

**chemBIOS – Unifying On-Chip Solution-Based Organic Synthesis,  
Characterization and Biological Screening in Drug Discovery**

Zur Erlangung des akademischen Grades eines

DOKTORS DER NATURWISSENSCHAFTEN

(Dr. rer. nat.)

von der KIT-Fakultät für Chemie und Biowissenschaften

des Karlsruher Instituts für Technologie (KIT)

genehmigte

DISSERTATION

von

Maximilian Benz

aus

Bruchsal, Deutschland

1. Referent: Prof. Dr. Pavel A. Levkin

2. Referentin: Prof. Dr. Ute Schepers

Tag der mündlichen Prüfung: 21.07.2020



Die vorliegende Arbeit wurde unter der Leitung von Prof. Dr. Pavel Levkin von September 2017 bis Juni 2020 am Institut für Biologische und Chemische Systeme (IBCS-FMS) des Karlsruher Instituts für Technologie (KIT, Campus Nord) angefertigt.

Die vorliegende Arbeit wurde nach den Vorgaben der Promotionsordnung des Karlsruher Instituts für Technologie (KIT) für die KIT-Fakultät für Chemie und Biowissenschaften Zur Erlangung des Doktorgrades der Naturwissenschaften vom 27. Juni 2017 angefertigt. Die vorliegende Dissertation wurde nach § 12 Dissertation Abs. (1) als monographische Dissertation unter Verwendung von Vorveröffentlichungen des Doktoranden (Maximilian Benz) erstellt. Hierfür wurden nach § 12 Dissertation Abs. (2) die Vorveröffentlichungen in einen thematisch kohärenten Zusammenhang gestellt und in die Dissertation mit einbezogen.

Hiermit versichere ich, Maximilian Benz, als Erstautor im Rahmen einer Mitautorenschaft einen signifikanten Beitrag der einbezogenen Vorveröffentlichungen selbstständig erbracht und die Teile deutlich kenntlich gemacht zu haben, die im Rahmen der vorliegenden Dissertation auf den Vorveröffentlichungen basieren oder übernommen wurden.

Versicherung gemäß § 13 Absatz 2 Satz 2 Ziffer 5 der Promotionsordnung des Karlsruher Instituts für Technologie (KIT) für die KIT-Fakultät für Chemie und Biowissenschaften

In die Dissertation wurden Vorveröffentlichungen einbezogen, bei denen ich im Rahmen einer Mitautorenschaft jeweils einen signifikanten Teil selbstständig erbracht habe. Eine Aufstellung mit den Angaben:

(1)

*Autoren:* Maximilian Benz, Mijanur R. Molla, Alexander Böser, Alisa Rosenfeld, Pavel A. Levkin

*Titel der Vorveröffentlichung:* Marrying chemistry with biology by combining on-chip solution-based combinatorial synthesis and cellular screening

*Veröffentlicht in:* Nature Communications (<https://doi.org/10.1038/s41467-019-10685-0>)

*Publisher:* Springer Nature

*Ausführliche Darlegung des selbstständig erbrachten, signifikanten Beitrages der Vorveröffentlichung:*

- Ausarbeitung und Weiterentwicklung der initialen Idee

- Design und Konstruktion der Geräte und Hilfsmittel
- Design des experimentellen Aufbaus
- Durchführung, Analyse und Interpretation der Daten
- Praktische, experimentelle Durchführung der Massenspektrometrie gemeinsam mit Alexander Böser
- Verfassen der Vorveröffentlichung in Rücksprache mit den Koautoren

*Rechte und Nutzungserlaubnis:*

Dieser Artikel steht unter einer Creative Commons Attribution 4.0 International Lizenz (CC BY 4.0), die die Nutzung, Teilen, Anpassung, Verbreitung und Vervielfältigung in jedem Medium und in jedem Format erlaubt, solange die ursprünglichen Autoren und die Quelle angemessen angegeben, einen Link zur Creative-Commons-Lizenz zur Verfügung gestellt, und darauf hingewiesen wird, ob Änderungen vorgenommen wurden. Die Bilder oder anderes Material von Dritten aus diesem Artikel sind in der Creative-Commons-Lizenz des Artikels enthalten, es sei denn, es wird in einem Verweis auf das Material anders angegeben.

Eine Kopie dieser Lizenz kann unter folgendem Link eingesehen werden:  
<https://creativecommons.org/licenses/by/4.0/>

(2)

*Autoren:* Maximilian Benz, Arndt Asperger, Meike Hamester, Alexander Welle, Stefan Heissler, Pavel A. Levkin

*Titel der Vorveröffentlichung:* A combined high-throughput and high-content platform for unified on-chip synthesis, characterization and biological screening

*Veröffentlicht in:* Nature Communications (aktueller Stand vom 28.08.2020: Manuskript angenommen)

*Publisher:* Springer Nature

*Ausführliche Darlegung des selbstständig erbrachten, signifikanten Beitrages der Vorveröffentlichung:*

- Vorschlag, Ausarbeitung und Weiterentwicklung der initialen Idee
- Design und Konstruktion der Geräte und Hilfsmittel
- Design des experimentellen Aufbaus

- Durchführung, Analyse und Interpretation der Daten
- Verfassen der Vorveröffentlichung in Rücksprache mit den Koautoren

*Rechte und Nutzungserlaubnis:*

Dieser Artikel steht unter einer Creative Commons Attribution 4.0 International Lizenz (CC BY 4.0), die die Nutzung, Teilen, Anpassung, Verbreitung und Vervielfältigung in jedem Medium und in jedem Format erlaubt, solange die ursprünglichen Autoren und die Quelle angemessen angegeben, einen Link zur Creative-Commons-Lizenz zur Verfügung gestellt, und darauf hingewiesen wird, ob Änderungen vorgenommen wurden. Die Bilder oder anderes Material von Dritten aus diesem Artikel sind in der Creative-Commons-Lizenz des Artikels enthalten, es sei denn, es wird in einem Verweis auf das Material anders angegeben.

Eine Kopie dieser Lizenz kann unter folgendem Link eingesehen werden:

<https://creativecommons.org/licenses/by/4.0/>

Bruchsal, 28.08.2020

Maximilian Benz

Eidesstattliche Erklärung

Hiermit versichere ich, dass ich die vorliegende Arbeit selbständig angefertigt und keine anderen als die angegebenen Quellen und Hilfsmittel benutzt, sowie wörtlich und inhaltlich übernommene Stellen als solche kenntlich gemacht habe. Die Satzung des Karlsruher Instituts für Technologie (KIT) zur Sicherung guter wissenschaftlicher Praxis in der gültigen Fassung wurde beachtet.

Bruchsal, 28.08.2020

Maximilian Benz



## Abstract<sup>1</sup>

Drug development often relies on high-throughput cell-based screening of large compound libraries. However, the lack of miniaturized and parallelized methodologies in chemistry as well as strict separation and incompatibility of the synthesis of bioactive compounds from their biological screenings make this process expensive and inefficient.<sup>1</sup> In this PhD thesis, a process was developed that combines on-chip solution-based synthesis of compound libraries with on-chip, highly sensitive compound characterization by mass spectrometry, IR and UV-Vis spectroscopy and high-throughput biological screenings in droplet arrays (chemBIOS workflow).

In the first part of this thesis, a method for miniaturized and parallelized, solution-based, high-throughput organic synthesis was investigated. Photochemically functionalized oleophilic-oleophobic patterned glass slides enabled the generation of dense droplet arrays with low surface tension liquids (such as most organic solvents). Each droplet functioned as an individual, spatially separated reaction vessel, that could be used for solution-based synthesis. Combinatorial synthesis enabled fast generation of large compound libraries. As a proof-of-principle, the chemBIOS platform was used to perform 75 parallel, three-component reactions to synthesize a library of lipid-like compounds (lipidoids).<sup>1</sup> Due to the flat two-dimensional substrate and the open architecture of the chemBIOS platform, chemicals and solutions could be added to individual spots of the array during a running experiment. A method for high-throughput, on-chip purification by miniaturized and parallelized liquid-liquid extraction was also developed. Additionally, a workflow for the post-synthetic application of on-chip synthesized compound libraries in an on-chip biological (cell-based) screening was demonstrated and optimized. This was achieved using a single-step sandwiching approach, where the on-chip synthesized lipidoid library was transferred to another polymer-based droplet array compatible with high surface tension liquids such as aqueous solutions and cell suspensions. The produced liposomes were complexed with a green fluorescent protein (GFP)

---

<sup>1</sup> Parts of the abstract are adapted from the following publications which are licensed under a Creative Commons Attribution 4.0 International License (CC BY 4.0; <https://creativecommons.org/licenses/by/4.0/>):

Benz, Maximilian, Molla, M.R., Böser, A., Rosenfeld, A. & Levkin, P.A. Marrying chemistry with biology by combining on-chip solution-based combinatorial synthesis and cellular screening. *Nature Communications* **10**, 2879 (2019).

Benz, Maximilian, Asperger, A., Hamester, M., Welle, A., Heissler, S. & Levkin, P.A. A combined high-throughput and high-content platform for unified on-chip synthesis, characterization and biological screening. Manuscript accepted.

plasmid DNA to form an on-chip library of different lipoplexes. The open infrastructure of the chemBIOS platform enabled off-line characterization of the on-chip generated lipoplex particles by dynamic light scattering (DLS) and zeta potential analysis. The transfection efficiency of the lipoplex library was investigated by reverse cell transfection using fluorescence microscopy. The entire process from the library synthesis to cell screening took only 3 days and about 1 mL of total solutions, demonstrating the potential of the chemBIOS technology to increase efficiency and accelerate screenings and drug development.<sup>1</sup>

The chemBIOS process enabled both miniaturized and parallelized, solution-based compound library synthesis and subsequent biological screening. However, the lack of miniaturized and parallelized analytical methods made the compound characterization difficult. Existing analytical methods are not designed for nanoliter scale, on-chip high-throughput approaches. Additional transfer steps between the synthesis platform (only compatible with low surface tension liquids (organic solvents)), analytical devices (with incompatible infrastructure) and the biological read-out platform (only compatible with high surface tension liquids (aqueous solutions)) hindered the entire workflow efficiency. The second part of this PhD research addressed these challenges. A dendrimer-based surface patterning was developed that enabled the generation of high-density nanodroplet arrays for both organic and aqueous liquids. Each droplet (among >50,000 droplets per plate) functioned as individual, spatially separated nanovessel, that could be used for solution-based synthesis or analytical assays. An additional indium-tin oxide coating enabled ultra-fast on-chip detection down to the attomole per droplet by matrix-assisted laser desorption/ionization mass spectrometry. The excellent optical properties of the chemBIOS platform allowed for on-chip characterization and *in situ* reaction monitoring in the ultraviolet, visible (on-chip UV-Vis spectroscopy and optical microscopy) and infrared (on-chip IR spectroscopy) regions. Finally, the platform is shown to be compatible with cell-biological screenings, which opens new avenues in the fields of high-throughput synthesis and drug discovery.<sup>2</sup>

## Zusammenfassung<sup>2</sup>

Die Medikamentenentwicklung beruht oft auf zellbasiertem Hochdurchsatz-Screening großer Wirkstoffbibliotheken. Der Mangel an miniaturisierten und parallelisierten Methoden in der Chemie, sowie die strikte Trennung und Inkompatibilität der Synthese bioaktiver Verbindungen von ihren biologischen Screenings macht den Prozess jedoch teuer und ineffizient.<sup>1</sup> In dieser Doktorarbeit wurde ein Verfahren entwickelt, das die Flüssigphasen-basierte on-chip Synthese von Wirkstoffbibliotheken mit hochsensitiver on-chip Charakterisierung von chemischen Substanzen durch Massenspektrometrie, IR- und UV-Vis Spektroskopie und biologischen Hochdurchsatz-Screenings in Tröpfchen-Arrays vereint (chemBIOS Workflow).

Im ersten Teil dieser Arbeit wurde eine Methode entwickelt, die eine miniaturisierte und parallelisierte, Flüssigphasen-basierte, organische Hochdurchsatz-Synthese ermöglicht. Funktionalisierte und photochemisch oleophil-oleophobisch gemusterte Glasobjektträger ermöglichten die Erzeugung dichter Tröpfchen-Arrays mit Flüssigkeiten mit niedriger Oberflächenspannung (z.B. organische Lösungsmittel). Jeder Tropfen fungierte als einzelnes, räumlich getrenntes Reaktionsgefäß, das für die Synthese in flüssiger Phase verwendet werden kann. Die kombinatorische Synthese ermöglichte die schnelle Generierung großer Molekülbibliotheken. In einer Proof-of-Principle Studie wurde die chemBIOS-Plattform verwendet, um 75 parallele 3-Komponenten-Reaktionen durchzuführen und so eine Bibliothek Lipid-ähnlicher Verbindungen (Lipidoide) zu synthetisieren.<sup>1</sup> Aufgrund des zweidimensionalen Substrats und der offenen Architektur der chemBIOS-Plattform konnten Chemikalien und Lösungen während eines laufenden Experiments zu einzelnen Spots des Arrays hinzugefügt werden. Es wurde eine Methode entwickelt, die on-chip im Hochdurchsatz-Verfahren eine Aufarbeitung durch miniaturisierte und parallelisierte Flüssigphasen-Extraktion ermöglichte. Zusätzlich wurde ein Workflow entwickelt, der eine post-synthetische Prozessierung der auf dem Chip synthetisierten Bibliothek ermöglichte, gefolgt von einem biologischen, zellbasierten on-chip Screening. Die on-chip synthetisierte Lipidoid-Bibliothek wurde durch einen

---

<sup>2</sup> Teile der Zusammenfassung wurde aus den folgenden Publikationen adaptiert, die unter einer Creative Commons Attribution 4.0 International Lizenz (CC BY 4.0; <https://creativecommons.org/licenses/by/4.0/>) lizenziert wurden: Benz, Maximilian, Molla, M.R., Böser, A., Rosenfeld, A. & Levkin, P.A. Marrying chemistry with biology by combining on-chip solution-based combinatorial synthesis and cellular screening. *Nature Communications* **10**, 2879 (2019).

Benz, Maximilian, Asperger, A., Hamester, M., Welle, A., Heissler, S. & Levkin, P.A. A combined high-throughput and high-content platform for unified on-chip synthesis, characterization and biological screening. Manuscript accepted.

einstufigen Sandwich-Vorgang auf eine andere Tröpfchen-Array-Plattform (mit zusätzlicher Polymerschicht) übertragen, die mit Flüssigkeiten mit hoher Oberflächenspannung, wie z.B. wässrige Lösungen und Zellsuspensionen, kompatibel war. Die Lipidoide wurden mit einem grün fluoreszierenden Protein (GFP)-Plasmid komplexiert und in wässriger Lösung zu Lipoplexen prozessiert. Die offene Infrastruktur der chemBIOS-Plattform ermöglichte die Offline-Charakterisierung der erzeugten Lipoplex-Partikel durch dynamische Lichtstreuung (DLS) und Zeta-Potenzial-Analyse. Die Transfektionseffizienz der Lipoplex-Bibliothek wurde durch reverse Transfektion mittels Fluoreszenzmikroskopie untersucht. Der gesamte Prozess von der Bibliothekssynthese bis zum Screening dauerte nur 3 Tage und benötigte etwa 1 mL Gesamtlösungen, was das Potenzial der chemBIOS-Technologie zur Effizienzsteigerung und Beschleunigung des Screenings und der Arzneimittelentwicklung demonstrierte.<sup>1</sup>

Das chemBIOS-Verfahren ermöglichte sowohl eine stark miniaturisierte und parallelisierte, Synthese von Molekül-Bibliotheken in flüssiger Phase als auch ein anschließendes biologisches Screening. Der Mangel an miniaturisierten und parallelisierten analytischen Methoden erschwert jedoch die Charakterisierung der Verbindungen. Die vorhandenen analytischen Methoden sind nicht für den Nanoliter-Maßstab und für on-chip Hochdurchsatz-Verfahren ausgelegt. Zusätzliche Transferschritte zwischen der Synthesepattform (nur kompatibel mit Flüssigkeiten mit niedriger Oberflächenspannung (organische Lösungsmittel)), den Analysegeräten (mit inkompatibler Infrastruktur) und der biologischen Screening-Plattform (nur kompatibel mit Flüssigkeiten mit hoher Oberflächenspannung (wässrige Lösungen)) schränken die Effizienz des gesamten Workflows ein. Der zweite Teil dieser Doktorarbeit befasste sich mit diesen Herausforderungen. Es wurde eine auf Dendrimern basierende Oberflächenstrukturierung entwickelt, die die Erzeugung von hochdichten Nanotröpfchen-Arrays sowohl für organische als auch für wässrige Flüssigkeiten ermöglichte. Jedes Tröpfchen (>50.000 Tröpfchen pro Platte) fungierte als ein einzelnes, räumlich getrenntes Nanogefäß, das für Flüssigphasen-basierte Synthese oder analytische Assays verwendet werden kann. Eine zusätzliche Indium-Zinnoxid-Beschichtung ermöglichte eine ultraschnelle on-chip Detektion bis in den Attomol-Bereich pro Tröpfchen mittels Matrix-unterstützter Laser-Desorption/Ionisation-Massenspektrometrie. Die hervorragenden optischen Eigenschaften der chemBIOS-Plattform ermöglichten eine on-chip Charakterisierung und *in situ* Reaktions-Monitoring im ultravioletten, sichtbaren (on-chip UV-Vis-Spektroskopie und optische Mikroskopie) und infraroten (on-chip IR-Spektroskopie) Bereich. Die Plattform ist mit verschiedenen zellbiologischen Screenings kompatibel, was neue Wege in den Bereichen Hochdurchsatzsynthese und Medikamentenentwicklung eröffnet.<sup>2</sup>

## Acknowledgments

Firstly, I would like to thank my supervisor, Prof. Dr. Pavel Levkin, for offering me the chance to work on this interesting topic, his consistent attention, teaching and supportive guidance through my PhD journey.

I would like to thank the members of the Thesis Advisory Committee, Dr. Gary Davidson (IBCS-FMS, KIT) and Prof. Dr. Joerg Lahann (IFG, KIT) for their feedback on the progress of my PhD research and for many thought-provoking scientific impulses.

Especially, I would like to thank Dr. Meike Hamester, Dr. Arndt Asperger and the whole team of the Bruker Corporation in Bremen for the great collaboration on MALDI-TOF MS. Thank you very much for your support, discussions and social events. I wish you guys all the best!

I thank Dr. Gerald Brenner-Weiß (IFG, KIT), Dr. Nicole Jung (IOC, KIT) and Dr. Dr. Michael Hirtz (INT, KIT) for providing training and access to MALDI-TOF MS, LC-MS and AFM.

I want to thank the Society for Laboratory Automation and Screening (SLAS) for providing me an international platform to present my research. I am proud to be part of SLAS by volunteering in the member sub-committee.

This PhD research was funded by ERC Starting Grant (DropCellArray, 337077), ERC Proof-of-Concept Grant (CellScreenChip, 680913), Baden-Württemberg Ministry of Science, Research and Arts (DrugMicroarray, 7533-7-11.10-7) and Helmholtz Association. I am very grateful for this. Furthermore, I am thankful for the support of the BioInterfaces International Graduate School (BIF-IGS) for educational training during my PhD study.

My deepest gratitude goes to my parents, Herbert and Sonja Benz, and my whole family, for always encouraging and supporting me throughout all situations of my life. I would never have gotten this far without you.

Finally, I am very thankful to Tanja Brenner, who accompanied me through the craziest times of my PhD study and always put a smile on my face.

# Table of Contents

Abstract .....	I
Zusammenfassung .....	III
Acknowledgments .....	V
Table of Contents .....	VI
List of Abbreviations .....	IX
Chapter 1 Introduction .....	1
1.1 Drug Discovery .....	1
1.2 Miniaturization and Parallelization of Chemical Synthesis .....	3
1.3 High-Throughput Biological Screenings .....	5
1.3.1 Droplet Microarray .....	7
1.4 Combing Chemistry, Analysis and Biology .....	11
Chapter 2 Objectives .....	13
Chapter 3 Marrying On-Chip Chemical Synthesis with Biological Cell-Screening .....	17
3.1 Results and Discussion .....	19
3.1.1 Manufacturing and characterizing the platform .....	19
3.1.2 On-chip synthesis and characterization of a lipidoid library .....	22
3.1.3 On-chip formation of liposomes and lipoplexes .....	27
3.1.4 On-chip cellular screening of produced lipoplexes .....	29
3.1.5 Discussion .....	30
Chapter 4 High-Throughput and High-Content On-Chip Compound Characterization .....	35

4.1	Results and Discussion .....	37
4.1.1	Manufacturing and characterization of the platform .....	37
4.1.2	On-chip MALDI-TOF mass spectrometry .....	41
4.1.3	On-chip IR spectroscopy .....	45
4.1.4	On-chip UV-Vis spectroscopy .....	46
4.1.5	Biological compatibility .....	50
4.1.6	Conclusions .....	51
Chapter 5	Summary and Future Perspectives .....	53
5.1	Miniaturization and Parallelization of Solution-Based Organic Synthesis .....	53
5.2	Marrying Chemistry with Biology .....	56
5.3	On-Chip High-Throughput Characterization.....	58
Chapter 6	Materials and Methods .....	63
6.1	Experimental Details to Chapter 3.....	63
6.2	Experimental Details to Chapter 4.....	70
References	.....	77
Appendix	.....	82
Curriculum Vitae	.....	99



## List of Abbreviations

A	absorbance
AFM	atomic force microscopy
ANSI	American National Standards Institute
c	concentration
CHCA	<i>alpha</i> -cyano-4-hydroxycinnamic acid
d	path length
DESI-MS	desorption electrospray ionization mass spectrometry
DIC	<i>N,N'</i> -diisopropylcarbodiimide
DLS	dynamic light scattering
DMA	droplet microarray
DMAP	4-dimethylaminopyridine
DMF	dimethyl formamide
DPMA	Deutsches Patent- und Markenamt
DMPK	drug metabolism and pharmacokinetics
DMSO	dimethyl sulfoxide
$\varepsilon$	extinction coefficient
eq.	equivalent
EtOH	ethanol
G	generation
GFP	green fluorescent protein
HCl	hydrochloric acid
HEK	human embryonic kidney cells
HeLa	cervical cancer cells
HEMA- <i>co</i> -EDMA	2-hydroxyethyl methacrylate- <i>co</i> -ethylene dimethacrylate
HSTL	high-surface tension liquids
HTS	high-throughput screening
IBCS-FMS	Institute of Biological and Chemical Systems – Functional Molecular Systems
IFG	Institute of Functional Interfaces

INT	Institute of Nanotechnology
IR	infrared
ITO	indium-tin oxide
KIT	Karlsruhe Institute of Technology
L	lipidoid (lipid-like structure)
LC-MS	liquid chromatography mass spectrometry
lipidoid	lipid-like compound
LSTL	low-surface tension liquid
MALDI-TOF MS	matrix-assisted laser desorption/ionization time-of-flight mass spectrometry
MTP	microtiter plate
NaOAc	sodium acetate
NaOH	sodium hydroxide
NH <sub>4</sub> H <sub>2</sub> PO <sub>4</sub>	ammonium dihydrogen phosphate
pDNA	plasmid DNA
PFDT	1 <i>H</i> ,1 <i>H</i> ,2 <i>H</i> ,2 <i>H</i> -perfluorodecanethiol
PI	propidium iodide
Ref	reference
Rq	surface roughness
rt	room temperature
S/N	signal-to-noise
SLAS	Society for Laboratory Automation and Screening
SPS	solid phase synthesis
SW	sandwiching
t <sub>1/2</sub>	reaction half-life
TE	transfection efficiency
ToF-SIMS	Time-of-flight secondary ion mass spectrometry
UV	ultraviolet
Vis	visible

## Chapter 1 Introduction<sup>3</sup>

### 1.1 Drug Discovery

The pharmaceutical industry struggles to meet the ever-increasing demand for new drugs. A decrease in the development of new drugs has been observed for years.<sup>3</sup> From 1991 to 2000, the total number of new drugs discovered in the 21 leading countries was 367, dropping to 251 for the period 2001-2010.<sup>4</sup> Fewer and fewer new drugs are being tested in clinical trials, and R&D takes longer to develop potential new drug candidates.<sup>1, 3</sup>

The process of developing drugs as well as various other fundamental and applied biological experiments begin from the organic synthesis of compound libraries, followed by their high-throughput screening in biological assays to identify few active molecules (hits) (**Figure 1**). Most of the compounds available in primary and secondary libraries are synthesized individually via standard organic synthesis usually involving large quantities of reagents and organic solvents. This makes library synthesis an extremely lengthy and costly process taking many years and consuming valuable resources. Despite these well-established procedures and methods, it often takes over 20 years and \$2-4 billion between a single drug's first synthesis, biological screening and ultimate approval.<sup>1</sup> For example, obeticholic acid, a drug to treat chronic liver diseases and a promising blockbuster drug, was first synthesized by Roda et al. in 1994.<sup>5</sup> Initial biological experiments were carried out at the turn of the millennium by Aldini and Pellicciari et al.,<sup>6, 7</sup> while worldwide approval was only in 2016.<sup>8</sup> Also Selexipag, a drug

---

<sup>3</sup> Parts of this chapter are adapted from the following publications which are licensed under a Creative Commons Attribution 4.0 International License (CC BY 4.0; <https://creativecommons.org/licenses/by/4.0/>):

Benz, Maximilian, Molla, M.R., Böser, A., Rosenfeld, A. & Levkin, P.A. Marrying chemistry with biology by combining on-chip solution-based combinatorial synthesis and cellular screening. *Nature Communications* **10**, 2879 (2019).

Benz, Maximilian, Asperger, A., Hamester, M., Welle, A., Heissler, S. & Levkin, P.A. A combined high-throughput and high-content platform for unified on-chip synthesis, characterization and biological screening. Manuscript accepted.

for pulmonary arterial hypertension based on a synthesis by Meanwell et al. in 1992<sup>9, 10</sup> was tested in biological studies beginning in 2007 by Kuwano et al.,<sup>11</sup> entering clinical trial II in 2012 and clinical trial III in 2016.<sup>12, 13</sup>

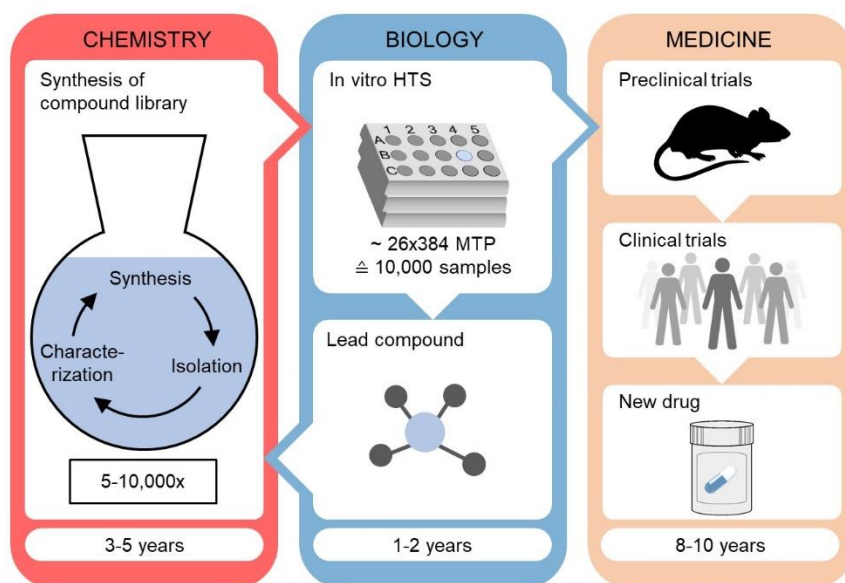


**Figure 1 | Schematic describing the process of drug discovery.** Strict separation between chemistry (synthesis) and biology (assays) makes the process of drug discovery inefficient. Modified from Ref<sup>1</sup>.

There are many reasons for such slow progress in developing drugs, ranging from typical problems such as poor lead optimization, limited specificity, and potential toxicity.<sup>1</sup> Most compounds already fail in primary biological screenings due to low biological activity. Few potential candidates passing the first *in vitro* screens after several cycles of lead optimization are then screened in preclinical *in vivo* studies before entering highly expensive clinical trials where the most promising drug candidates are tested on patients (**Figure 1**). The probability of a drug candidate to fail in this stage of drug development due to low target affinity, high clearance, low bioavailability or non-optimal metabolism causing low activity or unexpected side effects is about 75-99%.<sup>14-17</sup> Investigation of drug metabolism and pharmacokinetic (DMPK) profiles in early-stage drug discovery is a key technology to understand and predict drug properties to reduce the failure rate of a drug candidate and, thus, also reduce the costs and effort of the overall drug development process.<sup>18</sup> It is essential to collect as much information

as possible at an early stage of drug discovery. However, due to high costs and low availability, primary screenings are usually only done once (without repetitions and at different concentrations), and only in big pharmaceutical companies or screening centers.<sup>1</sup> There is a clear need to miniaturize and parallelize early-stage drug discovery to reduce the consumption of expensive and valuable chemicals, accelerate the process of compound library design, therefore, reduce the overall costs for preliminary drug screenings and, thus, making the process affordable for smaller research groups, too.

## 1.2 Miniaturization and Parallelization of Chemical Synthesis

The most arduous challenge in early drug discovery is the synthesis of novel, large compound libraries. Standard solution-based organic synthesis is performed in relatively large flasks requiring chemicals at least in the milligram and solvents in the milliliter scale to handle the amount of product in further isolation and characterization steps. A very simplified example demonstrates the challenge: If we had to synthesize 100,000 different compounds based on bimolecular reactions ( $A + B \rightarrow C$ ) for a subsequent biological screening, even if each reaction required only 10 mg of each reactant A and B and only 10 mL of solvents, the total amount of chemicals would be at minimum 2 kg and the total volume of organic solvents would amount to 1,000 L. The most important limitation, however, is the time needed for the synthesis part. For example, if one chemist had to do this library synthesis at a speed of five compounds per day, it would take him/her 55 years. This illustrates the underlying problem for the entire field of drug discovery and explains the slow development and exorbitant costs.<sup>1</sup> Miniaturization of chemical synthesis is essential to reduce the chemical consumption and resulting costs, and parallelization is required to accelerate and increase the throughput of the synthesis process.

Microarrays have been used to try to overcome these challenges. Solid-phase synthesis (SPS) in the microarray format is one example showing the potential of miniaturization and combination with the biological part. Microarrays of DNA, peptide microarrays, small molecule microarrays or oligosaccharide microarrays produced by SPS have been demonstrated.<sup>19-25</sup> Although these SPS methods have accelerated the development and investigation of large and diverse compound libraries because of their inherent miniaturization and parallelization, solution-based synthesis offers a much broader scope of chemical reactions. Moreover, most of the existing SPS methods are incompatible with more physiologically relevant cellular assays (2D or 3D cell culture) where freely diffusing compounds and therefore compartmentalization of individual cell experiments are required.<sup>1</sup>

Another strategy to miniaturize chemical synthesis is the use of microreactors and microfluidic devices.<sup>26-28</sup> Microfluidic chips consist, for example, of a glass, silicone or polymer substrate with incorporated microchannels that can be connected to external tubes and pumps (**Figure 2**).<sup>29</sup> Different chemicals can be mixed through the microchannels under a continuous flow and reactions can be carried out on-chip.

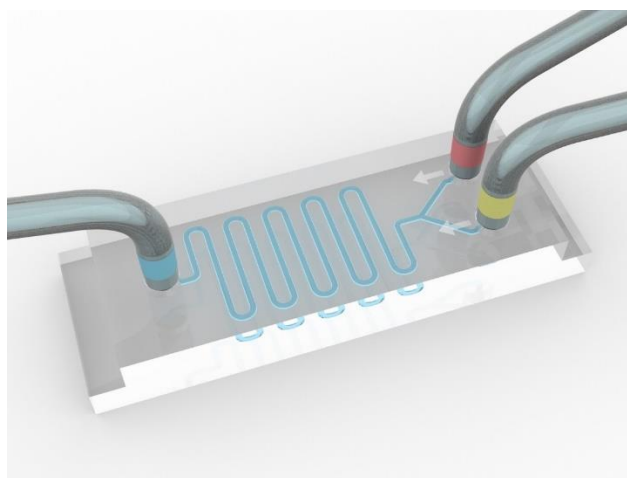


**Figure 2 | Schematic presenting an exemplary microfluidic system.** Tubes can be connected to the microfluidic chip and reactants mixed through microchannels to carry out, for example, an on-chip reaction under a continuous flow.

For example, Wang et al. designed a microfluidic chip enabling 32 parallel click reactions that can be carried out in approximately 30 mins requiring only 4  $\mu\text{L}$  volume per reaction.<sup>30</sup> Theberge et al. developed a chip to carry out 20 combinatorial Ugi-type reactions.<sup>31</sup> McMullen et al. designed an automated microfluidic system for optimizing on-chip Knoevenagel condensation reactions.<sup>32</sup> Although microfluidics have contributed significantly to the miniaturization of solution-based chemical synthesis, the possibility of parallelization is still lacking. In order to match existing biological ultra-high-throughput screenings, hundreds to thousands of compounds need to be synthesized simultaneously. Furthermore, each specific reaction type demands specific design of the microfluidic chip, and the complex setup limits the suitability for mass and daily use. The reaction chambers of microfluidic chips are very small (micro- to nanoliter range), however, the dead volume of the connected tubes for injecting the chemicals and solvents must also be considered. In addition, the whole equipment (chip substrate, tubes, pumps etc.) must be compatible with the chemicals used. The closed infrastructure of microfluidics hinders fast and direct intervention with running experiments and compatibility with independent, subsequent analytical and biological assays. There is a lack of technology that enables both miniaturized and parallelized, high-throughput, versatile, solution-based synthesis.

### 1.3 High-Throughput Biological Screenings

The principle of miniaturization and parallelization was perfected in biology by the development of microplates (so called Microtiter® plates, MTP). In 1951, the Hungarian scientist Gyula Takátsy developed a poly(methyl methacrylate) plate with 12x6 wells, followed by the well-known 96-well MTP in 1952, to overcome the shortage of test tubes during an influenza epidemic (**Table 1**).<sup>33</sup> In 1995, the Society for Biomolecular Screening (SBS; later

merged with the Association for Laboratory Automation (ALA) and renamed to the Society for Laboratory Automation and Screening (SLAS)) started to create standard definitions (footprint, height, bottom outside flange dimensions, well positions and well bottom elevation) of microplates, which had been published by the American National Standards Institute (ANSI). The ANSI/SLAS standards ensured a joint development of microplates and corresponding infrastructure (e.g. liquid handlers, plate readers etc.) within the screening industry.

**Table 1 | History of microplates.** Adapted from Ref<sup>34</sup>.

<b>Year</b>	<b>Innovator</b>	<b>Affiliation</b>	<b>Contribution</b>
1951	Takátsy, G.	N.I.P.H. Hungary	first 72-well (12x6) plate
1952	Takátsy, G.	N.I.P.H. Hungary	first 96-well plate
1992	Lennon, G. et al.	Lawrence Livermore	first 384-well plate
1995	SBS members	SBS	ANSI/SLAS standards
1996	Manns, R. & Young et al.	Whatman	first 1,536-well plate

Meanwhile, MTPs in various well arrangements are sold by different companies all over the world. The development of MTPs with smaller wells enabled reduction of the working volume and, thus, the material consumption, and at the same time increased the throughput through a higher well density (**Table 2**). While 96-well MTPs still requires up to 300  $\mu\text{L}$  of solution per well, the working volume of a well of a 1,536-well MTP is only about 1-15  $\mu\text{L}$ .

The development of robotic systems for automated liquid handling, optical imagers and data management software enabled both high-throughput and high-content screenings. Screening facilities can screen up to 100,000 compounds per day in ultra-high-throughput screenings.<sup>35</sup> For example, Dunn et al. screened two million compounds of a combinatorial compound collection for a target enzyme inhibitor within a couple of days using 1,536-well MTPs.<sup>36</sup>

**Table 2 | Technical properties of 96-, 384- and 1,536-well microtiter plates.**

	wells		volume [ $\mu$ L]
	amount	layout	
	96	8x12	100-300
	384	16x24	30-100
	1,536	32x48	1-15

The trend of modern biological screening is clear. Single-cell high-throughput and high-content drug screenings are increasingly coming into focus.<sup>37-39</sup> Considering a typical eukaryotic cell (e.g. hepatocyte) has a volume of 3.4 pL,<sup>40</sup> there is still much room for miniaturizing screening platforms. However, the capacity of miniaturizing microtiter plates is limited by physical properties. The material of the microplate and the physical walls that separate the wells from each other hinder increasing miniaturization. The capillary forces within a well increase with smaller well diameter making liquid handling impossible.<sup>41, 42</sup>

### 1.3.1 Droplet Microarray

Levkin et al. developed a so-called Droplet MicroArray (DMA) platform that enables massive miniaturization and parallelization of biological screening.<sup>43</sup> The technology behind DMA is inspired by nature. The Namib Desert beetle, also known as fogstand beetle, has an exceptional strategy to survive the extremely dry conditions of the Namib Desert. The wings of the beetle show a pattern of many small hydrophilic bumps, which are surrounded by hydrophobic troughs (**Figure 3a**). Finest water particles from fog arising from the Atlantic Ocean accumulate in small microdroplets on the hydrophilic bumps of the wings. Reaching a certain size, the droplets slide over the hydrophobic troughs to the mouthparts of the beetle and can be used for drinking water.<sup>44</sup> Levkin et al. adapted this hydrophilic-hydrophobic surface patterning and translated

the principle into a technical system. A poly(2-hydroxyethyl methacrylate-*co*-ethylene dimethacrylate) (HEMA-*co*-EDMA) polymer is grafted on the surface of a standard glass slide to increase the surface porosity. The polymer layer is then modified via an esterification with 4-pentynoic acid, followed by a photochemically thiol-yne click reaction sequentially applied through a photomask using different thiols. This results in the formation of hydrophilic spots (functionalized with 2-mercaptoethanol) which are surrounded by hydrophobic borders (functionalized with 1*H*,1*H*,2*H*,2*H*-perfluorodecanethiol (PFDT)) (**Figure 3c**).<sup>45, 46</sup>

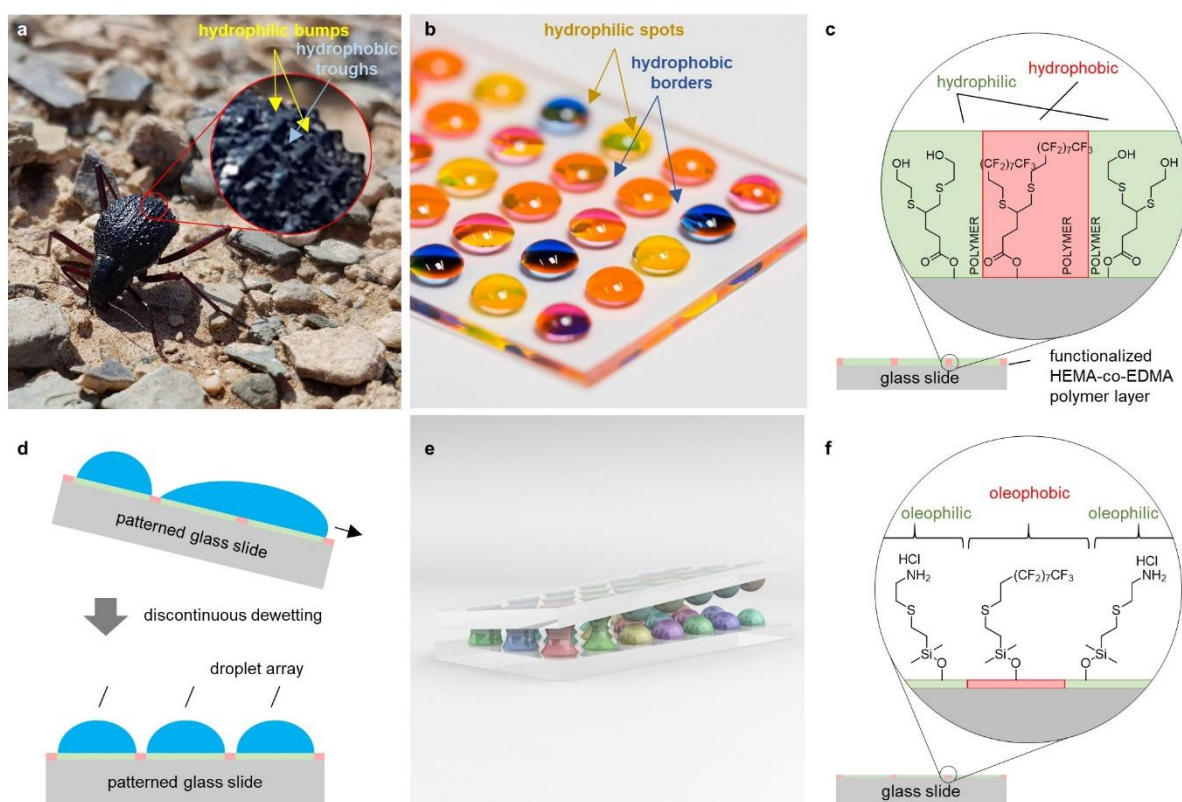


**Figure 3 | Droplet microarray.** (a) Photograph of a Namib Desert beetle found in the Hardap region of Namibia. The wings of the beetle show a pattern of hydrophilic bumps which attract water particles from fog and hydrophobic, water-repellent troughs. (b) Photograph of a droplet array applied to a hydrophilic-hydrophobic patterned glass slide. Modified from Ref<sup>1</sup>. (c) Schematic presenting the chemical composition of the surface of an hydrophilic-hydrophobic patterned polymer-layer grafted on a glass slide. Modified from Ref<sup>1</sup>. (d) Schematic describing the process of discontinuous dewetting. A large droplet is rolled over an hydrophilic-hydrophobic patterned glass slide resulting in the formation of microdroplets on the hydrophilic spots. Modified from Ref<sup>1</sup>. (e) Concept-Art showing the process of sandwiching two droplet arrays. (f) Schematic presenting the chemical composition of the surface of an oleophilic-oleophobic patterned glass slide. Modified from Ref<sup>1</sup>.

High contrast in wettability between highly hydrophilic, water-attracting spots ( $\theta_{\text{adv}}(\text{H}_2\text{O}) 19.2 \pm 1.6^\circ$ ,  $\theta_{\text{rec}}(\text{H}_2\text{O}) 6.3 \pm 1.1^\circ$ ) and hydrophobic, extremely water-repellent borders

( $\theta_{\text{adv}}(\text{H}_2\text{O}) 159.3 \pm 6.8^\circ$ ,  $\theta_{\text{rec}}(\text{H}_2\text{O}) 139.6 \pm 2.2^\circ$ ) enables the formation of droplet arrays (**Figure 3b**).<sup>1</sup> Due to the lack of physical walls between the spots and, therefore, nonexistent capillary forces, this array platform can be dramatically miniaturized and parallelized to generate ultra-dense droplet arrays with a working volume in the lower nanoliter range (**Table 3**). Each droplet of the array corresponds to one well of an MTP and can be used for carrying out individual assays. The extreme contrast in wettability of the hydrophilic-hydrophobic patterns allows to apply solutions via the effect of discontinuous dewetting (**Figure 3d**).<sup>47-51</sup> Solutions can also be applied by pipetting or, due to the standardized layout (meeting the ANSI/SLAS standards), dispensed by common robotic liquid handling systems (**Table 3**). Another benefit of the flat, wall-free architecture of the DMA is that entire arrays can be combined simultaneously by sandwiching and, thus, merging two droplet arrays (**Figure 3e**).<sup>52</sup> A broad variety of high-throughput applications have been shown using the DMA including the study of cell-cell communication,<sup>53</sup> cell culture and toxicity screenings in hydrogel micropads,<sup>50, 54</sup> drug and transfection screenings,<sup>52, 55, 56</sup> single cell screenings,<sup>57</sup> bacteria biofilm analysis,<sup>58</sup> culturing and screening of stem cells and embryoid bodies,<sup>59, 60</sup> spheroid screenings,<sup>61</sup> and even *in vivo* fish screenings.<sup>62</sup>

**Table 3 | Technical properties of droplet arrays of different spot sizes.** <sup>a)</sup> MTP-sized format meeting ANSI/SLAS standards

spot diameter	borders width	amount of spots <sup>a)</sup>	array layout <sup>a)</sup>	droplet volume
[ $\mu\text{m}$ ]	[ $\mu\text{m}$ ]			[nL]
2,828	1,672	384	24x16	1,000-5,000
900	225	6,144	96x64	50-150
500	62	24,576	192x128	10-30

The DMA technology opened new avenues for on-chip, miniaturized and parallelized high-throughput biological screenings. However, there is a fundamental limitation that makes most

chemical applications impossible. The porous HEMA-*co*-EDMA polymer increases the contrast in wettability of hydrophilic spots and surrounding hydrophobic borders for high surface tension aqueous solutions but it makes the entire surface oleophilic and, thus, incompatible with low surface tension liquids, such as most organic solvents that are required for solution-based synthesis. Therefore, Feng et al. developed another method of creating droplet arrays on a substrate without an additional porous polymer layer. The surface of a glass slide is silanized with chloro(dimethyl)vinylsilane resulting in a thiol-reactive monolayer of vinyl groups.<sup>47</sup> Next, the reactive surface is patterned via an UV-induced thiol-ene click reaction using PFDT and cysteamine hydrochloride subsequently through a photomask, resulting in the formation of oleophilic spots (functionalized with cysteamine hydrochloride) that are surrounded by oleophobic borders (functionalized with PFDT) (**Figure 3f**).<sup>47</sup> High contrast in wettability between this oleophilic-oleophobic patterns enables the generation of dense droplet arrays of low surface tension liquids, such as ethanol ( $\gamma_{lv}$  22.1 mN cm<sup>-1</sup>), acetone ( $\gamma_{lv}$  25.2 mN cm<sup>-1</sup>), dichloromethane ( $\gamma_{lv}$  26.5 mN cm<sup>-1</sup>) or dimethyl formamide ( $\gamma_{lv}$  37.1 mN cm<sup>-1</sup>).<sup>47</sup> However, the low contrast between the advancing water contact angle of the oleophobic parts ( $\theta_{adv}$  110.5±1.2°) and relatively high receding water contact angle of the oleophilic parts ( $\theta_{rec}$  33.7±0.8°) makes this substrate incompatible with high surface tension liquids, such as aqueous cell suspension and, thus, incompatible with biological screenings. An ultimate high-throughput platform that combines chemical and biological realms should be capable of handling both organic solutions for chemical synthesis and aqueous solutions for biological screenings.

## 1.4 Combing Chemistry, Analysis and Biology

Closer inspection of the individual disciplines of the drug discovery process above revealed the tremendous gap of miniaturized and parallelized high-throughput methodologies between chemical and biological realms. While existing ultra-high-throughput approaches in biology enable screenings of up to 100,000 drugs per day requiring only few micro- to nanoliters of solutions, the throughput in chemistry is still suffering from individual synthesis in large flasks (milliliter range), chemical diversity due to specialized solid-phase approaches, or low parallelization due to complex flow chemistry approaches. Combining chemical synthesis of large compound libraries with straightforward possibility of biological screening within a unified workflow is important to reduce additional transfer steps between individual platforms, labs or even companies which elaborates the entire drug discovery process and makes it cost-intensive. Low throughput of chemical synthesis entails the risk that large drug screenings will be only carried out using existing, commercially available compound libraries. This, however, limits the chemical space and the potential to discover novel active compounds. The obvious solution to elevate the throughput of chemical synthesis to the level of biological screening is to transfer and apply existing biological strategies and infrastructure to chemical systems. And, indeed, there are studies which used microtiter plates as synthesis platforms, followed by biological screenings. For example, Anderson et al. synthesized 2,350 cationic polymers in a combinatorial, solution-based approach using 96-well MTPs and identified 46 novel polymers that show high transfection efficiency in subsequent cell-based screenings.<sup>63</sup> Santanilla et al. used 1,536-well MTPs to investigate and optimize palladium-catalyzed C-O, C-N and C-C cross-coupling reactions requiring only about 1  $\mu$ L solutions per reaction (100 nmol of substrate).<sup>64</sup> These studies demonstrated the possibility of miniaturizing and parallelizing solution-based organic chemistry. However, they are suffering from several restrictions. The physicochemical properties of polystyrene microtiter plates limit the use to plastic-compatible

reaction medium such as water or dimethyl sulfoxide (DMSO). Reactions can only be carried out at ambient temperature.<sup>64</sup> Purification and dilution of compounds for subsequent biological screenings require additional transfer steps.<sup>63</sup> Furthermore, compound characterization is critical, since most common chemical analysis techniques are not designed for microtiter plates and the accompanying low volumes and low concentrations. Each of the 1,536 compounds of the study of Santanilla et al. have been transferred and characterized individually by liquid chromatography-mass spectrometry (LC-MS), which required a total analysis time of 52 h.<sup>64</sup> Hit compounds were resynthesized in larger quantities to investigate the isolated yield of the reactions.<sup>64</sup> It is very common to characterize only few members of a combinatorically synthesized compound library and assume similar results for other, untested compounds of the entire library, which could result in false-positive or false-negative hits. Beside the high-throughput chemical and biological applications there is a clear need to develop high-throughput on-line characterization methodologies to characterize and, furthermore, monitor the synthesis process.

Although it remains very challenging to unify chemical synthesis with characterization and the biological screening part to enable faster transfer and utilization of the synthesized compounds in biological screenings, this is the most efficient pathway to solve the aforementioned problems of the current early-stage drug discovery process.<sup>1</sup>

## Chapter 2 Objectives

The development of a new drug is extremely time- and cost-consuming, and the risk for a potential new drug to fail on its way to approval due to low biological activity or unexpected side effects is tremendously high in each stage of the drug discovery pipeline. There is a clear need to improve the drug discovery process to accelerate the development of new drugs and at the same time reduce the development costs. The focus of optimizing this process should be on an early stage of the drug discovery pipeline to increase the outcome of novel, promising compounds in preliminary screenings by high-throughput methods and to improve the chemical and biological characterization of those compounds by high-content approaches. The key technologies are miniaturization to reduce the consumption of expensive and valuable materials and agents, parallelization to increase the entire throughput, and unification to connect compound generation directly with biochemical and biological readout methods, thus, saving time, effort and money.

The first goal of this PhD research was to develop a method for miniaturized and parallelized solution-based synthesis to reduce the chemical consumption and increase the access to novel compound libraries (apart from existing, purchasable drug libraries), thus, expanding the chemical space for subsequent biological screenings. Oleophilic-oleophobic patterned glass substrates enable high-density compartmentalization of flat surfaces and the generation of droplet arrays of organic liquids. In this PhD thesis, this organic droplet array system should be evaluated for applying solution-based organic synthesis. Each droplet of the array (10-5,000 nL) represents a clearly defined and separated vessel that could be used for performing chemical reactions in liquid phase. In a proof-of-principle, a library of lipid-like compounds (lipidoids) should be synthesized on-chip by combinatorial synthesis. A critical step of solution-based synthesis is the need for purifying crude products. The current state of the art in standard

organic chemistry is performing reactions in flasks requiring agents and solvents in the milliliter range (or higher). Existing purification methods are developed to purify crude products at least in the milligram scale and, thus, are incompatible with miniaturized and parallelized on-chip chemistry. Another goal of this PhD thesis was to develop and evaluate the possibility of miniaturized on-chip high-throughput purification by liquid-liquid extraction. Hydrophilic-hydrophobic patterned glass substrates with an additional porous polymer layer enable the generation of droplet arrays with high surface tension liquids such as water. Sandwiching the water droplet array slide with another droplet array with droplets with a less polar organic solvent (such as octanol) should result in the formation of an interface between droplets containing immiscible liquids. A mixture of different compounds could be separated based on their relative solubilities in the polar or non-polar solvent. Furthermore, reaction monitoring and compound characterization are not designed for miniaturized and parallelized on-chip analysis in the nanoliter range. However, the optical properties of the patterned glass substrate promise the applicability of optical characterization methods such as UV-Vis or IR spectroscopy and should therefore be investigated in this PhD research to achieve on-chip high-throughput and high-content characterization. Recent developments of high-efficient lasers enable characterization of large compound libraries with high spatial resolution within seconds by matrix-assisted laser desorption/ionization time-of-flight mass spectrometry (MALDI-TOF MS).<sup>65-68</sup> However, MALDI-TOF MS requires a conductive substrate. Another aim of this PhD research was to develop a conductive surface patterning and, thus, enable on-chip characterization by MALDI-TOF MS, which has the potential to accelerate the process of on-chip compound library characterization. The sensitivity of each analytical method should be examined to observe the limitations of on-chip synthesis, on-chip monitoring and on-chip characterization.

Separation in time and space of the individual disciplines of early drug discovery – compound library synthesis, characterization and biological screening – resulted in a methodological gap and incompatibility between chemical, analytical and biological realms, which slows the entire drug discovery process, making it highly expensive. Finally, in this PhD thesis, a chemBIOS workflow should be developed which unifies on-chip compound library synthesis with the possibility of *in situ* reaction monitoring, on-chip characterization and subsequent on-chip biological screening. A lipidoid library should be synthesized on-chip, followed by on-chip processing of the lipidoids with an aqueous droplet array containing green fluorescent protein (GFP)-plasmids to generate an array of lipoplexes. This lipoplex library should be screened for the potential of transfecting cells by on-chip reverse cell transfection and validated via fluorescence microscopy.

In summary, the primary objectives of this PhD thesis are (i) miniaturization and parallelization of solution-based synthesis and possible purification technologies, (ii) development and evaluation of on-chip high-throughput and high-content compound characterization methods, and (iii) development of a workflow (chemBIOS) that unifies chemical synthesis of novel compound libraries, characterization and biological screening on the same platform, thus accelerating the process of drug discovery.



## Chapter 3 Marrying On-Chip Chemical Synthesis with Biological Cell-Screening<sup>4</sup>

Drug discovery is a lengthy and expensive process. The development of a single new drug often takes over 20 years and costs billions of dollars.<sup>2, 69-72</sup> Strict spatially and timely separation between individual disciplines in early-stage drug discovery – chemistry, analysis and biology – slows the drug discovery pipeline (**Figure 4**). Chemists synthesize, isolate and characterize thousands of compounds to create large compound libraries. The one-by-one synthesis approach of each single compound is dramatically time- and work-consuming. Furthermore, most solution-based syntheses are performed in relatively large borosilicate flasks requiring reagents and solvents at least in the milliliter-range to make it practicably possible to isolate, transfer and handle an essential amount of substance for further compound characterization. Large chemical consumption in the compound library synthesis process makes the drug discovery process additionally expensive. This is highly inefficient with regard to the reagent demands for biological drug screenings. High-throughput, automated biological drug screenings are already well-established using 96-, 384- or even 1536-well plates requiring only few microliters of total solutions.<sup>73-75</sup> Considering first dose response tests are mostly performed using concentrations between 1 nM to 100  $\mu$ M,<sup>76-80</sup> the working volume of one well per 1536-well plate is around 1.5  $\mu$ L and a potential drug candidates' molecular mass of less than 500 Daltons (Lipinski's rule of five) mean only around 75 ng per compound are actually needed for biological screening. The handling of those small amounts of substances is not

---

<sup>4</sup> This chapter is adapted from the following publication which is licensed under a Creative Commons Attribution 4.0 International License (CC BY 4.0; <https://creativecommons.org/licenses/by/4.0/>): Benz, Maximilian, Molla, M.R., Böser, A., Rosenfeld, A. & Levkin, P.A. Marrying chemistry with biology by combining on-chip solution-based combinatorial synthesis and cellular screening. *Nature Communications* **10**, 2879 (2019).

possible with standard organic techniques. Compounds need to be synthesized in larger quantities, then diluted and transferred to suitable platforms for biological screenings. This demonstrates the massive, inefficient chemical consumption between standard organic chemistry and biological screening and clearly demonstrates the need for designing a multi-disciplinary platform and straight-forward workflow that unifies all parts of early-stage drug discovery beginning from first compound synthesis to biological *in vitro* hit screening in a combined system.

In this PhD research, a microarray platform was developed that is compatible with miniaturized and parallelized, solution-based organic synthesis of combinatorial libraries of small molecules that are easily screenable in various biological and cell-based assays using the same platform (chemBIOS; **Figure 4**). As a proof-of-concept, the chemBIOS platform was used to synthesize a library of 25 lipid-like molecules (lipidoids), followed by the on-chip preparation of lipoplexes and the on-chip cell screening to identify transfection reagents.

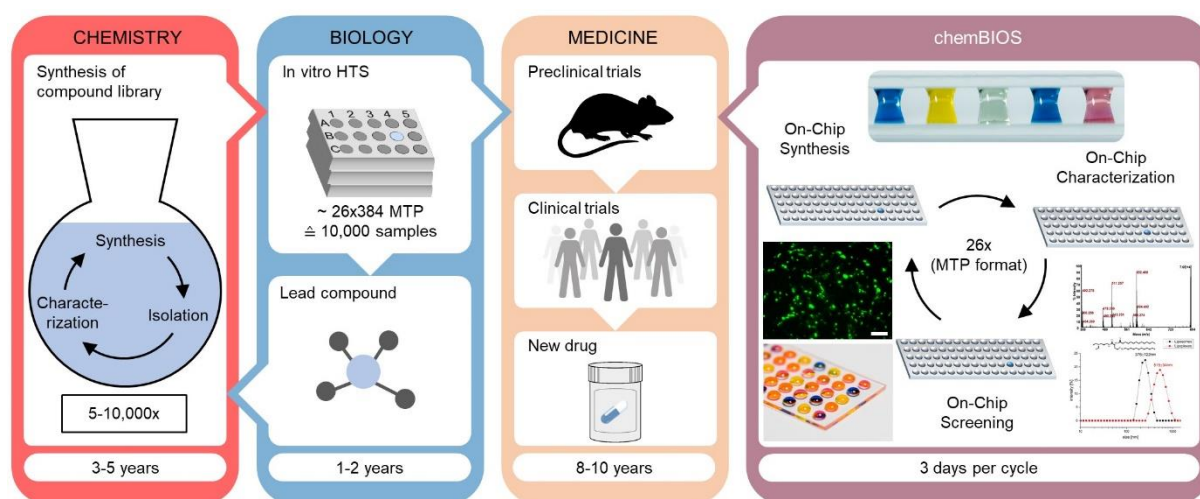


**Figure 4 | Schematic describing the integration of chemBIOS in the drug discovery process.** ChemBIOS unifies miniaturized solution-based chemical synthesis performed in a microarray format, characterization and biological screening, and thus, all steps in early-stage drug discovery take a few days rather than years. Scale bar: 200  $\mu\text{m}$ . Modified from Ref<sup>1</sup>.

## 3.1 Results and Discussion

### 3.1.1 Manufacturing and characterizing the platform

The entire validation of the chemBIOS process was conducted in four steps: (i) manufacturing and characterizing the platform, (ii) on-chip synthesis and characterization of a lipidoid library, (iii) on-chip formation of liposomes and lipoplexes, and (iv) on-chip cellular screening of produced lipoplexes.

A compound library was synthesized using omniphilic-omniphobic microarrays prepared on glass slides compatible with low surface tension organic liquids, thus called Low Surface Tension Liquids (LSTL) slides.<sup>47</sup> To manufacture LSTL slides, the surface of the glass slide was modified with chloro(dimethyl)vinylsilane to produce a monolayer of reactive vinyl groups on the surface. Afterwards, the photochemical patterning of the surface via the thiol-ene photoclick reaction (**Figure 7a**) led to the formation of omniphilic spots functionalized with cysteamine hydrochloride ( $\theta_{\text{adv}}(\text{DMSO}) = 32.9 \pm 2.4^\circ$ ,  $\theta_{\text{rec}}(\text{DMSO}) = 17.9 \pm 2.2^\circ$ ), spatially separated by omniphobic borders functionalized with 1*H*,1*H*,2*H*,2*H*-perfluorodecanethiol (PFDT) ( $\theta_{\text{adv}}(\text{DMSO}) = 87.0 \pm 3.5^\circ$ ,  $\theta_{\text{rec}}(\text{DMSO}) = 72.2 \pm 1.7^\circ$ ) (**Figure 7c** and **Appendix Figure 1**). +/- values of all contact angle measurements are standard deviations based on triplicate experiments. Due to the omniphilic-omniphobic properties of these patterns and excellent dewetting characteristics of the fluorinated regions, low surface tension liquids including various common organic solvents (such as n-hexane, ethanol, 1-decanol, DMF and DMSO (**Figure 5**)) could form arrays of microdroplets via the effect of discontinuous dewetting (**Figure 7e**).<sup>47</sup> The shape and volume of these droplets could be defined by varying the geometry of the patterns. Depending on the patterns and solvent, droplets from few picolitres up to microliters could be created.<sup>50</sup> However, LSTL slides cannot be used to form droplet arrays employing aqueous solutions with much higher surface tension, due to the relatively high

receding contact angle of the water on the hydrophilic regions ( $\theta_{\text{rec}}(\text{H}_2\text{O}) = 33.7 \pm 0.8^\circ$ ;

**Appendix Figure 1).**



**Figure 5 | Photograph of droplets of various organic solvents on a Low Surface Tension Liquids (LSTL) slide.** From left to right: n-hexane ( $\gamma_{\text{lv}} = 18.4 \text{ mN m}^{-1}$ ), ethanol ( $\gamma_{\text{lv}} = 22.1 \text{ mN m}^{-1}$ ), 1-decanol ( $\gamma_{\text{lv}} = 28.5 \text{ mN m}^{-1}$ ), DMF ( $\gamma_{\text{lv}} = 37.1 \text{ mN m}^{-1}$ ) and DMSO ( $\gamma_{\text{lv}} = 43.5 \text{ mN m}^{-1}$ ). Spot size: 2.83 mm; borders width: 1.67 mm; droplet volume: 5  $\mu\text{L}$ . Cited from Ref<sup>1</sup>.

Therefore, in the next step High Surface Tension Liquids (HSTL) slides were produced – glass slides coated with a porous polymer layer patterned with hydrophilic spots separated by hydrophobic barriers, leading to the effect of discontinuous dewetting of aqueous solutions.<sup>45</sup>

<sup>46</sup> The preparation of HSTL slides occurs via the photochemical patterning of a thin, porous layer of poly(2-hydroxyethyl methacrylate-*co*-ethylene dimethacrylate) (HEMA-*co*-EDMA polymer). Highly hydrophilic spots functionalized with 2-mercaptoethanol ( $\theta_{\text{adv}}(\text{H}_2\text{O}) = 19.2 \pm 1.6^\circ$ ,  $\theta_{\text{rec}}(\text{H}_2\text{O}) = 6.3 \pm 1.1^\circ$ ) and spatially separated by highly hydrophobic borders functionalized with PFDT ( $\theta_{\text{adv}}(\text{H}_2\text{O}) = 159.3 \pm 6.8^\circ$ ,  $\theta_{\text{rec}}(\text{H}_2\text{O}) = 139.6 \pm 2.2^\circ$ ) were generated via the photochemical thiol-yne photoclick reaction (**Figure 7b,d** and **Appendix Figure 1**). The combination of highly hydrophilic spots possessing very strong affinity to aqueous solutions and hydrophobic, extremely water-repellent regions enabled the formation of arrays of droplets of high surface tension aqueous solutions such as liposomes or cell suspension using discontinuous dewetting (**Figure 6**).

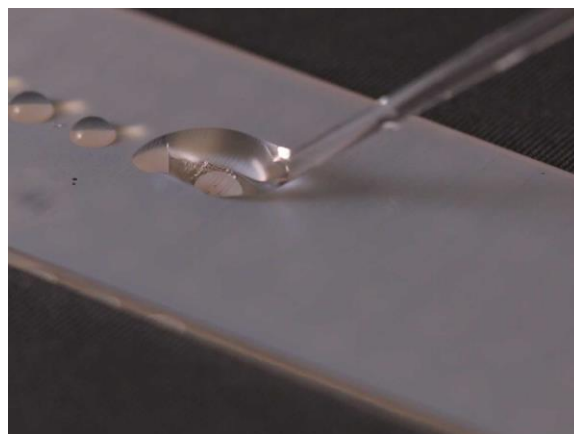


**Figure 6 | Rolling droplet.** Solutions can be applied row-by-row by rolling a large droplet over the photochemically patterned surface. Huge differences in wettability between hydrophilic/omniphilic spots and surrounding hydrophobic/omniphobic borders lead to the formation of microdroplets. Cited from Ref<sup>1</sup>.

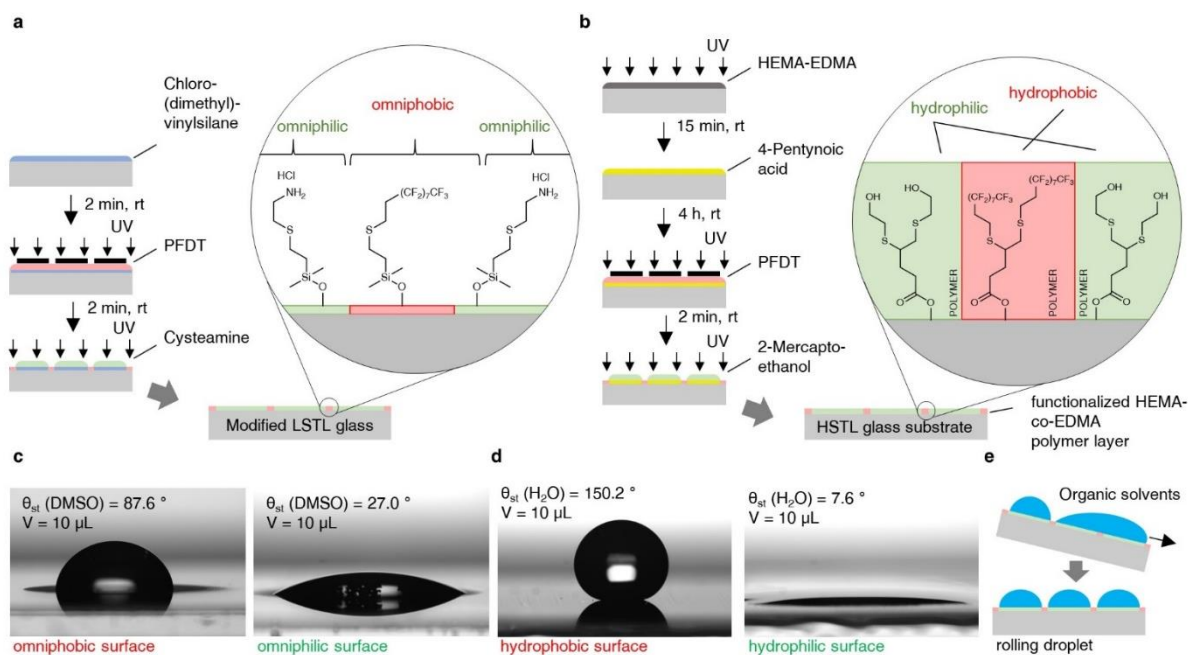


**Figure 7 | Manufacture and characterization of patterned slides used for the chemBIOS platform.** The chemBIOS platform consists of two types of patterned glass slides. (a) Slides compatible with Low Surface Tension Liquids (LSTL slides) are produced by silanizing the glass surface with chloro(dimethyl)vinylsilane and patterning via the photochemical thiol-ene click reaction. Omniphobic borders are generated by a reaction with perfluorodecanethiol (PFDT), followed by the formation of omniphilic spots by cysteamine hydrochloride. Spot diameter 2.83 mm; hydrophobic borders width 1.67 mm. (b) Slides for High Surface Tension Liquids (HSTL slides) are manufactured via a polymerization reaction to apply a porous polymer layer of poly(2-hydroxyethyl methacrylate-*co*-ethylene dimethacrylate). Functionalization with 4-pentynoic acid enables further surface patterning by thiol-yne photoclick chemistry. Hydrophobic borders are generated by PFDT, followed by the formation of hydrophilic spots using 2-mercaptoethanol. Spot diameter 2.83 mm; hydrophobic borders width 1.67 mm. (c) Photographs of droplets of DMSO on the omniphobic surface and omniphilic surfaces used for the LSTL patterns with corresponding static contact angle. Droplet volume: 10  $\mu$ L (d) Photographs of droplets of water on hydrophobic and hydrophilic surfaces used for the HSTL slides with corresponding static contact angle. Droplet volume: 10  $\mu$ L (e) Schematic showing the effect of discontinuous dewetting on patterned LSTL slides, which enables manual generation of organic droplet arrays. Cited from Ref<sup>1</sup>.

### 3.1.2 On-chip synthesis and characterization of a lipidoid library

LSTL slides were used to develop and optimize the parallel, combinatorial synthesis of cationic lipid-like molecules (lipidoids). For this purpose, a one-pot three-component reaction based on thiolactone opening by an amine, followed by a disulfide exchange reaction (**Figure 10b**) was carried out on-chip.<sup>81</sup> Two methods were used to apply solutions in droplet-array format to the slides: a printing method, where droplets were applied to each spot via a non-contact liquid dispenser system, and the rolling droplet method, where solutions were applied via discontinuous dewetting. The rolling droplet method was only used to synthesize the lipidoids characterized by MALDI-TOF mass spectrometric analysis and is described below. Solutions of various amines (A1-A5) in DMSO were applied in a column-by-column manner on an LSTL slide A to form an array of different amines in each row (**Figure 10a**). The thiolactone and pyridyl disulfide reactants were premixed together in DMSO in different combinations and applied on a LSTL slide B in row-by-row manner perpendicular to the columns in slide A (**Figure 10a**). By sandwiching both slides using an aligner device (**Figure 8**), the droplets on slides A and B were merged in array format, initiating the chemical reaction simultaneously in each droplet on the array (**Figure 10a**). Using this method, a library of 25 different compounds, each in triplicate was synthesized on one slide in a single step (**Appendix Table 1**). The reaction was carried out for 2 h at room temperature.

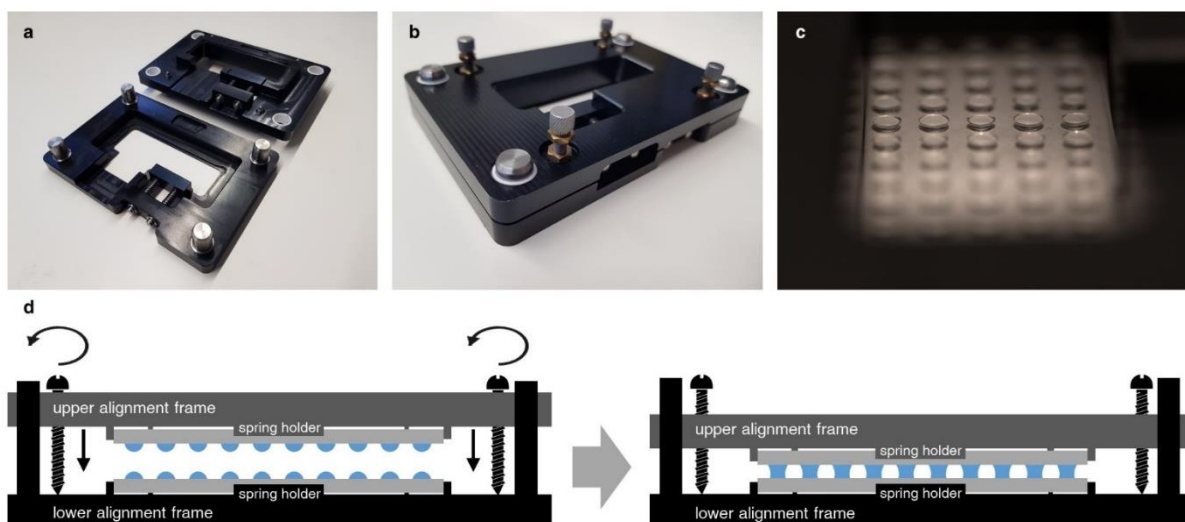


**Figure 8 | Alignment (sandwiching) device.** (a) Photograph of the opened alignment device. (b) Photograph of the closed alignment device during the synthesis step. (c) Photograph of two sandwiched slides in the alignment device during the synthesis step. (d) Schematic describing the process of precise sandwiching of two droplet arrays. The alignment device consists of a lower and upper frame. Slide A is set into the lower frame of the alignment device and fixed with a spring holder. Slide B is set into the upper frame of the alignment device and fixed, too. The lower frame shows round rods in each edge of the frame, whereas the upper frame shows round recesses on the same positions. The upper frame is put on the lower frame so that the rods from the lower frame slide into the recesses of the upper frame and therefore fix both frames in the lateral position. The distance in height of both frames can be precisely controlled by four screws until the droplets of slide B merge with the droplets of slide A. Cited from Ref<sup>1</sup>.

The released 2-thiopyridone was used to monitor the reaction kinetics and estimate the yield via UV-Vis spectroscopy. The extinction coefficient of 2-thiopyridon in DMSO/acetonitrile (1:10) was independently estimated to be  $2,040 \text{ M}^{-1} \text{ cm}^{-1}$  at 370 nm (**Figure 9a**). To monitor the progress of the reaction, one droplet from the array was taken, diluted in 90  $\mu\text{L}$  acetonitrile, and analyzed by UV-Vis. Based on those UV-Vis results, the reaction was complete after two hours (**Figure 9b**).

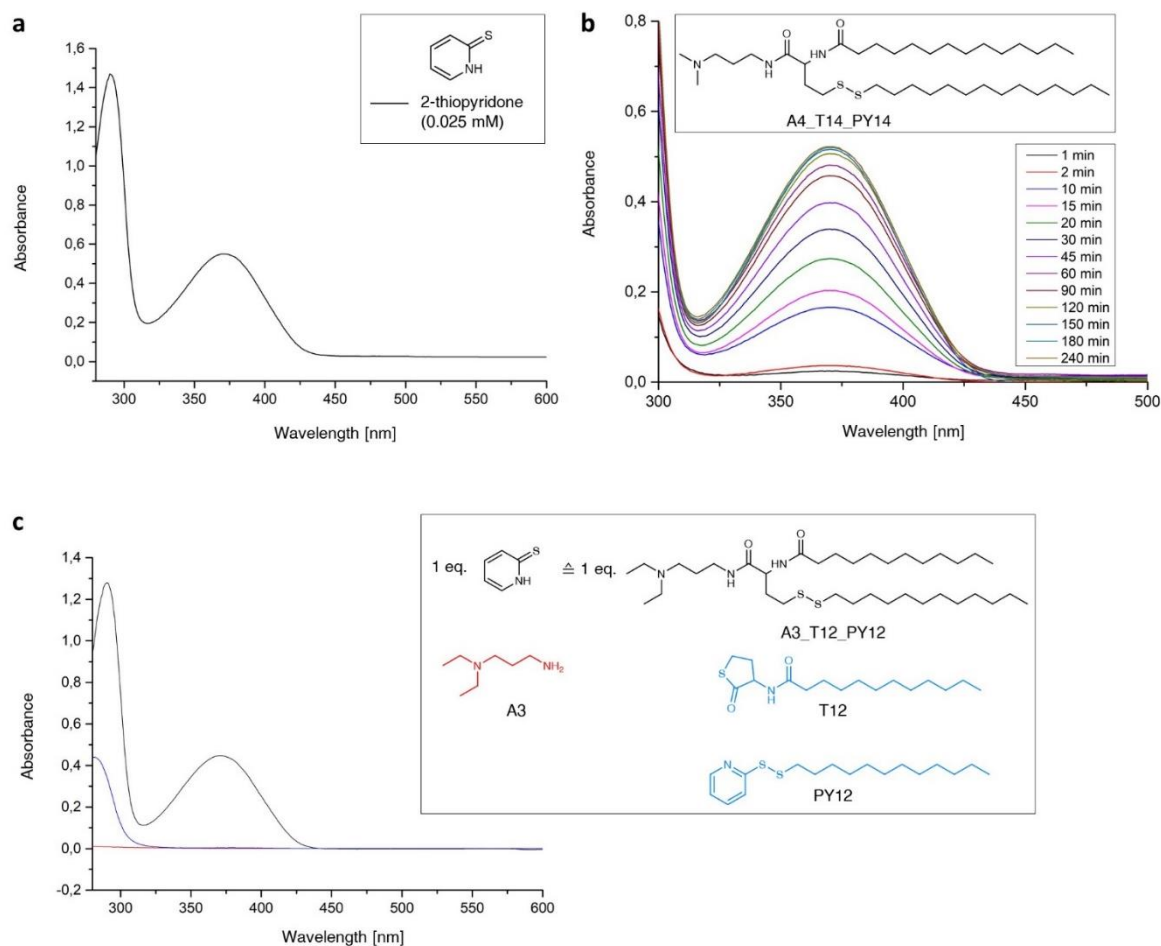


**Figure 9 | UV-Vis spectroscopy.** (a) Spectrum of 0.025 mM 2-thiopyridone in DMSO/acetonitrile (1:10). Extinction coefficient was estimated to be  $2040 \text{ M}^{-1} \text{ cm}^{-1}$  at 370 nm. (b) UV-Vis reaction kinetic measurements. UV-Vis absorbance of reaction mixture of sample A4\_T14\_PY14 was measured in range of 1-240 min. After approximately 2 h the reaction was completed. (c) Exemplary UV-Vis absorbance spectrum of raw product A3\_12\_12 (black) compared to UV-Vis absorbance spectra of educts (A3, red / T12\_PY12, blue). Optical depth: 1 cm. Cited from Ref<sup>1</sup>.

By quantifying the absolute concentration of 2-thiopyridone, the average yield of  $89 \pm 15 \%$  was calculated by Beer-Lambert law (**Figure 9c** and **Appendix Table 1**). +/- values of all reaction yields are standard deviations based on triplicate experiments. The products of the reaction were analyzed via MALDI-TOF mass spectrometry (MS). The open system and flat substrate of chemBIOS enabled to transfer and copy the entire compound library in a single step by stamping it onto a MALDI plate (**Figure 10c** and **Appendix Figure 2**). Moreover, the raw product was characterized by  $^1\text{H-NMR}$  (**Appendix Figure 3**) and on-chip ATR-IR spectroscopy (**Appendix Figure 4**).

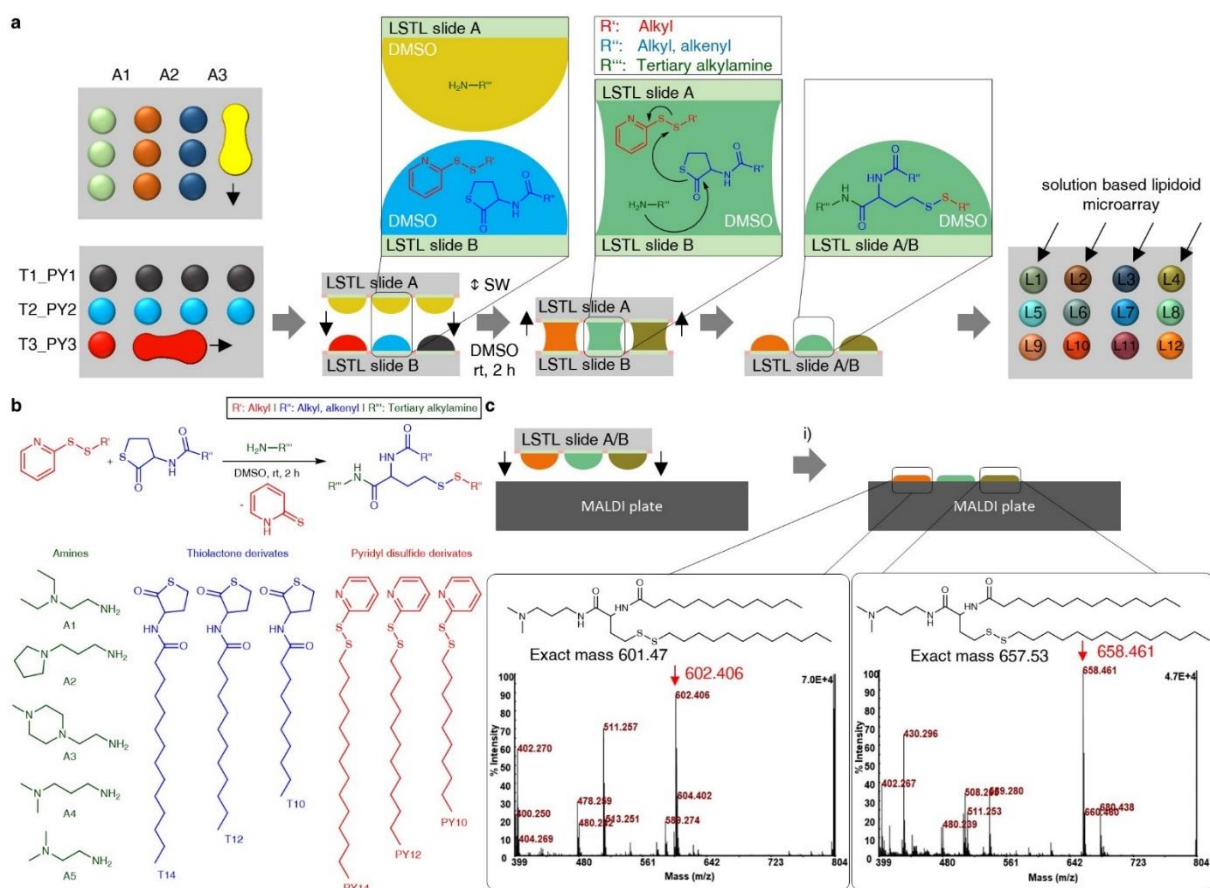


**Figure 10 | On-chip synthesis and characterization of a lipidoid library.** (a) Schematic description of combinatorial synthesis of lipidoids using the chemBIOS platform. In the first step, various amines dissolved in DMSO are applied column-by-column onto a low surface tension liquids (LSTL) slide A. Then, mixtures of thiolactone and pyridyl disulfide derivatives dissolved in DMSO are applied on a LSTL slide B in rows oriented orthogonally to the columns on slide A. The application is done by rolling a droplet of solution to form rows of separate droplets. In the next step, slide A and slide B are sandwiched (SW) with each other to bring individual droplets into contact to merge the droplets, thereby initiating the reaction. The reaction was completed after 2 h at room temperature. 25 different lipidoids per slide were synthesized in triplicates on a single slide. (b) Scheme of the reaction and a list of all different precursors for the reaction. (c) To characterize produced compounds, slide A was sandwiched onto a MALDI plate, followed by the adding of matrix and drying the plate. MALDI-TOF mass spectrometry measurement (examples of spectra shown in the insets, positive mode) enables rapid and convenient characterization of the entire library of synthesized compounds. i: sandwiching, followed by adding 10 mg mL<sup>-1</sup>  $\alpha$ -cyano-4-hydroxycinnamic acid solution of 1:1 acetonitrile:water containing 0.1% v/v trifluoroacetic acid. Cited from Ref<sup>1</sup>.

The open format of the chemBIOS system is compatible with further on-chip steps such as investigating, treating or converting the chemical compound library, to achieve high-throughput parallel on-chip purification. A proof-of-principle experiment proofed the possibility for on-chip purification by liquid-liquid-extraction (**Figure 11a,b**). Therefore, Nile red and methylene blue were dissolved in 1-octanol and applied to several spots on a LSTL slide D which resulted in dark blue droplets. LSTL slide D was sandwiched with an HSTL slide E containing water droplets, resulting in the formation of an octanol-water interface for each droplet (**Figure 11a**).

Methylene blue is highly water-soluble and was therefore extracted from the organic phase into the aqueous phase, while water-insoluble Nile red remained in the organic phase. The organic phase turned red after 10 min, while the aqueous phase turned blue, indicating successful separation.

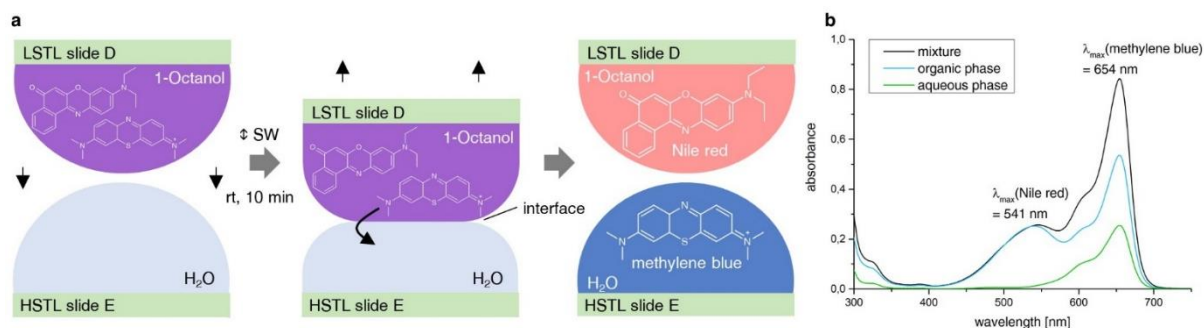


**Figure 11 | On-chip parallel liquid-liquid extraction.** (a) Schematic description of the on-chip two-phase liquid extraction process. A mixture of oleophilic Nile red and hydrophilic methylene blue in 1-octanol on an LSTL slide D was separated by sandwiching the slide with an HSTL slide E carrying water droplets for 10 min. An interface between the two non-miscible solvents was formed, and the water-soluble methylene blue was extracted into the aqueous phase. (b) Validation of the on-chip extraction via UV-Vis spectroscopy. The UV-Vis spectrum of the mixture reveals two local absorbance maxima: one at 541 nm corresponding to Nile red, and another at 654 nm corresponding to methylene blue. After the extraction, the intensity of the absorbance maximum of methylene blue in the organic phase decreased while the intensity of Nile red remained constant. In the aqueous phase, no Nile red could be detected. Cited from Ref<sup>1</sup>.

The mixture was analyzed before purification, as well as the organic and aqueous phases after purification by UV-Vis spectroscopy (Figure 11b and Appendix Figure 6) and liquid chromatography mass spectrometry (LC-MS) (Figure 12 and Appendix Figure 5). Both analytical methods yielded similar results. Using UV-Vis spectroscopy, the concentration of methylene blue measured  $11.9 \pm 0.5$  mM in the original organic phase mixture, and  $3.3 \pm 0.6$  mM and  $4.1 \pm 0.4$  mM in the organic and aqueous phase, respectively, after extraction. The concentration of Nile red was measured 6.0 mM in the original mixture, and  $4.3 \pm 0.3$  mM and  $0.3 \pm 0.04$  mM in the organic and aqueous phase after extraction. This corresponds to the purification of the methylene blue from 66% in the mixture to 91% in the aqueous phase and that of Nile red from 34% in the mixture to 57% in the organic phase via just one purification step. +/- values of all concentration measurements are standard deviations based on triplicate experiments.

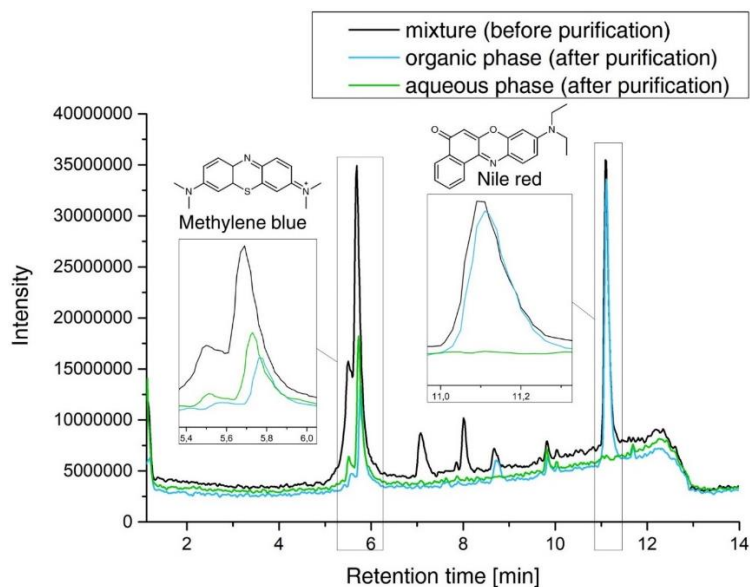


**Figure 12 | LC-MS characterization of the on-chip liquid-liquid extraction process.** A mixture of a solution of Nile red and methylene blue was purified by an on-chip two-phase liquid extraction. The mixture (black line), the organic (red line) and the aqueous phase (blue line) was analyzed by LC-MS. Methylene blue showed a retention time of about 5.7 min, Nile red showed a retention time of 11.1 min. The intensity of methylene blue in the organic phase decreased after the purification step, while the intensity of Nile red remained the same. No peak for Nile red could be detected in the aqueous phase. Flow rate: 1 mL min<sup>-1</sup>; detector: DAD (230 nm, 254 nm, 280 nm, 300 nm and 400 nm). Cited from Ref<sup>1</sup>.

### 3.1.3 On-chip formation of liposomes and lipoplexes

In the next step, the lipidoid library was transferred from the LSTL slide A to an HSTL slide C (**Figure 13a**). This step was performed to transfer lipidoids into aqueous cell-compatible droplets simultaneously, forming either liposomes or lipoplexes required for cell transfection experiments. To make lipoplexes or liposomes, the LSTL slide A containing dried lipidoids was sandwiched with HSTL slide C containing an array of droplets of an aqueous sodium acetate buffer (50 mM, pH 5) with or without plasmid pCS2-GFP (75 ng  $\mu\text{L}^{-1}$ ), respectively. The buffer also contained 0.04% w/v gelatin, 3.4% w/v sucrose, 0.002% w/v human fibronectin required for the subsequent reverse cell transfection experiment.<sup>82</sup> The sandwiched slides were incubated at 50 °C for 1.5 h to support the formation of liposomes/lipoplexes. As a result, the synthesis products were transferred to the HSTL slide C. Having been transferred into an aqueous environment, the amphiphilic lipidoids spontaneously formed liposomes, subsequently

complexing plasmid DNA to form lipoplexes (**Figure 13a**). Both liposome and lipoplex solutions were characterized by pipetting them directly from the HSTL slide C into a cuvette to analyze via dynamic light scattering (DLS) and zeta potential analysis. The lipoplex solutions revealed significantly larger particles than the corresponding liposome solutions (**Figure 13b**). Furthermore, lipoplex solutions demonstrated a lower zeta potential than the corresponding liposomes, indicating the formation of complexes between the positively charged headgroups of the lipoids and negatively charged DNA (**Figure 13b**).

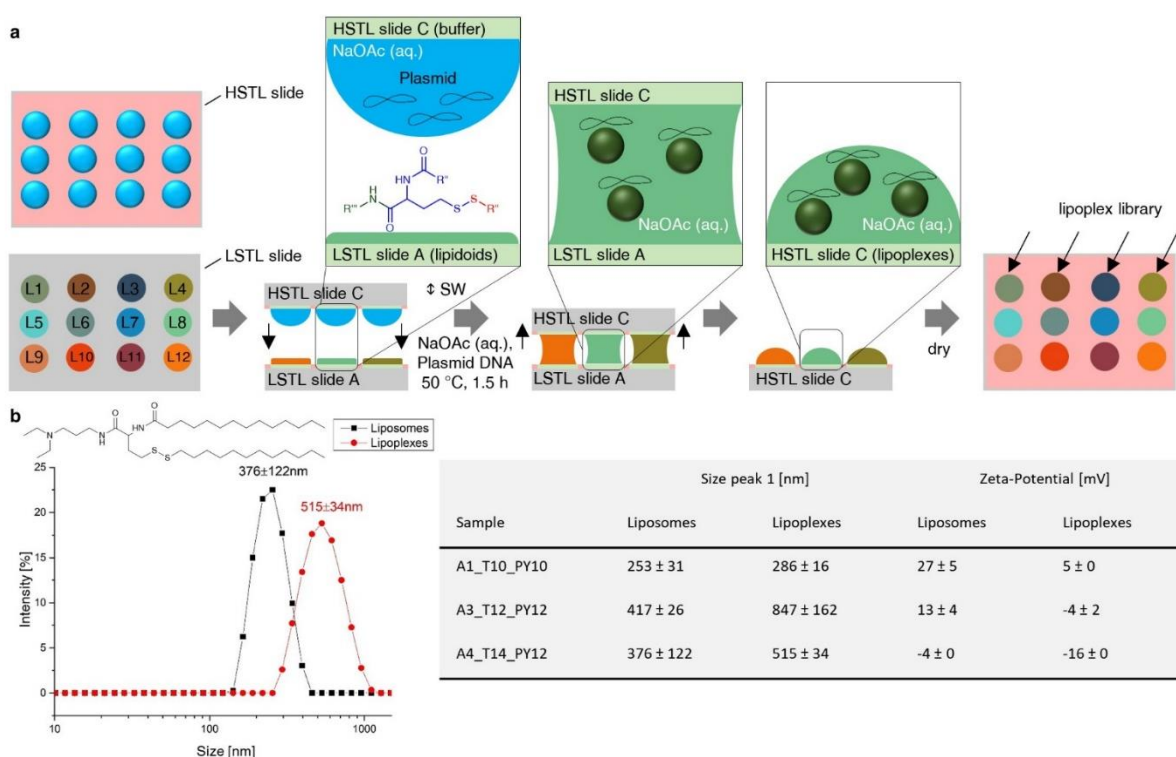


**Figure 13 | On-chip parallel formation of a library of liposomes or lipoplexes.** (a) Schematic description of lipoplex formation. An array (HSTL slide C) of aqueous sodium acetate buffer droplets containing sucrose, gelatin, fibronectin and pDNA (pCS2-GFP) was sandwiched with LSTL slide A containing a library of dried lipidoids, followed by incubation at 50 °C for 1.5 h and drying before using the slide C for the following reverse cell transfection experiment. Liposomes were produced in the same way without adding plasmid DNA. (b) Results of dynamic light scattering (DLS) and zeta potential analyses of lipoplexes and corresponding liposomes. Liposomes display smaller particles and higher zeta potential than corresponding lipoplexes. +/- values are standard deviations, n = 3 (number of replicates). Cited from Ref<sup>1</sup>.

### 3.1.4 On-chip cellular screening of produced lipoplexes

Next, the lipoplex library was investigated in an on-chip cell-based screening using reverse transfection of HEK293T cells (**Figure 14a**).

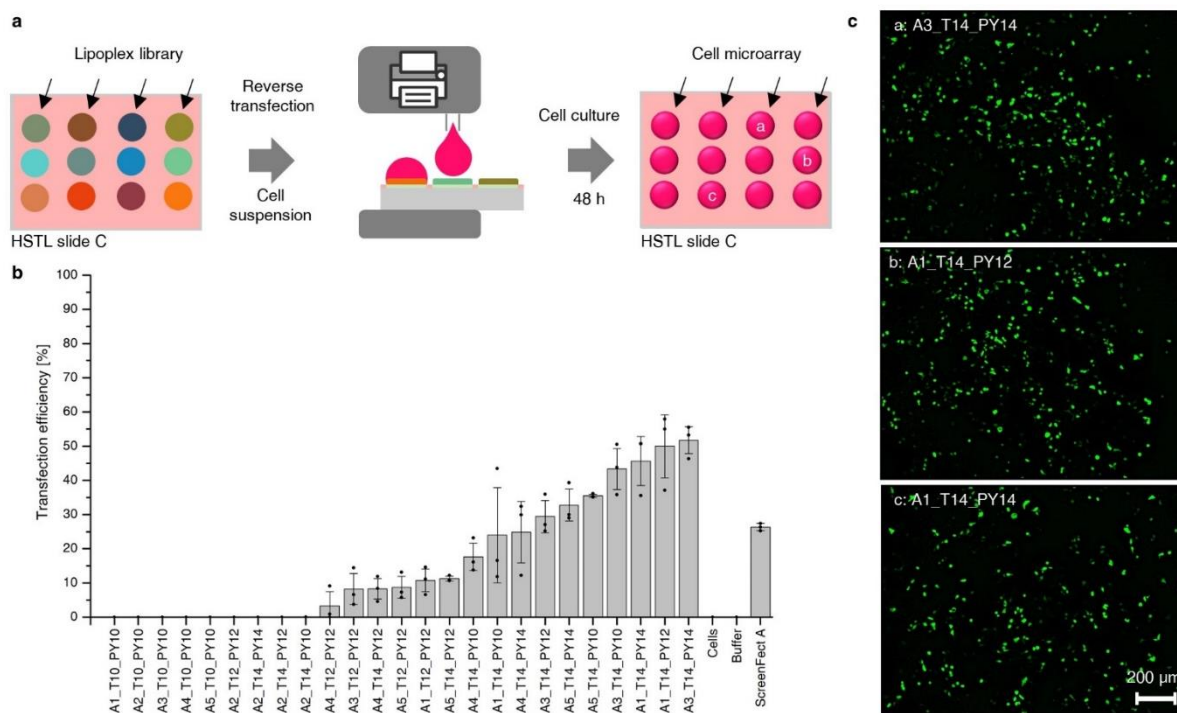


**Figure 14 | On-chip reversed cell transfection screening of the produced lipoplex library.** (a) Schematic showing the process of on-chip cell transfection screening. 5  $\mu\text{L}$  of HEK293T cell suspensions were printed into each hydrophilic spot on the HSTL slide C covered by the dried lipoplex cell transfection mixture. After incubating the array for 48 h at 36  $^{\circ}\text{C}$  and 5%  $\text{CO}_2$ , 1  $\mu\text{L}$  of staining solution was printed into each droplet, followed by 15 min incubation and fluorescence microscopy analysis. (b) Bar chart visualizing mean values of transfection efficiencies (number of GFP-transfected cells per total cell number) calculated based on three independent experiments (overlaid dot plots) covering the entire pipeline including on-chip library synthesis, formation of lipoplexes and cell transfection. A3\_T14\_PY14 lipidoid proved to be most efficient in this study, resulting in 52 $\pm$ 4% transfection efficiency. Error bars are standard deviations,  $n = 3$  (number of replicates);  $N = 3$  (repetitions including lipid synthesis). (c) Fluorescence microscopy images of pCS2-GFP transfected cells. Scale bar: 200  $\mu\text{m}$ . Cited from Ref<sup>1</sup>.

ScreenFect A was used as a positive control, while dilution buffer without pDNA and untreated cells served as negative controls. The transfection experiment was performed by printing 5  $\mu\text{L}$  of a suspension of  $6 \times 10^5$  HEK293T cells  $\text{mL}^{-1}$  into each spot on the dried lipoplex array slide using a non-contact liquid dispenser. After 48 h of cultivating and staining the cells with Hoechst and propidium iodide (PI), the transfection efficiency of each sample of the array was determined by fluorescence microscopy (**Figure 14b,c** and **Appendix Table 2**). Sample A3\_T14\_PY14 was observed to be the best performing transfection agent in the screening with

52±4% average transfection efficiency (**Figure 14b**). Viability of cells in the negative control experiment (spots without lipidoids and only treated with buffer solution) was 97±1%, while cells transfected with the most efficient lipoplexes demonstrated approx. 34% viability as measured by PI/Höchst staining (**Appendix Figure 7**).

### 3.1.5 Discussion

The process of developing biologically active compounds and potential drug candidates is difficult due to several factors. The transfer of commercially available drug libraries into a suitable screening format poses huge handling and logistics challenges. The parallel addition of reagents and solutions, and the transfer to another platform requires many multi-pipetting steps and thus large amounts of consumables as well as the loss of material due to large dead volumes. The handling of very large drug libraries is often impossible for a single individual to accomplish within a reasonable time. Additional labor costs make the development of bioactive compounds prohibitively expensive. Furthermore, commercially available drug libraries are extremely costly, and the number of available compounds remains limited. Synthesizing new compounds is very time- and resource-consuming, since traditional solution-based organic synthesis is not designed for miniaturized and parallelized applications. In addition, the temporal and spatial separation of synthesis, characterization, and biological screening significantly slows down entire biological discovery and drug development pipelines. There is currently no system that could efficiently hyphenate these parts.

The chemBIOS platform enables miniaturized combinatorial solution-based organic synthesis in the microarray format and unifies chemistry with biological high-throughput screenings, and, thus tries to solve these challenges in drug discovery pipelines. The platform uses Low Surface Tension Liquids (LSTL) slides with omniphobic-omniphilic patterns to form arrays of organic

solvents, where each droplet functions as a separate microreactor for solution-based organic synthesis. Furthermore, sandwiching the array with another droplet array enables the rapid and parallel addition, transfer, and copying of the whole library. For example, a 3-component lipidoid combinatorial synthesis was carried out to create a library of 25 small molecules in triplicates (**Figure 10b**). By sandwiching two droplet arrays, all educts in 75 droplets were simultaneously mixed, and, thus the synthesis of an entire library was initiated in a single step (**Figure 10a**). Although this platform can be readily utilized for many types of solution-based reactions using various organic or aqueous solvents, there are still some challenges in adapting other chemical techniques. Reactions at elevated temperatures and highly exothermic reactions as well as adding solid reagents or purging gaseous educts might be difficult to realize using the chemBIOS platform in its current state. Chemical reactions requiring a protective atmosphere or controlled pressure are feasible but would require a closed chamber with controlled pressure and atmosphere. On-chip parallel high-throughput purification is another key challenge. The advantages of the chemBIOS platform are that its configuration is open and flat, making all microcompartments accessible and potentially compatible with parallel high-throughput purification methods, e.g. on-chip extraction (**Figure 11a,b**).

Due to the low sensitivity, most organic synthesis characterization methods are often incompatible with the micro-, nano- or even picomolar scale reactions required for high-throughput miniaturized synthetic applications. MALDI-TOF mass spectrometry is the method of choice for characterizing small quantities of compounds in a parallel way. The open system of the chemBIOS platform enabled to copy the entire droplet-based library in a single step by stamping it onto a MALDI plate, followed by mass spectrometric analysis (**Figure 10c**). Besides MALDI-TOF MS, compounds synthesized on the chemBIOS platform can be characterized via on-chip IR spectroscopy (**Appendix Figure 4**). This demonstrates another important advantage of the chemBIOS platform's flat, open droplet microarray system. The

open and flat microarray format of the chemBIOS slides makes it compatible with other analytical methods such as Raman spectroscopy or surface sensitive methods including DESI-MS or time-of-flight secondary ion mass-spectrometry.

The chemical compounds from the LSTL slide could be transferred to a High Surface Tension Liquids (HSTL) slide in a parallel manner that enabled rapid and convenient hyphenation between the two realms – chemical and biological. HSTL slides were used to create highly hydrophilic-hydrophobic microarrays that could be used to form the arrays of aqueous droplets needed for biochemical and cellular screenings. Sandwiching of both types of slides enabled the single-step transfer of the entire lipidoid library from the platform for organic solvents (LSTL slide) to the platform for aqueous solvents (HSTL slide). The single-step formation of liposomes and lipoplexes during this transfer step was proved by dynamic light scattering and zeta potential analysis – observing higher zeta potentials for liposomes than for lipoplexes (**Figure 13b**). The lipoplexes were successfully screened with cells by printing cellular suspension into the individual spots containing lipoplexes to perform a reversed cell transfection experiment (**Figure 14**). The screening of lipidoids to determine their cell transfection efficiency using plasmid DNAs is an example of a biological assay that is combinable with synthesized libraries. Other possible biological experiments include, inter alia, CRISPR/Cas9-based gene editing, screening of membrane proteins, gene-knockdown, and the screening of cell spheroids or organoids. Overall, this demonstrates the possibility to hyphenate combinatorial organic chemistry with biological screenings using the chemBIOS platform. Unifying chemistry and biology both temporally and spatially on the same platform accelerates the entire process of developing bioactive compounds important for various applications. Using the chemBIOS platform, *in situ* synthesized small molecule libraries can be screened immediately for their biological activity, thereby saving time, effort, chemicals, cells, and other consumables. The entire procedure of synthesizing (3  $\mu$ L organic solvent),

transferring/processing (4.5  $\mu\text{L}$  aqueous solvent) and screening (5  $\mu\text{L}$  cell suspension + 1  $\mu\text{L}$  staining solution) of a single lipidoid took only 3 days and about 13.5  $\mu\text{L}$  of solutions, whereas the traditional bulk procedure requires at least several milliliters per compound. This allowed to repeat the whole process from the synthesis to the biological screening again and again; the final analysis of transfection efficiency by fluorescence microscopy yielded reproducible transfection results for all the library compounds (**Figure 14b**). The platform is compatible with further miniaturization, despite possible future challenges associated with further reductions in droplet size, such as faster solvent evaporation, difficult alignment during the sandwiching process, compatibility with and sensitivity of analytical methods.

In summary, the first prototype of the chemBIOS platform that is described in this chapter marries on-chip *in situ* miniaturized and parallelized solutions-based combinatorial synthesis of bioactive compounds with the on-chip biological and cellular screening and, thus, enables fast compound screenings of novel compound libraries. This will be useful not only for drug discovery but also for various other biological or biotechnological screening applications. Although rapid and fast characterization can be achieved by copying the library microarray onto a separated slide for analysis, the efficiency of the developed chemBIOS workflow at that point is slowed down by several transfer steps between the synthesis, characterization and screening part. Furthermore, offline MALDI-TOF MS characterization is the only possibility at that moment for high-throughput characterization of large compound libraries. Therefore, the next step for improving the chemBIOS workflow, which is topic of the following chapter of this PhD thesis, should focus on making the platform compatible for chemical, analytical and biological methodologies at the same slide, and developing further high-throughput and high-content approaches for online *in situ* monitoring and characterization.



## Chapter 4 High-Throughput and High-Content On-Chip Compound Characterization<sup>5</sup>

Miniaturization and parallelization of organic synthesis is crucial to enlarge the capacity of compound library design and reduce the effort, chemical consumption and associated costs. In the previous chapter, the chemBIOS platform was used in a proof-of-principle study demonstrating on-chip miniaturized solution-based synthesis of 75 transfection agents and subsequent on-chip cell-biological screening in a process that was completed in only three days and required only 1 mL of solutions.<sup>1</sup> However, these improvements have been hindered because the existing analytical methods are not designed for nanoliter scale, on-chip high-throughput approaches. Liquid handling of nanoliter-sized volumes and sample transfer of thousands of compounds between synthesis, characterization and screening platforms slows down the process of drug development and, thus, makes it expensive. There is a clear need to unify early-stage drug discovery on a multi-functional platform that enables sequential nano-scale synthesis of structurally diverse compounds, highly sensitive chemical characterization and high-throughput biological screening on the same chip.

In this this chapter, a dendrimer-based surface patterning method was developed that can be used to handle high-density nanodroplet arrays of both low (organic solvents) and high (aqueous solutions) surface-tension liquids, thus, enabling a broad range of chemical, analytical and biological applications (chemBIOS) (**Figure 15**). An indium-tin oxide (ITO) coating makes the platform conductive and therefore, compatible with on-chip high-throughput compound

---

<sup>5</sup> This chapter is adapted from the following publication which is licensed under a Creative Commons Attribution 4.0 International License (CC BY 4.0; <https://creativecommons.org/licenses/by/4.0/>): **Benz, Maximilian**, Asperger, A., Hamester, M., Welle, A., Heissler, S. & Levkin, P.A. A combined high-throughput and high-content platform for unified on-chip synthesis, characterization and biological screening. Manuscript accepted.

characterization by matrix-assisted laser desorption/ionization mass spectrometry (MALDI-TOF MS). We demonstrate highly sensitive on-chip approaches for infrared (IR) spectroscopy and high-content reaction monitoring by UV-Vis spectroscopy using this platform (**Figure 15**). The open infrastructure and standardized format make chemBIOS adaptable for well-established assays and commercial devices and for both high-throughput (>50,000 droplets/plate) and high-content (>50,000 results/experiment) chemical, analytical and biological screening (**Figure 15**).

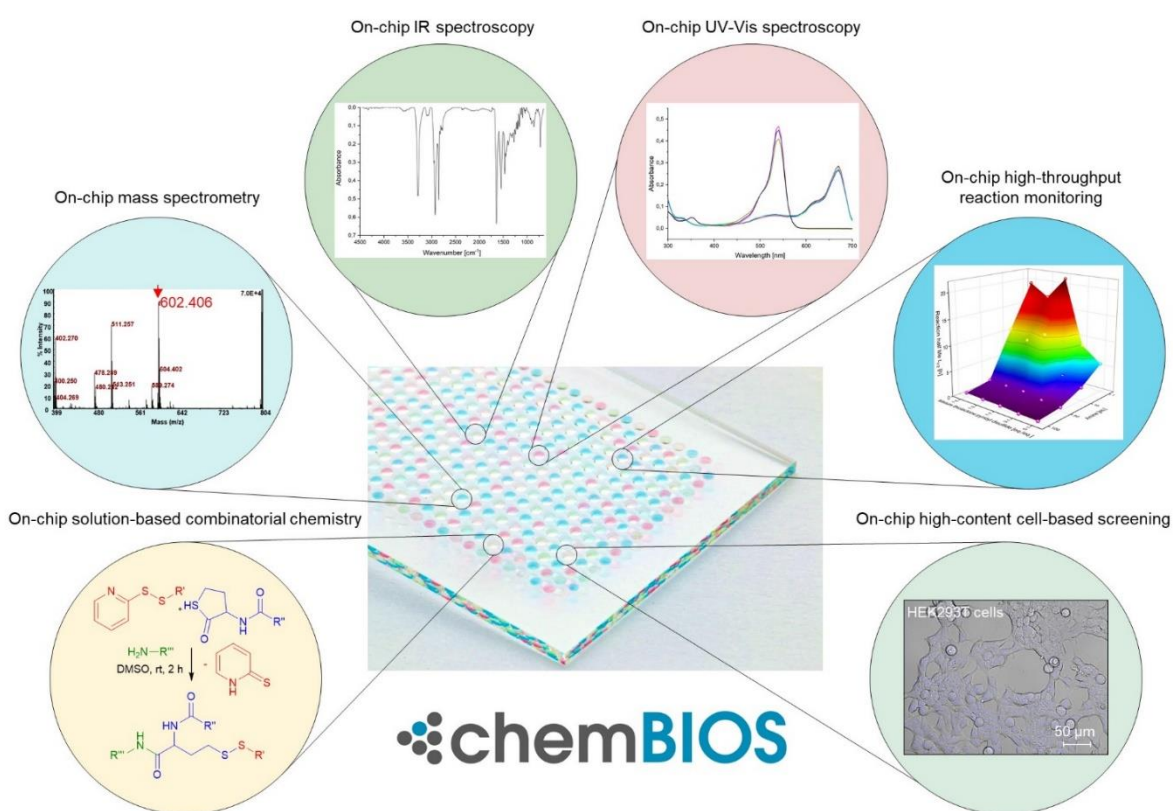


**Figure 15 | Schematic overview of the chemical, analytical and biological high-throughput methods compatible with the chemBIOS platform.** ChemBIOS enables on-chip solution-based synthesis, on-chip analytical characterization using various spectrometric and spectroscopic approaches for high-content screening and also unifies chemistry with biological high-throughput screening using nanodroplet arrays. Cited from Ref<sup>2</sup>.

## 4.1 Results and Discussion

### 4.1.1 Manufacturing and characterization of the platform

Previously reported hydrophilic-hydrophobic functionalized droplet arrays used for high-throughput cell screenings were based on porous polymer substrates, making the surface oleophilic and incompatible with organic solvents with low surface tension.<sup>1, 83, 84</sup> Feng et al. developed a flat oleophilic-oleophobic patterned substrate enabling the formation of droplet arrays of organic solvents used for miniaturized and parallelized solution-based organic synthesis.<sup>1, 47</sup> However, the low contrast between the advancing water contact angle of the oleophobic parts ( $\theta_{adv}$   $110.5 \pm 1.2^\circ$ ) and the receding water contact angle of the oleophilic parts ( $\theta_{rec}$   $33.7 \pm 0.8^\circ$ ) makes this substrate incompatible for handling high surface tension liquids.<sup>1</sup> To create arrays of droplets of both high and low surface tension liquids, the hydro-/oleophobic (omniphobic) patterns should have high advancing contact angles while the hydro-/oleophilic (omniphilic) parts should possess very low receding contact angles. A dendrimeric surface modification with high-density functional groups might increase the contrast of wettability properties leading to an omniphilic-omniphobic patterning. Therefore, a dendrimeric surface modification was developed based on a poly(thioether) dendrimer synthesis (**Figure 16a**).<sup>85</sup> The surface of a standard glass slide was silanized with triethoxyvinylsilane to produce a reactive, vinyl group-presenting surface. The dendrimeric layer was then synthesized in a repetitive two-step reaction cycle consisting of a photochemical thiol-ene click reaction with 1-thioglycerol followed by esterification with 4-pentenoic acid (**Figure 16b**); three cycles produce a dendrimerized surface decorated with high-density alkene groups. This surface can then be photochemically functionalized either with 1-thioglycerol or 1*H*,1*H*,2*H*,2*H*-perfluorodecanethiol (PFDT), to yield an omniphilic or omniphobic surface, respectively. Omniphilic-omniphobic micropatterns of defined geometry can be created by sequential functionalization through a quartz photomask (**Figure 16c**).

An increase in functional group density should correlate with the wettability properties of the surface. To test this hypothesis, the static water contact angle of different dendrimer generations was compared (G0–G4) (**Figure 17a**), starting with cysteamine hydrochloride functionalized surfaces.<sup>1,47</sup> A slight increase in the static water contact angle ( $8.6^\circ$ ) was observed between the PFDT-modified G0 ( $\theta_{\text{stat}}(\text{H}_2\text{O}) 104.3 \pm 1.9^\circ$ ) and G4 ( $\theta_{\text{stat}}(\text{H}_2\text{O}) 112.9 \pm 1.5^\circ$ ) surfaces. A much greater decrease ( $23.8^\circ$ ) was observed between the cysteamine-modified G0 ( $\theta_{\text{stat}}(\text{H}_2\text{O}) 55.9 \pm 3.0^\circ$ ) and G4 ( $\theta_{\text{stat}}(\text{H}_2\text{O}) 32.1 \pm 5.7^\circ$ ) surfaces (**Figure 17a**). There were no significant differences in  $\theta_{\text{stat}}(\text{H}_2\text{O})$  between the G2 and G4 surfaces. Therefore, the advancing and receding water contact angles of the G3 surfaces (**Figure 17b**) were analyzed in the next step. In addition to omniphobic PFDT-modified G3 surfaces ( $\theta_{\text{adv}}(\text{H}_2\text{O}) 124.9 \pm 2.9^\circ$ ,  $\theta_{\text{stat}}(\text{H}_2\text{O}) 116.6 \pm 3.6^\circ$ ,  $\theta_{\text{rec}}(\text{H}_2\text{O}) 111.2 \pm 2.7^\circ$ ), omniphilic cysteamine-modified surface ( $\theta_{\text{adv}}(\text{H}_2\text{O}) 62.1 \pm 3.0^\circ$ ,  $\theta_{\text{stat}}(\text{H}_2\text{O}) 33.0 \pm 3.0^\circ$ ,  $\theta_{\text{rec}}(\text{H}_2\text{O}) 6.7 \pm 2.9^\circ$ ) was investigated, which omniphilic nature was further improved by modifying the G3 surface with thioglycerol, leading to a surface with extremely low  $\theta_{\text{rec}}(\text{H}_2\text{O})$  ( $\theta_{\text{adv}}(\text{H}_2\text{O}) 32.6 \pm 2.2^\circ$ ,  $\theta_{\text{stat}}(\text{H}_2\text{O}) 24.0 \pm 0.3^\circ$ ,  $\theta_{\text{rec}}(\text{H}_2\text{O}) 1.2 \pm 0.6^\circ$ ).

A huge difference of  $123.7^\circ$  between the  $\theta_{\text{adv}}(\text{H}_2\text{O})$  of PFDT-modified G3 surface ( $124.9 \pm 2.9^\circ$ ) and the  $\theta_{\text{rec}}(\text{H}_2\text{O})$  of thioglycerol-modified G3 areas ( $\theta_{\text{rec}}(\text{H}_2\text{O}) 1.2 \pm 0.6^\circ$ ) enabled the generation of stable nanodroplet arrays of high surface tension liquids, such as water ( $\gamma_{\text{lv}} 72.8 \text{ mN m}^{-1}$ ) or cell suspensions. The difference between  $\theta_{\text{adv}}$  of PFDT-modified and  $\theta_{\text{rec}}$  of thioglycerol-modified G3 surface was above  $80 - 100^\circ$  even for organic solvents with a much lower surface tension ( $22.1 - 43.5 \text{ mN m}^{-1}$ ) than water ( $72.8 \text{ mN m}^{-1}$ ) enabling the generation of nanodroplet arrays of low surface tension liquids, including various common organic solvents such as ethanol ( $\gamma_{\text{lv}} 22.1 \text{ mN m}^{-1}$ ), 1-decanol ( $\gamma_{\text{lv}} 28.5 \text{ mN m}^{-1}$ ), dimethylformamide (DMF;  $\gamma_{\text{lv}} 37.1 \text{ mN m}^{-1}$ ), and dimethyl sulfoxide (DMSO;  $\gamma_{\text{lv}} 43.5 \text{ mN m}^{-1}$ ) on the same substrate, as well (**Figure 16d**, **Figure 17c** and **Appendix Table 3**).

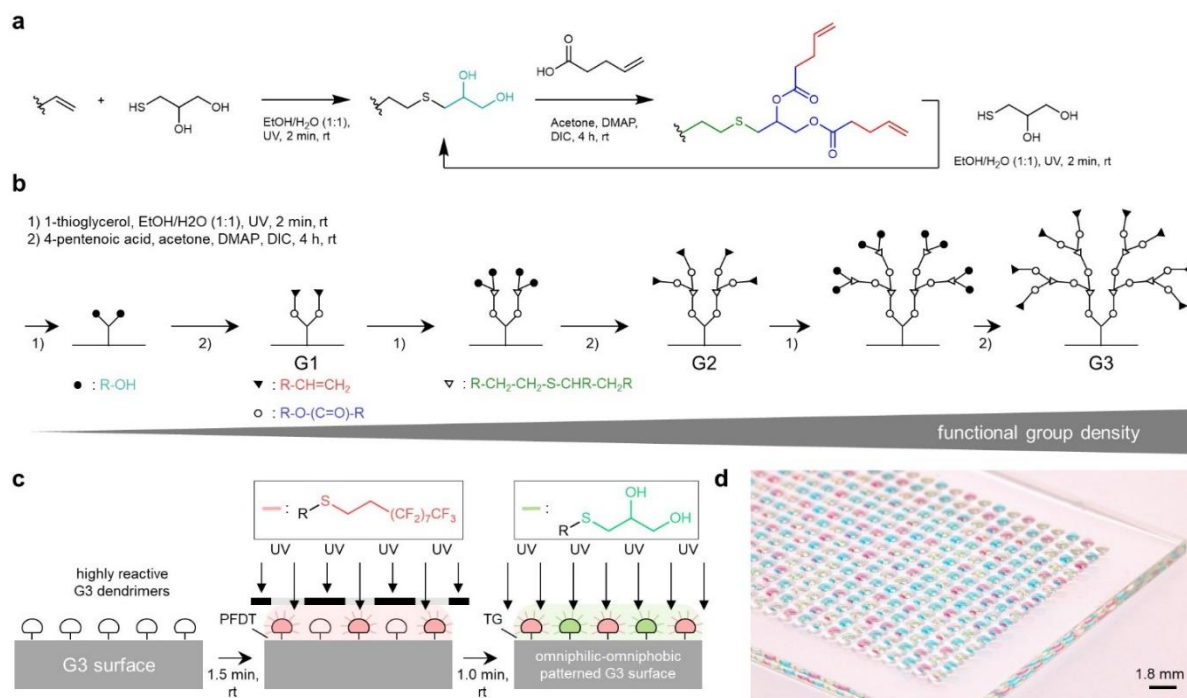


**Figure 16 | Manufacturing of patterned dendrimer slides based on grafted poly(thioether) dendrimers.** (a) The manufacture of dendrimeric slides begins with silanization of a glass slide with triethoxyvinylsilane, followed by a repetitive cycle involving a two-step reaction. An alkene reacts in a photochemical thiol-ene click reaction with 1-thioglycerol followed by an esterification with 4-pentenoic acid. (b) The amount of functional end-groups increases by  $2^n$  ( $n$ : amount of repetitions) for each dendrimer generation with reaching 8 reactive groups for the G3 surface. (d) A highly reactive, alkene-presenting dendrimer surface is patterned using the photochemical thiol-ene reaction. Omniphobic borders are generated by a reaction with perfluorodecanethiol (PFDT), followed by the formation of omniphilic spots by 1-thioglycerol (TG). (e) Photograph of a nanodroplet array of different compounds dissolved in dimethyl sulfoxide on an omniphilic-omniphobic patterned slide. Spot diameter: 900  $\mu\text{m}$ ; omniphilic border width: 225  $\mu\text{m}$ ; droplet volume: 100 nL; scale bar: 1.8 mm. Adapted from Ref<sup>2</sup>.

In the next step, thioglycerol-modified G0–3 surfaces were characterized by atomic force microscopy (AFM). An increase in surface roughness ( $R_q$ ) of  $90 \pm 5$  nm between each dendrimer generation was observed (Figure 17d, Appendix Figure 8 and Appendix Table 4). The thickness of each dendrimeric layer increased by  $1.1 \pm 0.2$  nm per generation, which is consistent with a calculated maximum growth of 1.6 nm in height per dendrimer generation (Figure 17e and Appendix Table 5 and Appendix Table 6). The increase in density of surface functional groups with dendrimer generation was confirmed using time-of-flight secondary ion mass spectrometry (ToF-SIMS) (Figure 18). The decrease in the  $\text{Si}^+$  signal arising from the silicone glass slide measured for each dendrimer generation matched the dendrimer growth. A well-defined chemical pattern was identified for the omniphilic-omniphobic patterned G3 surface

(**Figure 17f**). The lateral resolution between omniphilic patterns and surrounding omniphobic borders was approximately  $8\ \mu\text{m}$  (**Figure 17g**), enabling the generation of patterns with any defined geometry down to the low micrometer range (**Figure 17h**) by photolithography using highly reactive dendrimer substrates.

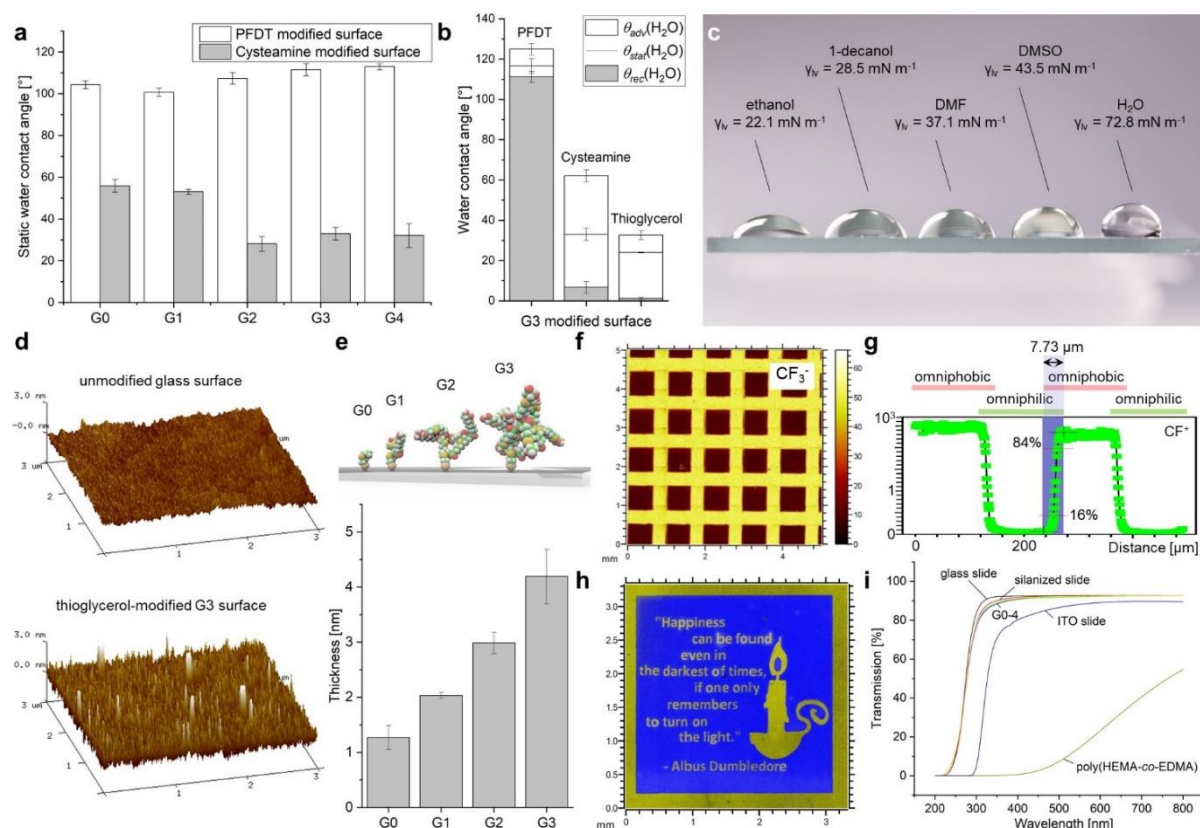


**Figure 17 | Characterization of dendrimer-grafted surfaces.** (a) Static water contact angles of PFDT-modified (omniphobic) and cysteamine-modified (omniphilic) G0–4 surfaces. (b) Advancing, static and receding water contact angles of G3 surface with different functionalization (PFDT, cysteamine and thioglycerol). (c) Photograph of droplets of various low and high surface tension liquids on an omniphilic-omniphobic patterned G3 surface. From left to right: ethanol ( $\gamma_{lv} = 22.1\ \text{mN m}^{-1}$ ), 1-decanol ( $\gamma_{lv} = 28.5\ \text{mN m}^{-1}$ ), dimethyl formamide ( $\gamma_{lv} = 37.1\ \text{mN m}^{-1}$ ), dimethyl sulfoxide ( $\gamma_{lv} = 43.5\ \text{mN m}^{-1}$ ) and water ( $\gamma_{lv} = 72.8\ \text{mN m}^{-1}$ ). (d) AFM images of an unmodified glass surface and a thioglycerol-modified G3 surface. (e) Schematic visualization of thioglycerol-modified G0–3 surfaces and corresponding coating thicknesses measured by AFM. (f) ToF-SIMS analysis of lateral distribution of  $\text{CF}_3^-$  signals showing PFDT-thioglycerol – omniphilic-omniphobic – surface patterning. Spot size:  $700 \times 700\ \mu\text{m}^2$ . (g)  $\text{CF}^+$  line scan perpendicular to a PFDT stripe pattern having  $250\ \mu\text{m}$  pitch, including indication of patterning fidelity by step analysis applying the 84/16% criterion. Lateral resolution of approximately  $8\ \mu\text{m}$  between PFDT- and thioglycerol-modified G3 areas. (h) ToF-SIMS stage scan of a customized pattern. Blue:  $\text{CF}_3^-$ ; yellow: Sum of  $\text{CH}_3\text{O}$ ,  $\text{C}_2\text{H}_5\text{O}$ , and  $\text{C}_4\text{H}_5\text{O}$ . (i) UV-Vis transmission spectra showing optical properties of thioglycerol-modified G0–4 glass surfaces, unmodified glass slide, ITO slide and poly(HEMA-co-EDMA) surface. Data represent mean  $\pm$  standard deviation based on triplicate experiments. Adapted from Ref<sup>2</sup>.

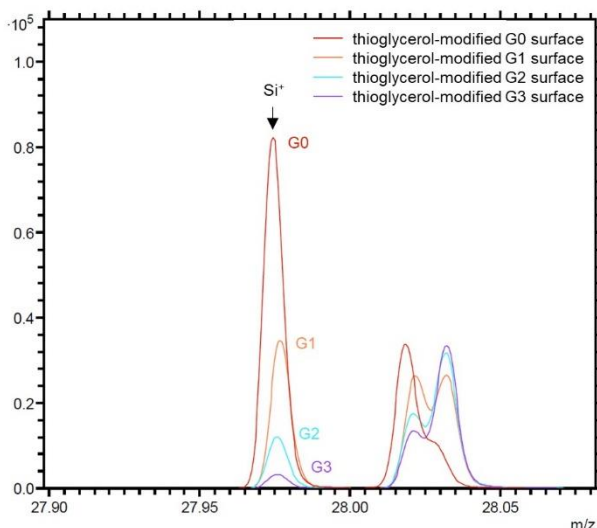


**Figure 18 | Time-of-flight secondary ion mass spectrometry (ToF-SIMS) surface characterization.** ToF-SIMS results comparing the  $\text{Si}^+$  signal intensity in positive polarity mode of thioglycerol-modified G0-3 surfaces. Cited from Ref<sup>2</sup>.

#### 4.1.2 On-chip MALDI-TOF mass spectrometry

Recent developments in on-chip miniaturized and parallelized solution-based synthesis have enabled rapid synthesis of hundreds to thousands of compounds on a single plate, although on-chip characterization of large compound libraries remains a challenge.<sup>1</sup> On-chip high-throughput synthesis requires novel on-chip analytical methods that are compatible with low volume, low concentration, high-density arrays and an on-chip platform. The goal of this research was to accelerate the drug development process by developing a combined platform for on-chip diverse chemical synthesis and straightforward compound characterization on the same plate. MALDI-TOF mass spectrometry (MS) enables characterization of thousands of compounds in seconds with high spatial resolution in the micrometer range using a conductive, flat and arrayed plate format, which is therefore ideal for characterizing large compound libraries.<sup>65-68</sup> In order to enable MALDI-TOF MS on the chemBIOS platform, the developed surface patterning method was applied to a conductive ITO slide (**Figure 20a**). Compounds can be applied or synthesized on-chip in an array format on the conductive slide followed by solvent

evaporation, processing with matrix solution and characterization by MS (**Figure 20a**). The slides remain transparent (**Figure 17i**) and are therefore suitable for use in correlative analysis by optical methods such as microscopy (**Figure 19b**), which is an advantage over standard MALDI stainless steel targets. All MALDI-TOF MS measurements of this study were performed on omniphilic-omniphobic patterned G3 ITO glass slides.

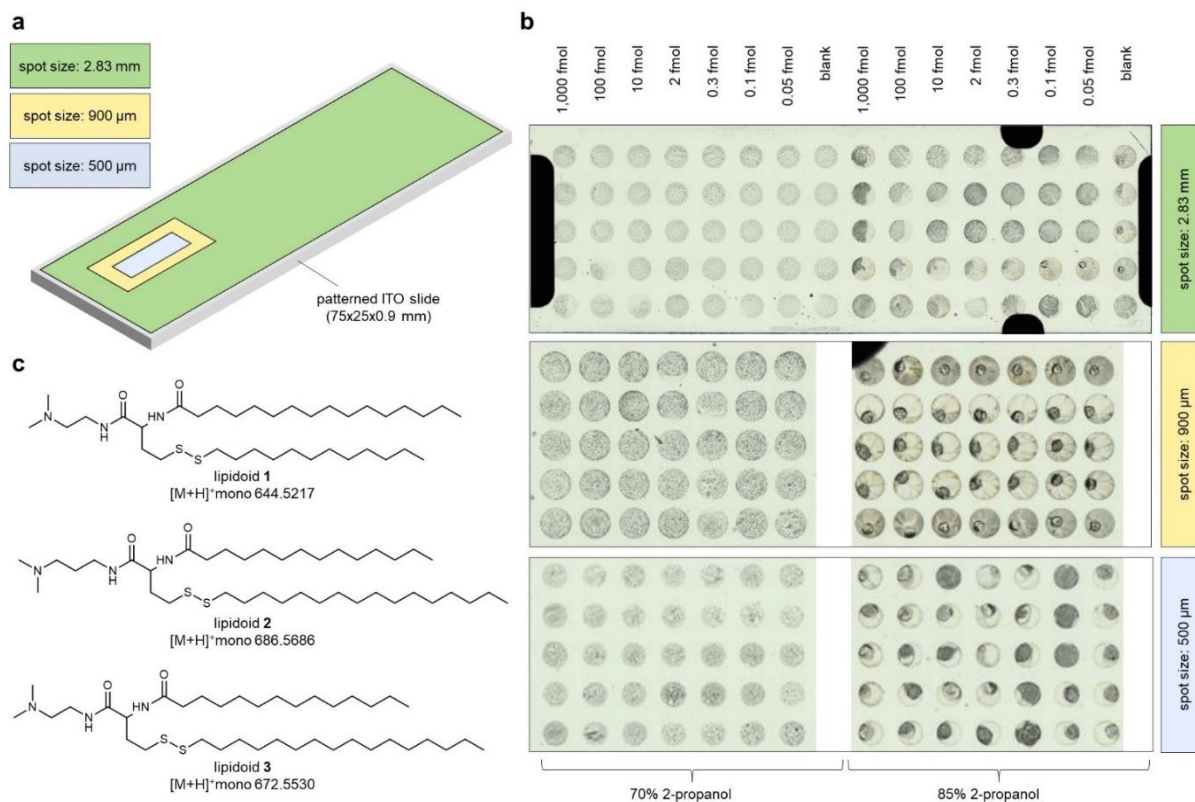


**Figure 19 | On-chip matrix-assisted laser desorption / ionization mass spectrometry (MALDI-TOF MS).** (a) Schematically comparing the required surface area on a omniphilic-omniphobic patterned ITO slide for applying lipidoid **1** in seven different concentrations, each in five replications, and 2x five blank spots (CHCA matrix without sample) on 2.83 mm (spot width: 1.67 mm), 900  $\mu\text{m}$  (spot width: 225  $\mu\text{m}$ ) and 500  $\mu\text{m}$  (spot width: 250  $\mu\text{m}$ ) round spots. (b) Microscopy images of omniphilic-omniphobic patterned ITO slides with different spot sizes (2.83 mm, 900  $\mu\text{m}$  and 500  $\mu\text{m}$  round spots) containing dried lipidoid **1** in different amounts of substance per spot (1,000, 100, 10, 2, 0.3, 0.1 and 0.05 fmol). Matrix solution was applied using 70 and 85% 2-propanol. (c) Chemical structure of lipidoid **1**, **2** and **3**. Cited from Ref<sup>2</sup>.

Miniaturizing chemical synthesis implies reduction of volumes and concentrations, respectively. The first aim of this project part was to investigate the sensitivity of the on-chip MALDI-TOF approach to determine the limits of miniaturization of the chemBIOS platform. Three different lipid-like structures, lipidoids **1** (m/z 643.522), **2** (m/z 686.569) and **3** (m/z

672.553), dissolved in 2-propanol were dispensed to round spots (diameter 2.83 mm; border width: 1.67 mm) to yield a final amount of substance per spot in the range of 0.05 to 1,000 fmol (Figure 19b). The samples were co-crystallized with  $\alpha$ -cyano-4-hydroxycinnamic acid (CHCA) matrix (Figure 20a). All three lipidoids were identified with a sensitivity of 100 fmol substance per spot and an average S/N ratio of  $38 \pm 10$  (Figure 20c and Appendix Table 7). The sensitivity was enhanced by a factor of four (S/N(100 fmol)  $148 \pm 25$ ) by additional on-target washing with the matrix buffer solution (Figure 20c and Figure 21, Appendix Figure 9, and Appendix Table 7).

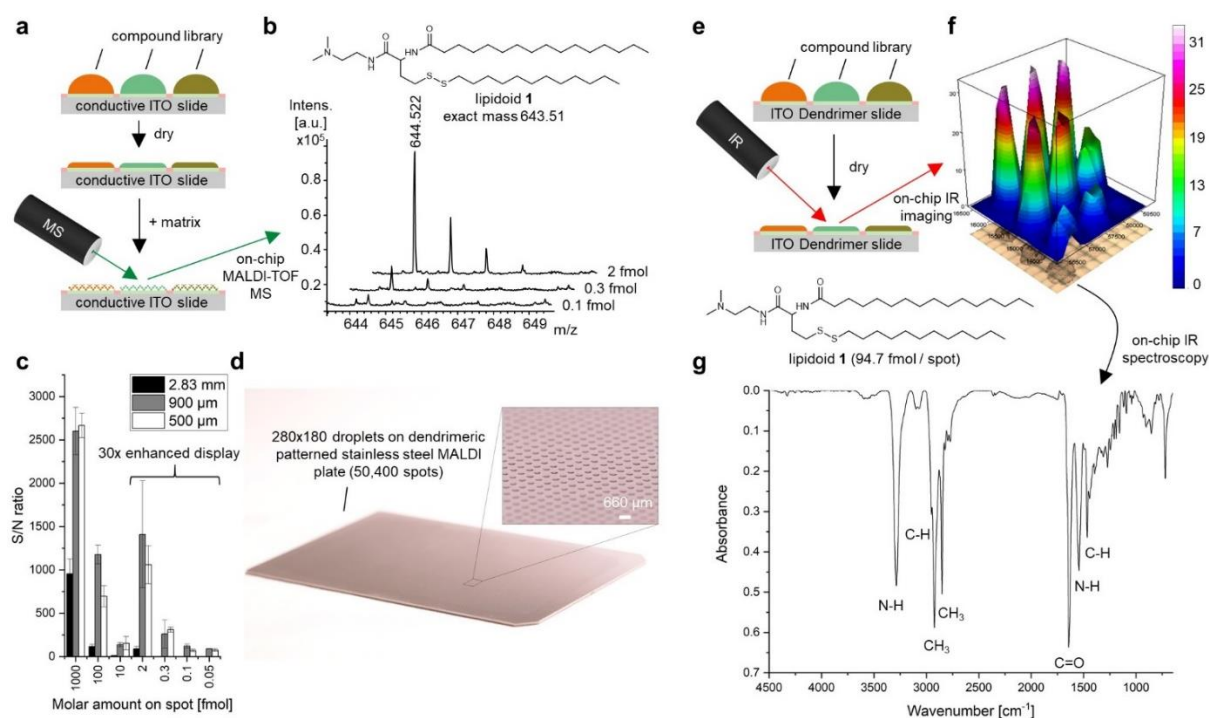


**Figure 20 | Indium-tin oxide substrates enable on-chip characterization by MALDI-TOF mass spectrometry and IR spectroscopy.** (a) Schematic showing the process of on-chip characterization by MALDI-TOF MS. A compound library generated on a conductive, dendrimer-modified and patterned ITO slide can be processed and co-crystallized with matrix solution prior to MALDI-TOF analysis. (b) MALDI-TOF mass spectra of 2, 0.3 and 0.1 fmol per spot of lipidoid 1. Spot diameter: 500  $\mu\text{m}$ ; spot distance: 250  $\mu\text{m}$ . The MALDI-TOF measurements were performed on patterned ITO glass slides. (c) Bar chart showing signal-to-noise (S/N) ratio obtained from on-chip MS analysis of lipidoid 1 in spots of different sizes. Data represent mean  $\pm$  standard deviation based on triplicate experiments. (d) Photograph of a dendrimer-modified and patterned stainless steel plate of microtiter plate size presenting 50,400 individual droplets. Spot size: 330x330  $\mu\text{m}^2$ ; spot distance: 60  $\mu\text{m}$ ; solvent: DMSO. The MALDI stainless steel plate was not used for MS measurements in this study. (e) Schematic diagram showing the process of on-chip characterization by IR spectroscopy. Non-invasive, on-chip characterization of a compound library by IR spectroscopy acquired after evaporation of the solvent. (f) On-chip IR imaging of several spots containing different amounts of lipidoid 1 per spot. (g) IR spectrum of lipidoid 1 (94.7 fmol per spot). Spot diameter: 500  $\mu\text{m}$ ; spot distance: 250  $\mu\text{m}$ . Adapted from Ref<sup>2</sup>.

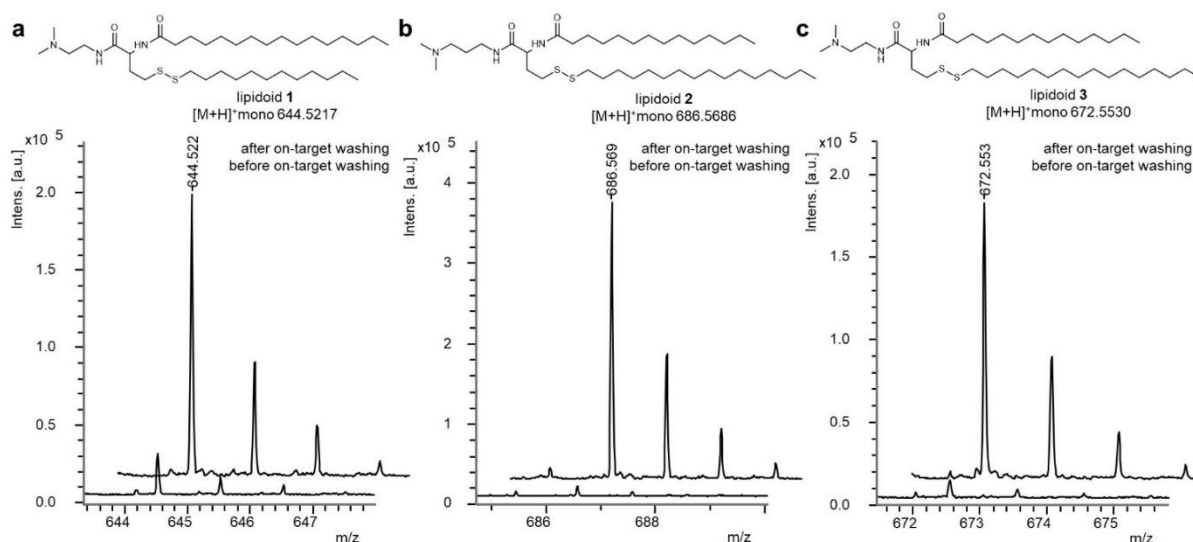


**Figure 21 | Effect of on-target washing on MALDI-TOF MS sensitivity.** MS spectra of (a) lipidoid 1 ( $[M+H]^+$ mono: 644.5217), (b) lipidoid 2 ( $[M+H]^+$ mono: 686.5686) and (c) lipidoid 3 ( $[M+H]^+$ mono: 672.5530) before and after on-target washing. Cited from Ref<sup>2</sup>.

The next aim was to reduce the spot size, thereby increasing the throughput, and to evaluate the effect of the spot size on the sensitivity of the on-chip MALDI-TOF MS method. Solutions of lipidoids 1, 2 and 3 were dispensed to spots with diameters of 900 and 500  $\mu\text{m}$  (border widths: 225 and 250  $\mu\text{m}$ , respectively) to yield an amount of substance between 1,000 and 0.05 fmol per spot. An equivalent amount of CHCA matrix solution was added to all samples. Miniaturization facilitated testing all three compounds on the same slide without altering the sample preparation parameters (**Figure 19a,b**). This improves the ease and comparability of experiments, reduces the cost of materials, and increases the throughput, thus, enhancing workflow efficiency. The limit of detection was 0.1 fmol for each lipidoid, demonstrating a 100-fold increase in the sensitivity of this method (**Figure 20b,c**, **Appendix Figure 9** and **Appendix Table 8**). The average S/N ratio for all 10 fmol samples on 900  $\mu\text{m}$  spots was  $117 \pm 37$ , which was 11 times higher than that of the 2.83 mm spots ( $S/N: 10.3 \pm 0.5$ ) (**Figure 20c**). However, further reduction of the spot diameter to 500  $\mu\text{m}$  did not yield a significant gain in MALDI-TOF sensitivity ( $S/N(10 \text{ fmol}) 208 \pm 92$ ) compared to that for 900  $\mu\text{m}$  spots (**Figure 20c**). Further optimization of critically important parameters (aliquot size, concentration and

matrix solvent composition) might improve the sensitivity for 500  $\mu\text{m}$  spots. Nevertheless, a sensitivity limit of approximately 100 amol allows detection of approximately only 60 million molecules on a single spot. Compared with standard chemical synthesis in flasks, where reactions are performed in the mol range (approximately  $0.6 \times 10^{24}$  molecules) in milliliter-sized volumes, the chemBIOS platform enables not only practicable handling but also analysis of ultra-small amounts of substances (attomole range) and volumes (pico- to nanoliters). Development of this ultra-sensitive chemBIOS platform for miniaturized and parallelized organic synthesis with integrated characterization is an important step toward high-throughput and high-content synthetic and analytical chemistry.

The dendrimeric surface modification and subsequent omniphilic-omniphobic patterning is not limited to silicon oxide or ITO-coated surfaces. Each hydroxy-presenting surface can be functionalized. A microtiter plate-sized MALDI stainless steel plates was modified and patterned accordingly to create a 280x180 droplet array (330x330  $\mu\text{m}^2$  spots separated by 60  $\mu\text{m}$  borders) enabling the application and characterization of 50,400 compounds on a single MALDI plate (**Figure 20d**). This demonstrates the potential for single plate ultra-high-throughput characterization.

#### 4.1.3 On-chip IR spectroscopy

ITO coating shows high transparency (>80% in the visible light region) (**Figure 17i**) and high reflectance (approximately 90% in the far-IR region),<sup>86, 87</sup> properties which are used in biology for conventional light microscopy and IR microscopy to yield additional chemical information.<sup>88, 89</sup> In this research, an on-chip IR spectroscopy approach should be developed that enables mapping of compound libraries and thereby, obtain structural information of compounds on individual spots. An ITO-coated, omniphilic-omniphobic patterned G3 glass slide was used as analytical platform. Lipidoid **1** was applied at different concentrations to

slides with round spots (diameter of 900 or 500  $\mu\text{m}$ ) (**Figure 20e,f**). The lipidoid was identified down to  $0.3 \mu\text{g mm}^{-2}$  (94.7 fmol per 500  $\mu\text{m}$  spot) (**Figure 20f**). The IR spectrum for each compound in the array was used for structural analysis (**Figure 20g**). Similar results were observed for spots with a diameter of 900  $\mu\text{m}$  (**Appendix Figure 10**). On-chip IR imaging in an array format offers the potential for non-destructive and position-coded collection of chemical information and characterization of synthesized compound libraries. Although the sensitivity of on-chip IR spectroscopy is lower than that of MALDI-TOF MS, it remains a highly sensitive and complementary method for on-chip characterization and thus, an essential technique in miniaturized and parallelized chemistry. However, light-scattering between the droplet-air interface limits this approach to measurements in the dried state. Further investigations are needed to develop methods for on-chip IR spectroscopy of liquids, which would be useful for on-chip *in situ* reaction monitoring, as well as a UV-Vis spectroscopy approach, which was developed in the next step of this research.

#### 4.1.4 On-chip UV-Vis spectroscopy

Many methods used for quantitative analysis of different reaction parameters are end-point driven and require numerous repetitions that are time-consuming and labor-intensive. Probe-based spectroscopy enables real-time reaction monitoring,<sup>90</sup> although this requires specialized devices and is limited in terms of miniaturization and parallelization potential. Another aim of this research was to develop a workflow for on-chip solution-based synthetic chemistry that enables miniaturized and parallelized high-throughput experimentation as well as *in situ* reaction monitoring. It was hypothesized that due to excellent optical properties, the chemBIOS platform should be compatible with on-chip UV-Vis monitoring. The transmittance of thioglycerol-modified G0–4 surfaces exceeded 90% in the visible region and 80% in the ultraviolet (UV-A/-B) region (**Figure 17i**).

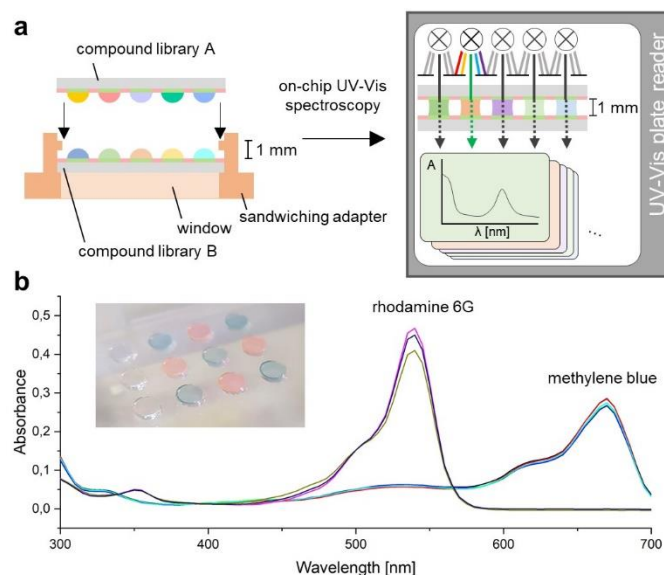


**Figure 22 | On-chip characterization by UV-Vis spectroscopy.** (a) Schematic diagram showing the process of on-chip UV-Vis spectroscopy. Droplets can be trapped between two slides sandwiched within a distance of 1 mm in a 3D-printed adapter. On-chip UV-Vis absorbance can be measured using commercial plate readers. (b) On-chip measured UV-Vis spectra of rhodamine 6G and methylene blue applied on-chip in a checkerboard pattern and trapped between two dendrimer slides. Cited from Ref<sup>2</sup>.

A slide adapter was designed and 3D-printed that meets the standards of ANSI/SLAS 1-2004 through ANSI/SLAS 4-2004, which is therefore compatible with standard UV-Vis plate readers (**Figure 23**). Droplet arrays can be trapped between two sandwiched patterned slides within a fixed distance (1 mm), allowing analysis of individual droplets using a plate reader (Fig. 5a). In a proof-of-principle study, droplets of rhodamine 6G and methylene blue were applied in a checkerboard pattern on slide A, inserted into the slide adapter, and sandwiched and trapped with slide B before UV-Vis absorbance measurement. Spatially separated UV-Vis spectra were observed from each individual droplet (**Figure 22b**).

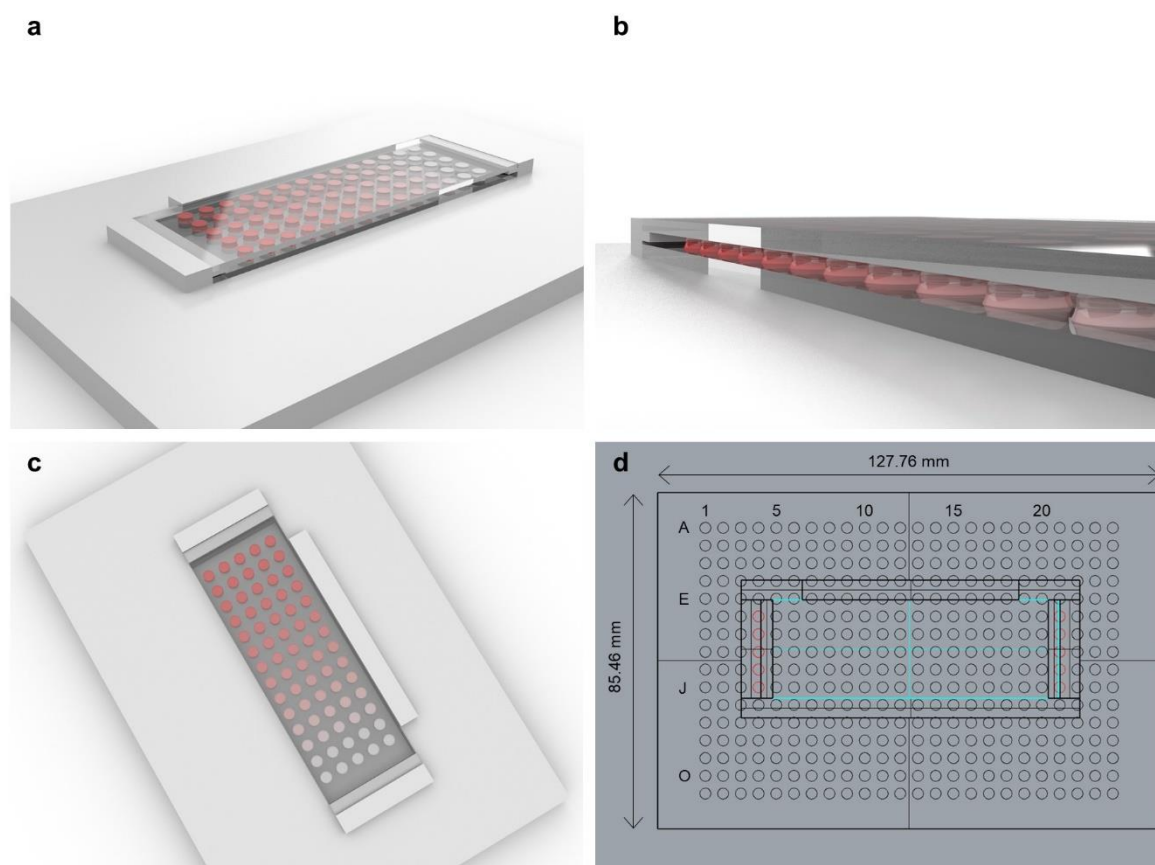


**Figure 23 | 3D-printed sandwiching adapter for UV-Vis measurements.** (a-c) Concept art images of a droplet array trapped between two dendrimer-modified, omniphilic-omniphobic patterned slides. The slides were sandwiched using a 3D-printed adapter. (d) Schematically showing the top view of the sandwiching adapter with overlaid 384-well microtiter plate patterns. Blue: omniphilic-omniphobic patterned glass slide. Adapted from Ref<sup>2</sup>.

Next, the on-chip UV-Vis approach was applied to investigate and optimize an one-pot synthesis of lipid-like structures.<sup>81</sup> The three-component reaction is initiated by an amine-based ring-opening of a thiolactone followed by a disulfide exchange with a pyridyl disulfide (**Figure 24a**). The resulting UV-absorbing by-product, 2-thiopyridone ( $\lambda_{\text{max}}$  365 nm) was used as an indicator to monitor the reaction progress. Two compound libraries were prepared: (i) slide A contained four blocks of amine A1 (1, 10, 50 and 100 eq.) in triplicate, and (ii) slide B contained mixtures with different ratios of thiolactone T14 to pyridyl disulfide PY12 (1:5, 1:3, 1:1, 3:1 and 5:1; eq./eq.) applied in rows perpendicular to the blocks of slide A (**Figure 24b**). Both slides were sandwiched in the slide adapter, thus, simultaneously initiating all reactions under equal environmental conditions (**Figure 24c**). All reactions were carried out at room

temperature and monitored by UV-Vis spectrometry at 5-min intervals over a period of 70 h. Twenty different reaction parameters, each in triplicates, were analyzed resulting in 50,400 data points within a single experiment (**Figure 24d**). The reaction half-life ( $t_{1/2}$ ) decreased as the thiolactone component ratio increased and decreased more rapidly as the amine concentration increased. This indicated that the first step of the reaction (ring-opening of the thiolactone by the amine) is rapid and the following disulfide exchange is rate-determining in the one-pot synthesis.

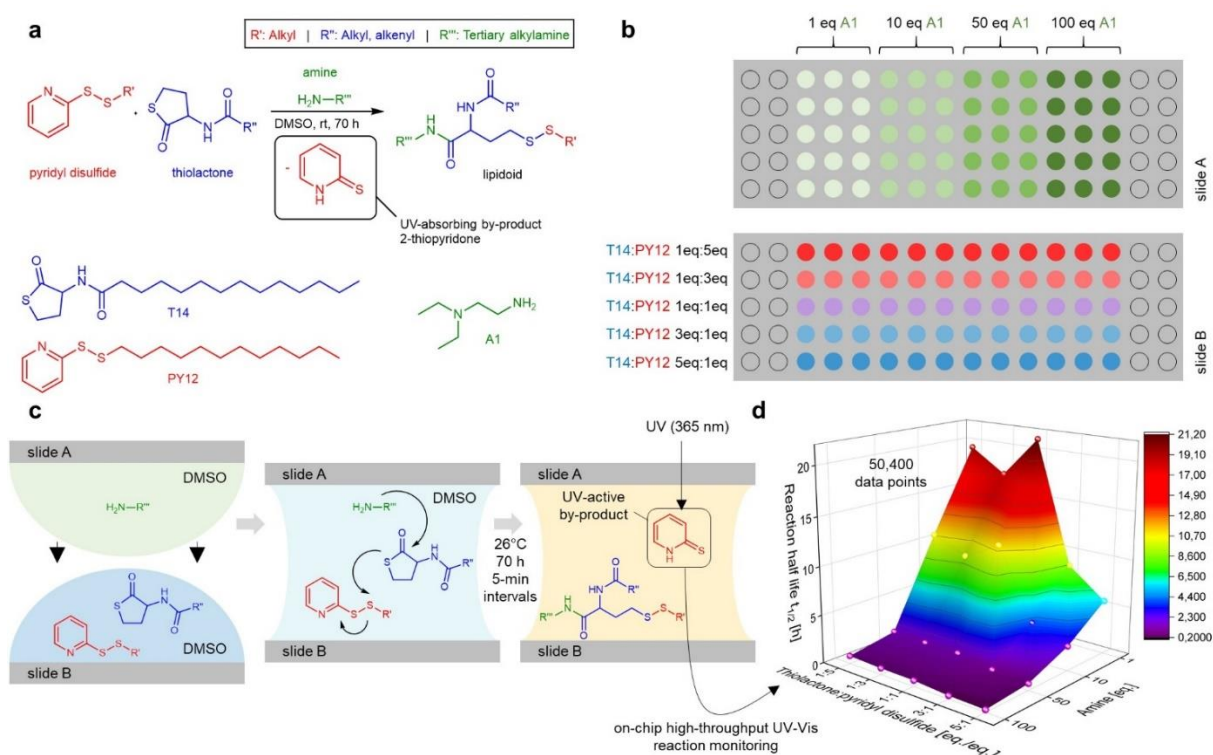


**Figure 24 | On-chip high-throughput reaction monitoring.** (a) Reaction scheme of the three-component lipidoid synthesis based on amine A1, thiolactone T14 and pyridyl disulfide PY12. (b) Array layout for parallel on-chip synthesis of sixty lipidoids. Amine A1 was dispensed in different concentrations column-by-column on slide A. Mixtures with different ratios of thiolactone T14 to pyridyl disulfide PY12 were dispensed row-by-row on slide B. All reactions were simultaneously initiated by sandwiching both slide. (c) Schematic visualization of the sandwiching process and resulting on-chip solution-based reaction. The UV-absorbing by-product 2-thiopyridone allowed on-chip *in situ* reaction monitoring by UV-Vis spectroscopy. (d) 3D plotting of the reaction half-life ( $t_{1/2}$  for each reaction condition) demonstrates the power of such a high-throughput system to investigate reaction parameters and mechanistical aspects of the reaction. Cited from Ref<sup>2</sup>.

#### 4.1.5 Biological compatibility

The ultimate goal of accelerating the screening of novel compound libraries and increasing throughput is to unify chemical processes, including compound library synthesis, characterization, and biological high-throughput screening.<sup>1, 91</sup> However, the lack of compatibility between the diverse platforms and infrastructures (flasks, tubes, bottles, polystyrene plates, plastic/glass pipettes, syringes, filters, etc.) of these methods with different material properties (chemical resistance vs. biological compatibility) limits the applicability of high-throughput approaches and slows drug and biotechnological development. Besides compatibility with a variety of organic and aqueous solutions, the platform must be cell compatible.

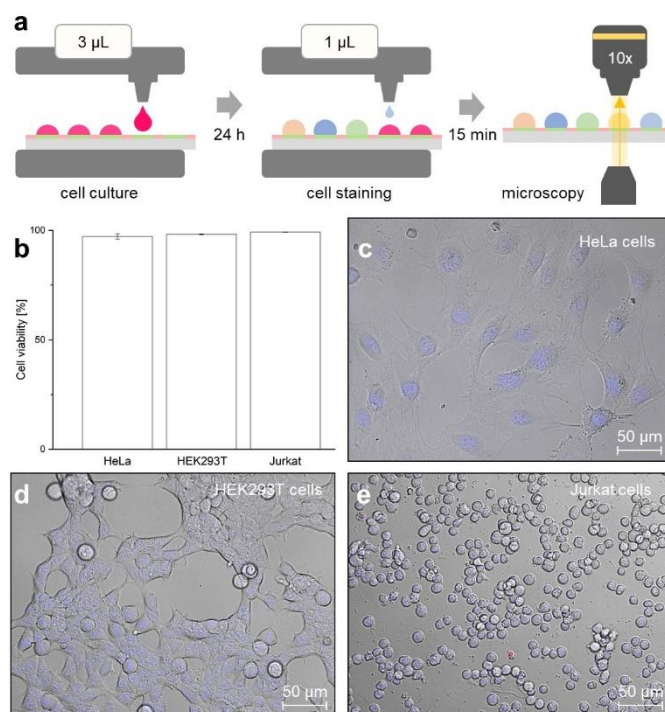


**Figure 25 | On-chip cell culture using dendrimer slides.** (a) Schematic diagram showing the process of cell culture and viability tests. Cell suspensions were dispensed to each spot of a dendrimer-based chemBIOS slide and cultured at 37°C under 5% CO<sub>2</sub> for 24 h. Cell staining solution (Hoechst 33342 and propidium iodide) was dispensed to individual droplets and cell viability was evaluated by fluorescence microscopy. (b) Cell viability of on-chip cultured HeLa, HEK293T and Jurkat cells. (c) Microscopy images of stained (Hoechst 33342 and propidium iodide) HeLa, (d) HEK293T, and (e) Jurkat cells. Scale bar: 50 µm. Data represent mean ± standard deviation based on triplicate experiments. Adapted from Ref<sup>2</sup>.

The viability of three cell lines (HeLa, HEK293T and Jurkat) dispensed to each spot of a thioglycerol-modified G3 slide and cultured for 24 h was evaluated by fluorescence microscopy after life/death staining (**Figure 25**). The viability of each cell line exceeded 97%, demonstrating the compatibility of this platform for biological studies, such as cell screening.

#### 4.1.6 Conclusions

In this research, a covalent surface modification was developed based on a surface-grafted poly(thioether) dendrimer resulting in an increase in the density of surface presentation of reactive alkene groups (**Figure 16a,b**). Further photochemical patterning of this surface with 1-thioglycerol and 1*H*,1*H*,2*H*,2*H*-perfluorodecanethiol (PFDT) sequentially through a photomask resulted in the formation of omniphilic spots surrounded by omniphobic borders (**Figure 16c**). The high contrast of advancing and receding contact angles of both aqueous and organic liquids between the omniphilic and omniphobic patterns, presenting high contrast in surface wettability, enabled the formation of nanodroplet arrays (1–3,000 nL depending on the spot size) of both low surface tension (organic) and high surface tension (aqueous) liquids (**Figure 16d** and **Figure 17b,c**). This offers the potential for use in a broad range of chemical, analytical and biological applications, such as miniaturized and parallelized on-chip solution-based synthesis or on-chip biological screening (chemBIOS). Each nanodroplet forms a distinct vessel that can be used individually. Chemicals, agents or cell suspension can be added at any time during an assay or whole compound libraries can be combined within a single step (**Figure 22a** and **Figure 25a**). In this study, the sensitivity of various analytical methods was analyzed and their compatibility for on-chip compound characterization was evaluated. An additional indium-tin oxide (ITO) coating made the chemBIOS surface conductive and, thus, compatible with matrix-assisted laser desorption/ionization mass spectrometry (MALDI-TOF MS) (**Figure 20a**). The sensitivity of the on-chip MALDI-TOF MS approach was investigated using an

exemplar lipid-like compound class. An increased sensitivity down to the attomole range per spot was observed for spots of increasingly smaller size (diameter 900 and 500  $\mu\text{m}$ ) (**Figure 20b,c**). The synergy between higher sensitivity for smaller spot sizes enable miniaturization and, thus, parallelization of the on-chip approach. Fabrication of a nanodroplet array in the microtiter plate size containing 50,400 droplets (330x330  $\mu\text{m}^2$  spots; border width: 60  $\mu\text{m}$ ) demonstrated the possibility for ultra-high-throughput screening (**Figure 20d**). Furthermore, the infrared-reflective properties of the ITO coating enabled IR imaging of a compound array and on-chip IR spectroscopy of selected compound spots (**Figure 20e–g**). The sensitivity of the IR spectroscopy approach was found to be 95 fmol per 500  $\mu\text{m}$  spot (**Figure 20g**). The dendrimer-modified chemBIOS platform showed excellent transparency in the visible and UV region (**Figure 17i**) and is therefore compatible with optical analysis methods, enabling on-chip high-throughput *in situ* reaction monitoring using UV-Vis spectroscopy (**Figure 22** and **Figure 24**). An on-chip, solution-based, combinatorial three-component reaction was carried out to demonstrate the possibility of an on-chip chemical reaction optimization with on-line reaction progress monitoring. 60 reactions were simultaneously screened resulting in the generation of 50,400 data points within a single experiment (**Figure 24**). The results provided insights into the reaction mechanism that could be used for reaction optimization. ChemBIOS is compatible with various adherent and suspension cell lines (HeLa, HEK293T and Jurkat) and is therefore suitable for high-throughput cell-based screening (**Figure 25**). ChemBIOS combines on-chip high-throughput chemical synthesis, high-content reaction monitoring, highly sensitive compound characterization and biological screening and, thus, unifies all areas of early-stage drug discovery.

## Chapter 5 Summary and Future Perspectives

The current state of the art drug discovery process is very length, expensive and inefficient. Several thousand compounds must be synthesized, isolated, characterized, screened and tested on biological systems which requires decades of effort and billions of dollars. Most of the compounds fail on their way to approval due to low biological activity or unexpected side effects making the entire process barely affordable, especially for rare diseases and almost impossible for smaller companies. From a technical point of view, early-stage drug discovery process suffers from three main challenges:

- (i) the lack of miniaturized and parallelized methodologies for high-throughput, solution-based organic synthesis
- (ii) spatial and temporal separation of chemical compound library synthesis (including lack of miniaturized high-throughput purification methods) from biological screening
- (iii) missing analytical methods for high-throughput characterization of low volumes / concentrations

In this PhD thesis, a chemBIOS workflow was developed to address and solve the aforementioned challenges.

### 5.1 Miniaturization and Parallelization of Solution-Based Organic Synthesis

Miniaturization and parallelization of chemical synthesis is important to reduce the material consumption of valuable chemicals and to accelerate the compound library synthesis for subsequent drug screenings. Microtiter plates have been used for parallel solution-based

synthesis, thereby reducing chemical consumption from milliliter (in flasks) to microliter (per well) range.<sup>63, 64</sup> However, the physicochemical properties of polystyrene microtiter plates limit the chemical compatibility (chemical durability and harsh reaction conditions) and further miniaturization (increasing capillary forces in smaller wells) which is needed to reach the nanoliter and sub-nanomole range, respectively, for subsequent biological screenings. Compartmentalization is important in chemical synthesis to avoid cross-contamination and undesired side reactions. In chapter 3 of this PhD thesis, highly dense droplet arrays have been used to demonstrate solution-based high-throughput organic synthesis. The surface of a standard glass slide was silanized with chloro(dimethyl)vinylsilane, followed by an UV-induced thiol-ene patterning resulting in the formation of oleophilic spots (functionalized with cysteamine hydrochloride) and surrounding oleophobic, organic-liquid-impermeable borders (functionalized with perfluorodecanethiol (PFDT)). Due to the flat substrate no capillary forces are exerted. High contrast in wettability between the oleophilic-oleophobic patterns enabled the generation of droplet arrays and, thus, highly dense compartmentalization. Droplet arrays with droplet volumes in the lower nanoliter up to the microliter range could be generated depending on the spot geometry. Defined and spatially separated droplets formed small vessels that could be used for miniaturized, solution-based synthesis. In chapter 3, a combinatorial three-component reaction is demonstrated to synthesize a library of lipid-like compounds (lipidoids) on-chip. The reaction was adapted from a bulk synthesis that was described by Molla et al.<sup>81</sup> Molla synthesized 288 structurally diverse lipidoids, which required about 2.3 L of total solvents (4 mL solvent per reaction + 4 mL solvent per purification).<sup>81</sup> Considering a working day of 8 h, a reaction time of 3 h and a purification time of 30 mins per lipidoid,<sup>81</sup> 10 compounds of this library could be synthesized per day. This means, the generation of the entire lipidoid library using standard chemical techniques would take 29 working days under optimal conditions. Using the on-chip chemBIOS approach, which was developed in this PhD thesis, the entire library of 288 lipidoids could be synthesized simultaneously in 3 h requiring only

about 0.000864 L (3  $\mu$ L per reaction) of organic solvents. This corresponds to an acceleration of the entire effort by the factor of about 80 and a reduction of material consumption by the factor of about 2.7 thousand which clearly demonstrates the potential of the chemBIOS approach to accelerate and enhance the efficiency of compound library synthesis in early drug discovery.

On-chip purification is one of the most critical challenges of the demonstrated chemBIOS approach for miniaturized and parallelized, solution-based synthesis. A proof-of-principle liquid-liquid extraction was developed and described in chapter 3 of this PhD thesis to demonstrate the possibility of on-chip purification. Mixtures of Nile red and methylene blue dissolved in octanol droplets could be separated simultaneously by sandwiching the droplet array of the mixtures with another droplet array with water droplets resulting in the formation of an interface between the organic and aqueous droplets and extraction of methylene blue from the organic into the aqueous droplets. Potential purification techniques such as product precipitation, crystallization, evaporation of by-products or parallelized liquid chromatography are currently being under investigation and promise to expand the spectrum of on-chip high-throughput purification methods. Precise handling of low volumes in sub-nanoliter range place special demands on automated liquid handling systems and evaporation of volatile solvents (especially of low volume droplets) is critical and must be addressed in future to expand the reaction toolbox. Miniaturized and parallelized synthesis could sustainably change conventional chemistry, minimize the material consumption, accelerate the throughput and, thereby, reduce the entire costs of drug discovery.

## 5.2 Marrying Chemistry with Biology

The current state of the art of the drug discovery pipeline is clearly separated into a chemical part, where compound libraries are synthesized, isolated and characterized, and a biological part, where those compound libraries are screened for biological activity. Slow individual synthesis, large reaction batches (compared to the actual amount of substance required for biological screenings), lots of transfer steps (between individual platforms, labs and companies) and infrastructure incompatibility elaborate the entire workflow and make it highly inefficient and expensive. There is a clear need in modern interdisciplinary research and development to unify chemical and biological realms. A major goal of this PhD thesis was to develop a chemBIOS workflow that enables straightforward combination of chemical synthesis, characterization and biological readout (**Figure 26**). Miniaturized and parallelized solution-based organic synthesis with low-surface tension liquids (LSTL) can be done in droplet arrays generated on oleophilic-oleophobic patterned glass slides (LSTL slides) (chapter 3). Cell-based screening requires the handling of aqueous, high-surface tension liquids (HSTL) that are incompatible with the surface properties of LSTL slides (low contrast between advancing water contact angle of the oleophobic barriers ( $\theta_{adv}$   $110.5 \pm 1.2^\circ$ ) and the receding water contact angle of the oleophilic spots ( $\theta_{rec}$   $33.7 \pm 0.8^\circ$ )).<sup>1</sup> Thus, biological screening requires another surface with a larger contrast between advancing and receding water contact angle to handle high-surface tension liquids such as water or cell suspension. An additional surface-grafted poly(2-hydroxyethyl methacrylate-*co*-ethylene dimethacrylate) (HEMA-*co*-EDMA) polymer made the surface of a standard glass slide rough and porous. Subsequent esterification with 4-pentynoic acid, followed by patterning the surface via an UV-induced thiol-yne reaction resulted in the formation of hydrophilic spots (functionalized with 2-mercaptoethanol) which are surrounded by hydrophobic borders (functionalized with 1*H*,1*H*,2*H*,2*H*-perfluorodecanethiol (PFDT)) (HSTL slides).<sup>45, 46</sup> Droplet arrays of high-surface tension liquids can be generated due to the

high contrast of advancing water contact angle of the hydrophobic barriers ( $\theta_{adv}$   $159.3 \pm 6.8^\circ$ ) and receding water contact angle of the hydrophilic spots ( $\theta_{rec}$   $6.3 \pm 1.1^\circ$ ). The flat and opened infrastructure of both type of slides (LSTL for synthesis and HSTL for screening) enabled dispensing liquids to individual spots and droplets or even single-step merging of entire droplet arrays by sandwiching two slides. In chapter 3, a method was developed for straight-forward biological screening of an on-chip synthesized lipidoid compound library. The synthesis of 75 structurally diverse lipidoids was performed as described above on LSTL slides. The lipidoid library was sandwiched with an HSTL slide presenting an array of aqueous buffer droplets containing green fluorescent protein (GFP)-plasmids which resulted in the transfer of the lipidoids from the LSTL slide to the water-compatible HSTL slide (**Figure 26a**). At the same time, mixing the amphiphilic lipidoids with aqueous buffer droplets resulted in the formation of a lipoplex library on the HSTL slide. The lipoplex library was screened in an on-chip reverse transfection cell screening (**Figure 26a**). The entire chemBIOS workflow starting from the compound library synthesis of 75 lipidoids to cell-based transfection screening took only 3 days and about 1 mL of total solvents and solutions which clearly demonstrated the potential of accelerating and improving the drug discovery process (chapter 3).

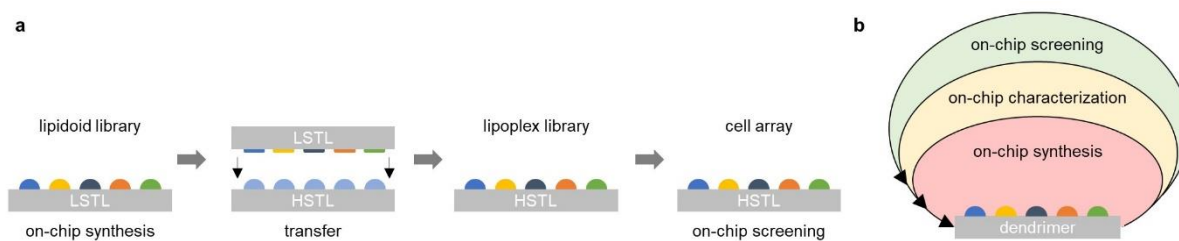


**Figure 26 | chemBIOS workflow.** (a) Schematically describing an exemplary chemBIOS workflow for discovering novel transfection agents consisting of on-chip synthesis of a lipidoid library on a low-surface tension liquids (LSTL) slide, followed by transferring the lipidoid library on an high-surface tension liquids (HSTL) slide by sandwiching, resulting in the formation of a lipoplex library and subsequently on-chip reverse transfection cell screening. (b) Schematically describing the chemBIOS workflow using a dendrimer-modified, omniphilic-omniphobic patterned slide that enables the handling of both low-surface tension liquids (organic solvents) and high-surface tension liquids (aqueous solutions / cell suspension) on the same substrate. On-chip synthesis, characterization and screening can be performed using one slide without the need of additional transfer steps. Adapted from Ref<sup>2</sup>.

The porous HEMA-*co*-EDMA polymer of an HSTL slide enabled the formation of high-surface tension liquid droplet arrays, but it also made the entire surface oleophilic and, thus, incompatible for generating droplet arrays of low-surface tension liquids (most organic solvents). Due to the incompatibility to handle both organic and aqueous solutions the chemBIOS workflow still required two different types of platforms (LSTL and HSTL slides) and an additional transfer step between the compound library synthesis and subsequent cell-based screening. Therefore, another goal of this PhD research was to develop a surface modification that enables the handling of both low-surface tension liquids (organic solvents) and high-surface tension liquids (aqueous solutions) on the same substrate (chapter 4). A poly(thioether) dendrimer was covalently grafted on the surface of a standard glass slide resulting in an increase in the density of surface-immobilized reactive alkene groups, followed by an UV-induced patterning of the surface via thiol-ene click reactions. The contrast of advancing contact angle of PFDT-modified barriers and receding contact angle of thioglycerol-modified spots was  $123.7^\circ$  for water and above  $80\text{-}100^\circ$  for organic solvents. The omniphilic-omniphobic surface patterning enabled the generation of droplet arrays with both organic solvents and aqueous solutions and, thus, is ideally suited to marry chemistry with biology (**Figure 26b**).

### 5.3 On-Chip High-Throughput Characterization

Existing analytical techniques have been developed to be compatible with standard chemistry which is done in flasks requiring relatively large volumes and amounts of substances. Thus, most characterization technologies are not compatible with on-chip high-throughput character, low volumes and low concentrations. However, compound characterization and reaction monitoring are essential in drug discovery to obtain as much information as possible on the

investigated substances and to enable an assessment and prediction of the compound's interaction with biochemical / biological systems, thereby reducing the failure rate in later stages. In chapter 4 of this PhD thesis, the compatibility of several characterization techniques was evaluated to be used in the chemBIOS workflow, and methods were developed to enable fast on-chip compound library characterization. Suitable analytical techniques for high-throughput characterization must be highly sensitive, fast, parallelizable and automatable, and compatible with the substrate (glass slide). Slides functionalized with the dendrimer modification method showed excellent optical properties. The transmittance of the thioglycerol-modified omniphilic spots exceeded 90% in the visible and 80% in the ultraviolet region, thus, behave similar to unmodified glass, making the substrate compatible with optical analysis methods such as UV-Vis spectroscopy. UV-Vis spectroscopy is particularly interesting for monitoring reactions where an UV-absorbing product is released, or the absorption maxima change during the reaction. The application of the Beer-Lambert law ( $A = \epsilon * c * d$ ;  $A$ : absorbance;  $\epsilon$ : extinction coefficient [ $M^{-1} \text{ cm}^{-1}$ ];  $c$ : concentration [ $M$ ];  $d$ : path length [ $\text{cm}$ ]) enables quantitative analysis of the reaction progress and estimation of the yield. In chapter 4 of this PhD thesis, a slide adapter was designed which could be used to trap a droplet array at a fixed distance between two omniphilic-omniphobic patterned slides, thus, defining the path length  $d$ . The adapter was designed to meet the ANSI/SLAS standards, thus, the system is compatible with most common plate readers enabling automated readout. The on-chip UV-Vis approach was used to investigate and optimize the lipidoid reaction as an exemplary miniaturized, solution-based on-chip synthesis. The high-throughput character of the chemBIOS platform enabled screening of twenty different reaction parameters (different concentrations and ratios of the precursor compounds), each in triplicate, in a single experimental workflow resulting in the generation of 50,400 data points. The generated data enabled investigation of the reaction mechanism and allowed to optimize the reaction conditions. This clearly demonstrated the power of on-chip high-throughput characterization

and potential usage for monitoring the synthesis of large compound libraries. Readout based on optical spectroscopy offers potential applications in high-throughput absorbance, colorimetric, fluorescence and luminescence assays. The standardized format of the chemBIOS platform and corresponding adapters make it possible to implement this technology into existing workflows and devices.

Modern high-efficient laser technology enables ultra-fast, label-free characterization of large compound libraries by MALDI-TOF mass spectrometry and would therefore be an important addition to the chemBIOS workflow. However, MALDI-TOF MS requires a conductive substrate. In chapter 4, a method was developed to produce such a conductive substrate by modifying an indium-tin oxide (ITO) coated glass slide via the dendrimer surface modification protocol, subsequently followed by omniphilic-omniphobic surface patterning. Thus, large compound libraries could be synthesized or applied on-chip followed by MALDI-TOF MS characterization (chapter 4). The sensitivity of this MALDI-TOF approach was systematically investigated by applying lipidoids in different concentrations to the patterned, conductive glass substrate. The lipidoids could be identified down to the attomole range per round omniphilic spot with a diameter of 500  $\mu\text{m}$  (omniphobic borders width: 250  $\mu\text{m}$ ). A total amount of 1,152 compounds could be characterized using one standard glass slide (75x25 mm) with the aforementioned pattern dimensions.

High reflectance of light in the far-IR region is another property of the ITO coating, which enabled the development of an additional on-chip characterization method by IR spectroscopy. An on-chip lipidoid compound library could be characterized by IR microscopy and the obtained chemical information of each individual spot could be converted into IR spectra and used for chemical structure analysis (chapter 4). The sensitivity of this on-chip IR spectroscopy approach was in the femtomole range per 500  $\mu\text{m}$  spot making IR spectroscopy a suitable analysis technique for miniaturized and parallelized on-chip synthesis.

In summary, in this PhD thesis, a dendrimer-based omniphilic-omniphobic patterned platform was developed that enabled the generation of both organic and aqueous, highly dense droplet arrays, which could be used for chemical, analytical and biological applications. A chemBIOS workflow was developed that enabled miniaturized and parallelized solution-based synthesis of large compound libraries and monitoring of the micro- to nanoliter-sized reactions by on-chip UV-Vis spectroscopy, followed by on-chip characterization of the compound library (in particular by MALDI-TOF MS and IR spectroscopy), post-synthetic processing of the library, and subsequently biological cell-based screening. Thus, chemBIOS covered and unified all parts of early drug discovery and showed the potential to accelerate the process of drug development in pharmaceutical and biotechnological research.



## Chapter 6 Materials and Methods<sup>6</sup>

### 6.1 Experimental Details to Chapter 3

#### Preparation of High Surface Tension Liquids (HSTL) slides

Activation of the surface of standard microscope glass slides (25x75x1 mm, width x length x thickness, Schröder Spezialglas) was done by immersing them in 1 M NaOH (Carl Roth) for 1 h, followed by neutralization in 1 M HCl (Merck) for 30 min. Activated glass slides were modified with 20% v/v solution of 3-(trimethoxysilyl)propyl methacrylate (Sigma-Aldrich) in ethanol (Merck) for 40 min at room temperature. Next, 35  $\mu$ L of polymerization mixture (24 wt% 2-hydroxyethyl methacrylate (Sigma), 16 wt% ethylene dimethacrylate (Sigma-Aldrich), 12 wt% 1-decanol (Merck), 48 wt% cyclohexanol (Sigma), and 0.4 wt% 2,2-dimethoxy-2-phenylacetophenone (Sigma-Aldrich)) was applied onto a fluorinated glass slide and covered with a modified glass slide to introduce a polymer layer. Polymerization was carried out by UV irradiation (OAI model 30) with 4 mW cm<sup>-2</sup> intensity and 260 nm wavelength for 15 min. Fluorination of glass slides was done by incubating slides in a closed vacuumed desiccator in the presence of an open vial containing 30  $\mu$ L of trichloro(1*H*, 1*H*, 2*H*, 2*H*-perfluorooctyl)silane (Sigma) for 16 h under 50 mbar vacuum. Modification of the polymer layer was done by incubating the slides in modification mixture (56 mg of 4-(dimethylamino)pyridine (Novabiochem), 111.6 mg 4-pentynoic acid (Sigma-

---

<sup>6</sup> This chapter is adapted from the following publications which are licensed under a Creative Commons Attribution 4.0 International License (CC BY 4.0; <https://creativecommons.org/licenses/by/4.0/>):

Benz, Maximilian, Molla, M.R., Böser, A., Rosenfeld, A. & Levkin, P.A. Marrying chemistry with biology by combining on-chip solution-based combinatorial synthesis and cellular screening. *Nature Communications* **10**, 2879 (2019).

Benz, Maximilian, Asperger, A., Hamester, M., Welle, A., Heissler, S. & Levkin, P.A. A combined high-throughput and high-content platform for unified on-chip synthesis, characterization and biological screening. Manuscript accepted.

Aldrich) and 180  $\mu\text{L}$  *N,N'*-diisopropylcarbodiimine (Alfa Aesar) in 45 mL dichloromethane (Merck) for 4 h while stirring at room temperature. The surface was patterned by first generating the hydrophobic borders. 300  $\mu\text{L}$  of a 8% v/v solution of 1*H*, 1*H*, 2*H*, 2*H*-perfluorodecanethiol (Sigma-Aldrich) in acetone (Merck) was applied onto the polymer surface and the thiol-yne click reaction carried out by irradiating the slide through a photomask (Rose Fotomasken) with 260 nm UV light (OAI model 30) at 4  $\text{mW cm}^{-2}$  intensity for 1 min. Round hydrophilic spots with a diameter of 2.83 mm were formed by applying 200  $\mu\text{L}$  of a 10% v/v  $\beta$ -mercaptoethanol (Alfa Aesar) solution in 1:1 water:ethanol onto the patterned surface and irradiating the slide with 260 nm, UV light (OAI model 30) at 4  $\text{mW cm}^{-2}$  intensity for 1 min.

### **Preparation of Low Surface Tension Liquids (LSTL) slides**

An activated glass slide was modified by inverting into modification mixture (0.8 mL triethylamine (VWR), 50 mg of 4-dimethylaminopyridine (Merck), 0.2 mL chloro(dimethyl)vinyl silane (Sigma-Aldrich) in 49 mL dichloromethane) for 2 min under stirring at room temperature. The slide surface was patterned by first applying 300  $\mu\text{L}$  of a 20% v/v solution of 1*H*, 1*H*, 2*H*, 2*H*-perfluorodecanethiol (Sigma-Aldrich) in acetone onto the modified surface and carried out a thiol-ene photoclick reaction by irradiating the slide through a photomask (Rose Fotomasken) with 260 nm UV light (OAI model 30) at 4  $\text{mW cm}^{-2}$  intensity for 1 min to create omniphobic borders. Round omniphilic spots with a diameter of 2.83 mm were formed by applying 200  $\mu\text{L}$  of a 10 wt% cysteamine hydrochloride (Alfa Aesar) solution in 1:2 water:ethanol onto the patterned surface and irradiating the slide with 260 nm, UV light (OAI model 30) at 4  $\text{mW cm}^{-2}$  intensity for 1 min.

## Surface characterization

The surface of each slide was characterized by contact angle measurements using Drop Shape Analyzer DSA25 (Krüss). For HSTL slides the advancing, static and receding contact angle were measured by applying 40  $\mu\text{L}$  (speed  $0.3 \mu\text{L s}^{-1}$ ) deionized water on hydrophobic and hydrophilic surfaces. For LSTL slides the advancing, static and receding contact angle were measured by applying 40  $\mu\text{L}$  (speed  $0.3 \mu\text{L s}^{-1}$ ) DMSO (VWR) and deionized water on omniphobic and omniphilic surfaces.

## Synthesis and characterization of a lipidoid library

On-chip synthetic procedure was performed in a standard chemistry fume hood. Stock solutions of different amines (Sigma-Aldrich) 1:24 v/v in DMSO and stock solutions of mixtures of different thiolactones ( $1.67 \text{ mg mL}^{-1}$ ) and pyridyl disulfides ( $1.75 \text{ mg mL}^{-1}$ ) in DMSO were prepared. The on-chip synthesis of a lipidoid library via the rolling droplet method was performed by applying 3  $\mu\text{L}$  of different amine solutions to each spot column-by-column in an array on a LSTL slide A and 3  $\mu\text{L}$  of different mixtures of thiolactones and pyridyl disulfides to each spot row-by-row in an array on a LSTL slide B perpendicular to the columns on slide A by discontinuous dewetting. The reaction was carried out by sandwiching both slides using an alignment frame for 2 h at room temperature. For characterization, the synthesized library was stamped onto a MALDI plate (Applied Biosystems). Solvent was evaporated in a desiccator under vacuum. Mass spectrum of each raw product was measured by 4800 MALDI TOF/TOF Analyzer (Applied Biosystems) using a  $10 \text{ mg mL}^{-1}$   $\alpha$ -cyano-4-hydroxycinnamic acid (Alfa Aesar) solution of 1:1 acetonitrile:water containing 0.1% v/v trifluoroacetic acid (Merck). Further characterization by UV-Vis was done by Lambda 35 UV-Vis spectrometer (PerkinElmer). On-chip ATR-IR spectroscopy was done by Tensor 27 (Bruker). For

characterization by  $^1\text{H-NMR}$  spectroscopy (Bruker 400 MHz), one lipidoid was synthesized on a whole array as described above, then evaporated the solvent and washed down the raw product with dichloromethane (Merck) from LSTL slides into a round bottle flask. The solvent was evaporated under high vacuum and dissolved the raw product in deuterated chloroform (VWR) for analysis.

The on-chip synthesis of a lipidoid library via the printing method was performed by printing 1.5  $\mu\text{L}$  of different amine solutions to each spot column-by-column in an array on a LSTL slide A using a non-contact liquid dispenser (I-DOT; Dispendix). Next, 1.5  $\mu\text{L}$  of different mixtures of thiolactones and pyridyl disulfides were printed to each spot row-by-row on the same array perpendicular to the columns of previously printed amine solutions using a non-contact liquid dispenser (I-DOT; Dispendix). The reaction was carried for 2 h at room temperature before the solvent was evaporated in a desiccator under vacuum.

This synthesizing method was used for all experiments except the characterization experiments by MALDI TOF MS.

### **On-chip purification**

On-chip purification was performed in a standard chemistry fume hood.

3  $\mu\text{L}$  per spot of a mixture of Nile red (2.1  $\text{mg mL}^{-1}$ ; Sigma-Aldrich) and methylene blue hydrate (2.7  $\text{mg mL}^{-1}$ ; Thermo Fisher) in 1-octanol (Sigma-Aldrich) were applied to several spots of an LSTL slide. 5  $\mu\text{L}$  per spot of deionized water was applied to several spots on a HSTL slide corresponding to the spots on the LSTL slide. Both slides were sandwiched for 10 min and then separated. 1  $\mu\text{L}$  of both the organic and aqueous phase of each spot were diluted separately in 1 mL acetonitrile for characterization by a Lambda 35 UV-Vis

spectrometer (PerkinElmer). 1  $\mu\text{L}$  of both the organic and aqueous phase of each spot were diluted separately in 50  $\mu\text{L}$  acetonitrile for characterization by an Agilent 1100 LC/MS (Agilent Technologies).

### **Preparation and characterization of liposomes/lipoplexes**

On-chip preparation of liposomes/lipoplexes was performed under sterile conditions using a standard sterile clean bench.

A sterile filtered (0.45  $\mu\text{m}$  sterile syringe filter) transfection solution of 0.04% w/v gelatin (Sigma-Aldrich), 3.4% w/v sucrose (Sigma-Aldrich), 0.002% w/v human fibronectin (Sigma-Aldrich) and – in case of formation of lipoplexes – plasmid DNA (75  $\text{ng } \mu\text{L}^{-1}$  of pCS2+-GFP) in aqueous sodium acetate buffer (50 mM, pH 5, Merck) was prepared for post-synthetic processing of the lipidoid library to form a liposome or lipoplex library. 4.5  $\mu\text{L}$  of prepared transfection mixture was printed onto each spot of a HSTL slide C by a non-contact liquid dispenser (I-DOT; Dispendix), followed by sandwiching the slide C with dried LSTL lipidoid library slide A for 1.5 h at 50  $^{\circ}\text{C}$  using an alignment frame to form liposomes or lipoplexes. For characterization via dynamic light scattering (DLS) and zeta potential, 2  $\mu\text{L}$  of processed liposome/lipoplex solution of a single spot were pipetted into 1 mL sodium acetate buffer (50 mM, pH 5) for analysis by Malvern Zetasizer Nano ZS (Malvern). Data were collected at 25  $^{\circ}\text{C}$  with an acquisition time of 15 s and the diameter size was averaged over 3x15 runs.

ScreenFect dilution buffer containing 0.04% w/v gelatin, 3.4% w/v sucrose and 0.002% w/v human fibronectin was used as positive control. In a PCR tube 12.6  $\mu\text{L}$  of ScreenFect A (Screenfect) was mixed into 23.7  $\mu\text{L}$  ScreenFect dilution buffer and incubated for 5 min at room temperature. In a separate PCR tube, 1.67  $\mu\text{L}$  plasmid DNA (2.05  $\mu\text{g } \mu\text{L}^{-1}$  of pCS2+-GFP) was

mixed into 6.93  $\mu\text{L}$  ScreenFect dilution buffer. The ScreenFect A solution was mixed into the plasmid DNA and incubated for 20 min at room temperature. Thus, led into to formation of lipoplexes with the same calculated pDNA to lipid ratio of the synthesized samples of  $0.273 \mu\text{g} \mu\text{L}^{-1}$ . 4.5  $\mu\text{L}$  of prepared ScreenFect solution was applied to unused spots of the library array after processing of the lipidoid library to liposome/lipoplex library. For negative control 4.5  $\mu\text{L}$  buffer solution was applied to unused spots after liposome/lipoplex formation. Furthermore, spots without any compounds were screened as negative control. All spots were dried under atmosphere pressure and sterile conditions for 2 h before continuing with cell seeding for reverse transfection.

### **Reverse transfection and cell culture**

On-chip reverse transfection was performed under sterile conditions using a standard sterile clean bench.

The transfection experiments were performed using human embryonic kidney (293T (ATCC® CRL3216™)) cells provided by the Institute of Toxicology and Genetics (ITG) at Karlsruhe Institute of Technology (KIT). Cells were cultured in Dulbecco's Modified Eagle Medium (Life Technologies) supplemented with 10% v/v fetal bovine serum (PAA Laboratories) and 1% v/v penicillin-streptomycin (Life Technologies) in a humid incubator at 37 °C with 5% CO<sub>2</sub>, and were passaged every 2-3 days. Cells were washed with phosphate buffered saline (Life Technologies), detached with 0.25% trypsin/EDTA solution (Life Technologies) and counted by Countess Automated Cell Counter (Life Technologies). Cells were stained by mixing 10  $\mu\text{L}$  cell suspension into 10  $\mu\text{L}$  trypan blue stain solution (Life Technologies). 10  $\mu\text{L}$  of this mixture were applied into cell counting chamber (Life Technologies) for counting the cells.

Culture medium for on-chip transfection experiments contained 15% v/v fetal bovine serum and 1% v/v PenStrep. After detachment of the cells from culture plate, the cells were centrifuged at 1200 x g for 3 min at room temperature to form a cell bead. The old medium was removed and then the cells resuspended again with freshly prepared medium. Cell suspension containing 60 000 cells mL<sup>-1</sup> were prepared and 5 µL of that suspension was printed onto each spot of the lipoplex slide C using a non-contact liquid dispenser (I-DOT; Dispindex). The seeded cell slide was placed in a Petri dish whose lid had been prepared with a 7 mL phosphate buffer saline soaked sterile tissue (Clean and Clever) – to prevent media evaporation of the droplets. The whole Petri dish was then placed in a humid incubator for 48 h at 37 °C with 5% CO<sub>2</sub>. After culturing the cells for reverse transfection, cells were stained by dispensing 1 µL staining solution onto each spot of the array containing Hoechst 33342 in dilution of 1:900 (10 mg mL<sup>-1</sup>, Invitrogen) to stain the nucleus and propidium iodide in a dilution of 1:1350 (1.00 mg mL<sup>-1</sup>, (Invitrogen)) to stain dead cells.

### **Image acquisition and analysis**

Fluorescence images were obtained using the microscope Keyence BZ9000 (Keyence). The exposure times were set and kept the same for all experiments and repetitions. Images were taken using a 10x objective.

Objective: Nikon x10 Plan Apo NA 0.45/4.00 mm

Resolution: 8-bit

Format: 1360x1024px

Light source: mercury vapor lamp

Cells were counted by adjusting the threshold of the 8-bit images and then using the Analyze Particles function in ImageJ. The ration of transfected cells in GFP channel and total number of cells in Hoechst channel revealed transfection efficiency of a sample. All date sets were depicted as mean  $\pm$  standard deviation. At least three replicates per slide and at least three slides were tested for each transfection sample.

## 6.2 Experimental Details to Chapter 4

### **Preparation of dendrimeric-modified and patterned surfaces**

The surface of standard microscope glass slides (25x75x1 mm, width x length x thickness, Schott Nexterion) was cleaned for 10 min using an UVO-Cleaner 42-220 (Jelight) and then silanized in the gas phase using 400  $\mu$ L triethoxyvinylsilane (Sigma–Aldrich) at 80°C for 20 h. The slide was washed with acetone and ethanol and then dried by compressed air. The solid-phase synthesis of one dendrimer generation consisted of two steps: (i) 300  $\mu$ L 10% (v/v) 1-thioglycerol (Sigma–Aldrich) in ethanol/water (1:1, v/v, Merck Millipore) containing 1 wt% 2,2-dimethoxy-2-phenylacetophenone (DMPA, Sigma–Aldrich) was applied to the alkene-presenting surface. A thiol-ene click reaction was carried out by irradiating the surface with 260 nm UV light (OAI model 30) at 3 mW cm<sup>-2</sup> intensity for 1.5 min. The slide was washed with ethanol and then dried by compressed air. (ii) Esterification of the hydroxy-presenting surface was performed by incubating the slides in esterification mixture (112 mg 4-(dimethylamino)pyridine (Novabiochem), 250  $\mu$ L pentenoic acid (Sigma–Aldrich) and 180  $\mu$ L *N,N'*-diisopropylcarbodiimine (Alfa Aesar) in 90 mL acetone (Merck Millipore)) for 4 h while shaking at room temperature. The surface was patterned by first applying 300  $\mu$ L 10% (v/v) 1*H*,1*H*,2*H*,2*H*-perfluorodecanethiol (Sigma–Aldrich) in acetone containing 1 wt% DMPA (Sigma–Aldrich). The thiol-ene photoclick reaction was carried out by irradiating the surface

through a photomask (Rose Fotomasken) with 260 nm UV light (OAI model 30) at  $3 \text{ mW cm}^{-2}$  intensity for 1 min to create omniphobic borders. The slide was washed with acetone and then dried by compressed air. Omniphilic spots were formed by applying 300  $\mu\text{L}$  10% (v/v) 1-thioglycerol (Sigma–Aldrich) in ethanol/water (1:1, v/v, Merck Millipore) containing 1 wt% DMPA (Sigma–Aldrich) onto the patterned surface and irradiating the surface with 260 nm UV light (OAI model 30) at  $3 \text{ mW cm}^{-2}$  intensity for 1.5 min. The slide was washed with ethanol and then dried by compressed air.

Dendrimeric modification and omniphilic-omniphobic patterning of ITO-coated slides were carried out using the protocol described above using commercial ITO slides (Bruker). Modification and patterning of stainless steel HTS sample plates (Bruker) was conducted accordingly.

### **Surface characterization**

Advancing, static, receding contact and sliding angles were measured using a Drop Shape Analyzer DSA25 (Krüss). Solvents were purchased without further purification from Merck Millipore.

AFM was performed using a Dimension Icon AFM (Bruker) under the following conditions: tapping mode, scan rate 1 Hz, sample/line 512 and AFM Cantilevers HQ:NSC15/AI BS-15 (Innovative Solutions Bulgaria Ltd.). Thickness was measured by scratching the surface with a tweezer and analyzing the depth of the scratch compared to the intact dendrimer surface surrounding the scratch.

ToF-SIMS experiments were performed by Dr. Alexander Welle (IFG, KIT) using a ToF-SIMS-5 instrument (ION-TOF GmbH) equipped with a Bi cluster primary ion source and a reflectron-type ToF analyzer. UHV base pressure during analysis was  $< 2 \times 10^{-9}$  mbar. For high

mass resolution the Bi source was operated in a bunched mode providing short  $\text{Bi}_3^+$  primary ion pulses at 25 keV energy, a lateral resolution of approx. 4  $\mu\text{m}$ , and a target current of 0.4 pA. The short pulse length of 1 ns allowed for high mass resolution (8500  $\text{m}/\Delta\text{m}$ ). For large fields of view (Fig. 3(f) and Fig. 3(h)) the primary beam and the sample stage were rastered, for high lateral resolution (Fig. 3(g)) the primary gun was operated in a non-bunched mode combined with delayed extraction. The lateral resolution of the instrument is better than 0.5  $\mu\text{m}$  in this case. For charge compensation on glass slide without ITO an electron flood gun (21 eV) was applied and the reflectron tuned accordingly. Primary ion dose was held below the static limit of  $1 \times 10^{11}$  ions  $\text{cm}^{-2}$ , spectra were mass calibrated on the omnipresent signals  $\text{C}^+$ ,  $\text{CH}^+$ ,  $\text{CH}_3^+$ ,  $\text{C}_2\text{H}^+$  or  $\text{C}^-$ ,  $\text{CH}^-$ ,  $\text{CH}_2^-$   $\text{C}_2^-$ .

Transparency analysis was performed using a Lambda 35 UV-Vis spectrometer (PerkinElmer) equipped with a solid sample holder (PerkinElmer).

### **On-chip MALDI-TOF mass spectrometry**

Three lipidoids 1, 2 and 3 ( $\geq 5$  replicates per slide) were tested on 2.83 mm, 900  $\mu\text{m}$  and 500  $\mu\text{m}$  spots of dendrimer-modified and patterned ITO slides by MALDI-TOF MS. Using a non-contact liquid dispenser (I-DOT, Dispendix) at a dispensing pressure set to 50–75 LA, sample solution was dispensed as follows: 500 nL per 2.83 mm spot, 50 nL per 900  $\mu\text{m}$  spot and 31 nL per 500  $\mu\text{m}$  spot. Therefore, stock solutions of 1  $\mu\text{mol mL}^{-1}$  of all three samples in 2-propanol (Merck Millipore) were prepared. Aliquots were prepared out of this stock solution to reach an absolute amount of substance per spot of 1,000 fmol, 100 fmol, 10 fmol, 2 fmol, 0.3 fmol, 0.1 fmol and 0.05 fmol. The solvent was evaporated at room conditions after dispensing. Subsequently, 500 nL 5  $\text{mg mL}^{-1}$   $\alpha$ -cyano-4-hydroxycinnamic acid (CHCA; Alfa Aesar) dissolved in 70% 2-propanol with 0.1% trifluoroacetic acid (Sigma–Aldrich) and 1 mM

ammonium dihydrogen phosphate (Merck Millipore) as additives were dispensed to each sample of a 2.83 mm spot, resulting in a matrix concentration of 397 ng mm<sup>-2</sup>. Similarly, 50 nL (resulting in 391 ng mm<sup>-2</sup>) and 31 nL (resulting in 388 ng mm<sup>-2</sup>) of a 2.5 mg mL<sup>-1</sup> CHCA solution with the same solvent and additive conditions were printed onto each sample of a 900 μm and 500 μm spot. The solvent was dried at room conditions. MALDI-TOF MS measurements were performed by Dr. Arndt Asperger (Bruker Corporation, Bremen) in reflector positive operation mode using a Bruker rapifleX MALDI-TOF/TOF system. The laser repetition rate was 10,000 Hz and 10,000 laser shots were accumulated per spectrum from 50 different raster positions within a sample spot. Spectra were acquired from three replicate spots for each sample dilution level. Peak areas/intensities and S/N ratios were determined using a centroid peak finder.

An additional on-target washing of prepared spots was carried out by applying 2 μL washing buffer (1 mM NH<sub>4</sub>H<sub>2</sub>PO<sub>4</sub>, 0.1% TFA in water) to each 2.83 mm spot. The solution was removed after an incubation time of 1 s. On-target washing of slides with 900 and 500 μm spots as performed by immersing the slide into a washing buffer reservoir for 1 s. The slide was then dried at room temperature.

### **On-chip IR spectroscopy**

Aliquots of lipidoid 1 (40.4 mg mL<sup>-1</sup>) dissolved in toluene (Merck Millipore) were dispensed to dendrimer-modified and patterned ITO slides (30 nL per 500 μm spot; 100 nL per 900 μm spot) using a non-contact liquid dispenser (I-DOT, Dispendix) at the following final concentrations: 6.3 μg mm<sup>-2</sup>, 3.2 μg mm<sup>-2</sup>, 0.7 μg mm<sup>-2</sup> and 0.3 μg mm<sup>-2</sup> per 900 μm spot (dispensed volume: 100 nL), and 6.1 μg mm<sup>-2</sup>, 4.2 μg mm<sup>-2</sup>, 3.0 μg mm<sup>-2</sup>, 2.4 μg mm<sup>-2</sup>, 1.8 μg mm<sup>-2</sup>, 1.2 μg mm<sup>-2</sup>, 0.6 μg mm<sup>-2</sup>, 0.3 μg mm<sup>-2</sup> and 0.06 μg mm<sup>-2</sup> per 500 μm spot

(dispensed volume: 30 nL). The solvent was allowed to dry at room conditions. Fourier-transform IR microscopy and spectroscopy were performed by Stefan Heissler (IFG, KIT) using a Bruker HYPERION 3000 microscope equipped with a 15x IR objective. The spectral range of 4500-650  $\text{cm}^{-1}$  was recorded with a spectral resolution of 4  $\text{cm}^{-1}$  (32 scans per spot) using gold substrate as a reference.

### **On-chip UV-Vis spectroscopy**

Aliquots (5  $\mu\text{L}$ ) of 36  $\mu\text{M}$  methylene blue (Sigma–Aldrich) and 40  $\mu\text{M}$  rhodamine 6G (Sigma–Aldrich) dissolved in DMSO were dispensed to a G3 dendrimer slide (spot diameter: 2.83 mm, spot pitch: 1.67 mm) in a checkerboard pattern using a non-contact liquid dispenser (I-DOT, Dispendix). The slide was sandwiched with another G3 dendrimer slide in a 3D-printed sandwiching adapter with a distance of 1 mm between both slides. The UV-Vis absorbance spectrum of each spot was measured by a BioTek Synergy H1 plate reader within a spectral range of 300–700 nm and a spectral resolution of 5 nm.

### **On-chip UV-Vis high-content screening**

The following stock solutions were prepared: thiolactone T14 in DMSO (Sigma–Aldrich) at 1.31  $\text{mg mL}^{-1}$ , 3.93  $\text{mg mL}^{-1}$  and 6.55  $\text{mg mL}^{-1}$ ; pyridyl disulfide PY12 in DMSO at 1.25  $\text{mg mL}^{-1}$ , 3.74  $\text{mg mL}^{-1}$  and 6.23  $\text{mg mL}^{-1}$ ; amine A1 in DMSO at 0.47  $\text{mg mL}^{-1}$  (1 eq.), 4.65  $\text{mg mL}^{-1}$  (10 eq.), 23.25  $\text{mg mL}^{-1}$  (50 eq.) and 46.50  $\text{mg mL}^{-1}$  (100 eq.). Aliquots of T14 and PY12 were mixed 1:1 (v/v) resulting in the following mixtures: 1:5, 1:3, 1:1, 1:3 and 1:5 eq./eq. (T14:PY12). Subsequently, 1.5  $\mu\text{L}$  of T14 and PY12 solutions was dispensed row-by-row on a G3 dendrimer glass slide A (spot diameter: 2.83 mm, spot pitch: 1.67 mm) and 1.5  $\mu\text{L}$  of each amine solution was dispensed in four replicates column-by-column on a G3

dendrimer glass slide B (spot diameter: 2.83 mm, spot pitch: 1.67 mm). Slides A and B were sandwiched in an 3D-printed sandwiching adapter within a distance of 1 mm. On-chip UV-Vis absorbance of each spot was measured at 365 nm at 5-min intervals over a period of 70 h using a BioTek Synergy H1 UV-Vis plate reader set to 26°C.

### **Cell culture**

Human cervical carcinoma HeLa cells (ATCC® CCL-2™) and human embryonic kidney (293T cells (ATCC® CRL3216™) provided by the Institute of Biological and Chemical Systems (IBCS) at Karlsruhe Institute of Technology (KIT) were cultured in Dulbecco's Modified Eagle Medium (Life Technologies) supplemented with 10% v/v fetal bovine serum (PAA Laboratories) and 1% v/v penicillin-streptomycin (Life Technologies) in a humidified incubator at 37°C under 5% CO<sub>2</sub>. Cells were washed with phosphate buffered saline (Life Technologies) and detached with 0.25% trypsin/EDTA solution (Life Technologies). Jurkat T lymphocytes (ATCC® TIB-152™) provided by IBCS were maintained in RPMI-1640 cell culture medium (Life Technologies) supplemented with 10% heat-inactivated fetal bovine serum (PAA Laboratories). Cells were passaged every 2–3 days. Cells were counted using the trypan blue staining (Life Technologies) method in a cell counting chamber (Life Technologies) and analyzed by a Countess Automated Cell Counter (Life Technologies). The cells were centrifuged at 1,200 xg for 3 min at room temperature and the cell pellet was resuspended in freshly prepared medium. Cell suspensions containing 50,000 cells mL<sup>-1</sup> were prepared and 3 µL was dispensed onto each spot of a dendrimeric-modified slide (spot diameter: 2.83 mm, spot pitch: 1.67 mm) using a non-contact liquid dispenser (I-DOT, Dispendix). The slide was placed into a Petri dish fitted with sterile tissue (Clean and Clever) soaked with 7 mL PBS to prevent evaporation of the droplets and incubated in a humidified incubator for 24 h at 37°C under 5% CO<sub>2</sub>. The cells were then stained by adding 1 µL Hoechst 33342 staining solution

(1:900 v/v (10 mg mL<sup>-1</sup>, Invitrogen) and 1:1,350 v/v propidium iodide (1.00 mg mL<sup>-1</sup>, Invitrogen).

### **Image acquisition and analysis**

Fluorescence images were obtained using a BZ9000 (Keyence) fluorescence microscope. The exposure times were set and kept the same for all experiments and repetitions.

Objectives: Nikon x10 PlanApo NA 0.45/4.00 mm; Nikon x20 PlanFluor ELWD DM 0.45/8.10 mm; Nikon x40 PlanFluor ELWD DM 0.60/3.70 mm

Resolution: 8-bit

Format: 1360 x 1024 px

Light source: mercury vapor lamp

Cells were counted by adjusting the threshold of the 8-bit images and then using the Analyze Particle function in ImageJ. Cell viability was calculated as the live cell:total cell ratio. All datasets were depicted as mean  $\pm$  standard deviation. At least three replicates per cell line and per slide were tested for each viability screening.

## References

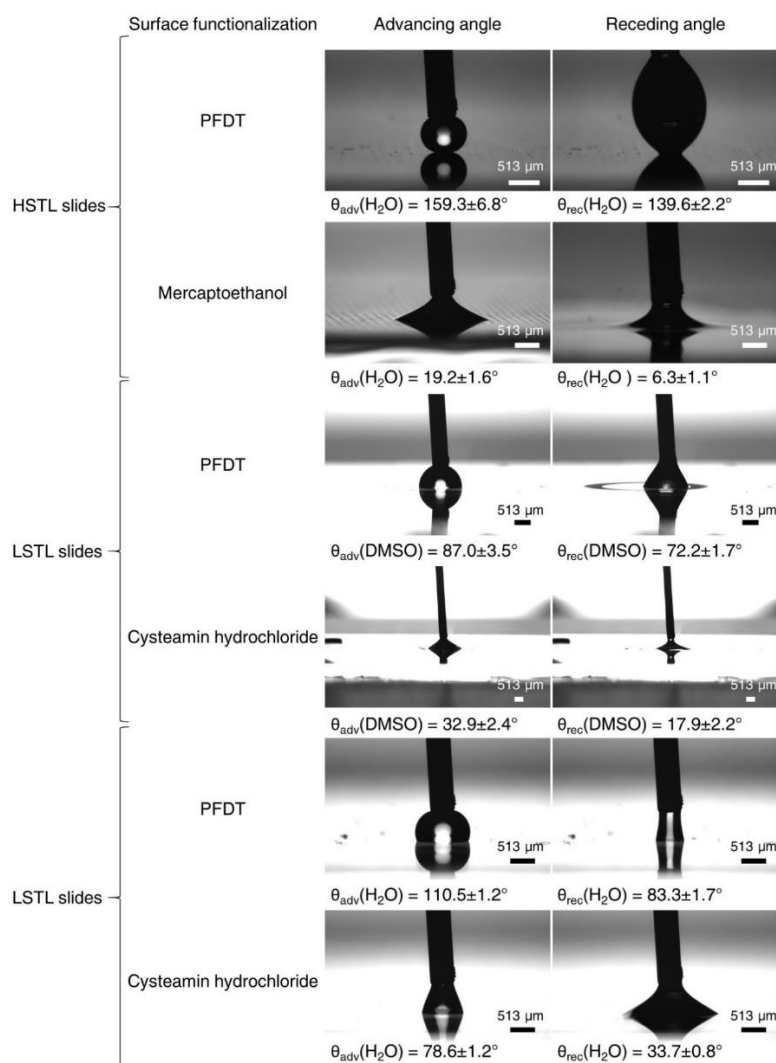
1. Benz, M., Molla, M.R., Böser, A., Rosenfeld, A. & Levkin, P.A. Marrying chemistry with biology by combining on-chip solution-based combinatorial synthesis and cellular screening. *Nature Communications* **10**, 2879 (2019).
2. Benz, M. et al. A combined high-throughput and high-content platform for unified on-chip synthesis, characterization and biological screening. *Manuscript accepted* (2020).
3. Drews, J. Strategic trends in the drug industry. *Drug Discovery Today* **8**, 411-420 (2003).
4. Weaver, I.N. & Weaver, D.F. Drug Design and Discovery: Translational Biomedical Science Varies Among Countries. *Clinical and Translational Science* **6**, 409-413 (2013).
5. Roda, A. et al. New 6-substituted bile acids: physico-chemical and biological properties of 6 alpha-methyl ursodeoxycholic acid and 6 alpha-methyl-7-epicholic acid. *Journal of Lipid Research* **35**, 2268-2279 (1994).
6. Aldini, R. et al. Relationship between structure and intestinal absorption of bile acids with a steroid or side-chain modification. *Steroids* **61**, 590-597 (1996).
7. Pellicciari, R. et al. 6 $\alpha$ -Ethyl-Chenodeoxycholic Acid (6-ECDCA), a Potent and Selective FXR Agonist Endowed with Anticholestatic Activity. *Journal of Medicinal Chemistry* **45**, 3569-3572 (2002).
8. Markham, A. & Keam, S.J. Obeticholic Acid: First Global Approval. *Drugs* **76**, 1221-1226 (2016).
9. Asaki, T., Hamamoto, T., Sugiyama, Y., Kuwano, K. & Kuwabara, K. Structure–activity studies on diphenylpyrazine derivatives: A novel class of prostacyclin receptor agonists. *Bioorganic & Medicinal Chemistry* **15**, 6692-6704 (2007).
10. Meanwell, N.A. et al. Structure-activity relationships associated with 3,4,5-triphenyl-1H-pyrazole-1-nonanoic acid, a nonprostanoid prostacyclin mimetic. *Journal of Medicinal Chemistry* **35**, 389-397 (1992).
11. Kuwano, K. et al. 2-{4-[(5,6-Diphenylpyrazin-2-yl)(isopropyl)amino]butoxy}-N-(methylsulfonyl)acetamide (NS-304), an Orally Available and Long-Acting Prostacyclin Receptor Agonist Prodrug. *Journal of Pharmacology and Experimental Therapeutics* **322**, 1181-1188 (2007).
12. Simonneau, G. et al. Selexipag: an oral, selective prostacyclin receptor agonist for the treatment of pulmonary arterial hypertension. *European Respiratory Journal* **40**, 874-880 (2012).
13. Hardin, E.A. & Chin, K.M. Selexipag in the treatment of pulmonary arterial hypertension: design, development, and therapy. *Drug Design, Development and Therapy* **10**, 3747-3754 (2016).
14. Cummings, J.L., Morstorf, T. & Zhong, K. Alzheimer's disease drug-development pipeline: few candidates, frequent failures. *Alzheimer's Research & Therapy* **6**, 37 (2014).
15. Wong, C.H., Siah, K.W. & Lo, A.W. Estimation of clinical trial success rates and related parameters. *Biostatistics* **20**, 273-286 (2018).
16. Dowden, H. & Munro, J. Trends in clinical success rates and therapeutic focus. *Nature reviews. Drug discovery* **18**, 495 (2019).
17. Harrison, R.K. Phase II and phase III failures: 2013–2015. *Nature Reviews Drug Discovery* **15**, 817-818 (2016).

18. Morgan, P. et al. Impact of a five-dimensional framework on R&D productivity at AstraZeneca. *Nature Reviews Drug Discovery* **17**, 167-181 (2018).
19. Adomas, A. et al. Comparative analysis of transcript abundance in *Pinus sylvestris* after challenge with a saprotrophic, pathogenic or mutualistic fungus. *Tree Physiology* **28**, 885-897 (2008).
20. Wang, D.G. et al. Large-Scale Identification, Mapping, and Genotyping of Single-Nucleotide Polymorphisms in the Human Genome. *Science* **280**, 1077 (1998).
21. Lindblad-Toh, K. et al. Loss-of-heterozygosity analysis of small-cell lung carcinomas using single-nucleotide polymorphism arrays. *Nature Biotechnology* **18**, 1001 (2000).
22. MacBeath, G., Koehler, A.N. & Schreiber, S.L. Printing Small Molecules as Microarrays and Detecting Protein-Ligand Interactions en Masse. *Journal of the American Chemical Society* **121**, 7967-7968 (1999).
23. Falsey, J.R., Renil, M., Park, S., Li, S. & Lam, K.S. Peptide and Small Molecule Microarray for High Throughput Cell Adhesion and Functional Assays. *Bioconjugate Chemistry* **12**, 346-353 (2001).
24. Seeberger, P.H. & Werz, D.B. Synthesis and medical applications of oligosaccharides. *Nature* **446**, 1046 (2007).
25. Lee, M.-Y. et al. Three-dimensional cellular microarray for high-throughput toxicology assays. *Proceedings of the National Academy of Sciences* **105**, 59 (2008).
26. Brivio, M., Verboom, W. & Reinhoudt, D.N. Miniaturized continuous flow reaction vessels: influence on chemical reactions. *Lab on a Chip* **6**, 329-344 (2006).
27. Dittrich, P.S. & Manz, A. Lab-on-a-chip: microfluidics in drug discovery. *Nature Reviews Drug Discovery* **5**, 210-218 (2006).
28. Elvira, K.S., i Solvas, X.C., Wootton, R.C.R. & deMello, A.J. The past, present and potential for microfluidic reactor technology in chemical synthesis. *Nature Chemistry* **5**, 905-915 (2013).
29. Ren, K., Zhou, J. & Wu, H. Materials for Microfluidic Chip Fabrication. *Accounts of Chemical Research* **46**, 2396-2406 (2013).
30. Wang, J. et al. Integrated Microfluidics for Parallel Screening of an In Situ Click Chemistry Library. *Angewandte Chemie International Edition* **45**, 5276-5281 (2006).
31. Theberge, A.B. et al. Microfluidic platform for combinatorial synthesis in picolitre droplets. *Lab on a Chip* **12**, 1320-1326 (2012).
32. McMullen, J.P. & Jensen, K.F. An Automated Microfluidic System for Online Optimization in Chemical Synthesis. *Organic Process Research & Development* **14**, 1169-1176 (2010).
33. Takátsy, G. The Use of Spiral Loops in Serological and Virological Micro-Methods. *Acta Microbiologica* **3**, 191-202 (1955).
34. Manns, R. Microplate History 2nd Edition May 1999, presented at MipTec-ICAR'99, May 17-21, 1999, Montreux, Switzerland; Astle, Thoma. Recollections of Early Microplate Automation. *Journal of the Association for Laboratory Automation* **5**, 30-31 (2000).
35. Martis, E.A., Radhakrishnan, R. & Badve, R.R. High-throughput screening: the hits and leads of drug discovery-an overview. *Journal of Applied Pharmaceutical Science* **1**, 2-10 (2011).
36. Dunn, D. et al. Ultra-High Throughput Screen of Two-Million-Member Combinatorial Compound Collection in a Miniaturized, 1536-Well Assay Format. *Journal of Biomolecular Screening* **5**, 177-187 (2000).
37. Krutzik, P.O., Crane, J.M., Clutter, M.R. & Nolan, G.P. High-content single-cell drug screening with phosphospecific flow cytometry. *Nature Chemical Biology* **4**, 132-142 (2008).

38. Mazutis, L. et al. Single-cell analysis and sorting using droplet-based microfluidics. *Nature Protocols* **8**, 870-891 (2013).
39. Lindström, S. & Andersson-Svahn, H. Miniaturization of biological assays — Overview on microwell devices for single-cell analyses. *Biochimica et Biophysica Acta (BBA) - General Subjects* **1810**, 308-316 (2011).
40. Lodish, H. et al. Molecular cell biology 4th edition. *National Center for Biotechnology Information, Bookshelf* (2000).
41. Berg, M. et al. Evaluation of Liquid Handling Conditions in Microplates. *Journal of Biomolecular Screening* **6**, 47-56 (2001).
42. Burbaum, J.J. The evolution of miniaturized well plates. *Journal of biomolecular screening* **5**, 5-8 (2000).
43. Feng, W., Ueda, E. & Levkin, P.A. Droplet Microarrays: From Surface Patterning to High-Throughput Applications. *Advanced Materials* **30**, 1706111 (2018).
44. Nørgaard, T. & Dacke, M. Fog-basking behaviour and water collection efficiency in Namib Desert Darkling beetles. *Frontiers in Zoology* **7**, 23 (2010).
45. Geyer, F.L., Ueda, E., Liebel, U., Grau, N. & Levkin, P.A. Superhydrophobic–Superhydrophilic Micropatterning: Towards Genome-on-a-Chip Cell Microarrays. *Angewandte Chemie International Edition* **50**, 8424-8427 (2011).
46. Feng, W. et al. Surface Patterning via Thiol-Yne Click Chemistry: An Extremely Fast and Versatile Approach to Superhydrophilic-Superhydrophobic Micropatterns. *Advanced Materials Interfaces* **1** (2014).
47. Feng, W., Li, L., Du, X., Welle, A. & Levkin, P.A. Single-Step Fabrication of High-Density Microdroplet Arrays of Low-Surface-Tension Liquids. *Advanced Materials* **28**, 3202-3208 (2016).
48. Xia, Y., Qin, D. & Yin, Y. Surface patterning and its application in wetting/dewetting studies. *Current Opinion in Colloid & Interface Science* **6**, 54-64 (2001).
49. Jackman, R.J., Duffy, D.C., Ostuni, E., Willmore, N.D. & Whitesides, G.M. Fabricating Large Arrays of Microwells with Arbitrary Dimensions and Filling Them Using Discontinuous Dewetting. *Analytical Chemistry* **70**, 2280-2287 (1998).
50. Ueda, E., Geyer, F.L., Nedashkivska, V. & Levkin, P.A. DropletMicroarray: facile formation of arrays of microdroplets and hydrogel micropads for cell screening applications. *Lab on a Chip* **12**, 5218-5224 (2012).
51. Kobaku, S.P.R., Kota, A.K., Lee, D.H., Mabry, J.M. & Tuteja, A. Patterned Superomniphobic–Superomniphilic Surfaces: Templates for Site-Selective Self-Assembly. *Angewandte Chemie International Edition* **51**, 10109-10113 (2012).
52. Popova, A.A. et al. Droplet-Array (DA) Sandwich Chip: A Versatile Platform for High-Throughput Cell Screening Based on Superhydrophobic–Superhydrophilic Micropatterning. *Advanced Materials* **27**, 5217-5222 (2015).
53. Efremov, A.N., Stanganello, E., Welle, A., Scholpp, S. & Levkin, P.A. Micropatterned superhydrophobic structures for the simultaneous culture of multiple cell types and the study of cell–cell communication. *Biomaterials* **34**, 1757-1763 (2013).
54. Neto, A.I. et al. Fabrication of Hydrogel Particles of Defined Shapes Using Superhydrophobic-Hydrophilic Micropatterns. *Advanced Materials* **28**, 7613-7619 (2016).
55. Popova, A.A., Demir, K., Hartanto, T.G., Schmitt, E. & Levkin, P.A. Droplet-microarray on superhydrophobic–superhydrophilic patterns for high-throughput live cell screenings. *RSC Advances* **6**, 38263-38276 (2016).
56. Ueda, E., Feng, W. & Levkin, P.A. Superhydrophilic–Superhydrophobic Patterned Surfaces as High-Density Cell Microarrays: Optimization of Reverse Transfection. *Advanced Healthcare Materials* **5**, 2646-2654 (2016).

57. Jogia, G.E., Tronser, T., Popova, A.A. & Levkin, P.A. Droplet Microarray Based on Superhydrophobic-Superhydrophilic Patterns for Single Cell Analysis. *Microarrays* **5**, 28 (2016).
58. Bruchmann, J., Pini, I., Gill, T.S., Schwartz, T. & Levkin, P.A. Patterned SLIPS for the Formation of Arrays of Biofilm Microclusters with Defined Geometries. *Advanced Healthcare Materials* **6**, 1601082 (2017).
59. Tronser, T., Popova, A.A., Jaggy, M., Bastmeyer, M. & Levkin, P.A. Droplet Microarray Based on Patterned Superhydrophobic Surfaces Prevents Stem Cell Differentiation and Enables High-Throughput Stem Cell Screening. *Advanced Healthcare Materials* **6**, 1700622 (2017).
60. Tronser, T., Demir, K., Reischl, M., Bastmeyer, M. & Levkin, P.A. Droplet microarray: miniaturized platform for rapid formation and high-throughput screening of embryoid bodies. *Lab on a Chip* **18**, 2257-2269 (2018).
61. Popova, A.A. et al. Facile One Step Formation and Screening of Tumor Spheroids Using Droplet-Microarray Platform. *Small* **15**, 1901299 (2019).
62. Popova, A.A. et al. Fish-Microarray: A Miniaturized Platform for Single-Embryo High-Throughput Screenings. *Advanced Functional Materials* **28**, 1703486 (2018).
63. Anderson, D.G., Lynn, D.M. & Langer, R. Semi-Automated Synthesis and Screening of a Large Library of Degradable Cationic Polymers for Gene Delivery. *Angewandte Chemie International Edition* **42**, 3153-3158 (2003).
64. Buitrago Santanilla, A. et al. Nanomole-scale high-throughput chemistry for the synthesis of complex molecules. *Science* **347**, 49 (2015).
65. Ly, A. et al. Site-to-Site Reproducibility and Spatial Resolution in MALDI-MSI of Peptides from Formalin-Fixed Paraffin-Embedded Samples. *PROTEOMICS – Clinical Applications* **13**, 1800029 (2019).
66. Spraggins, J.M. et al. Next-generation technologies for spatial proteomics: Integrating ultra-high speed MALDI-TOF and high mass resolution MALDI FTICR imaging mass spectrometry for protein analysis. *PROTEOMICS* **16**, 1678-1689 (2016).
67. Ogrinc Potočnik, N., Porta, T., Becker, M., Heeren, R.M.A. & Ellis, S.R. Use of advantageous, volatile matrices enabled by next-generation high-speed matrix-assisted laser desorption/ionization time-of-flight imaging employing a scanning laser beam. *Rapid Communications in Mass Spectrometry* **29**, 2195-2203 (2015).
68. Lin, S. et al. Mapping the dark space of chemical reactions with extended nanomole synthesis and MALDI-TOF MS. *Science* **361**, eaar6236 (2018).
69. DiMasi, J.A., Hansen, R.W. & Grabowski, H.G. The price of innovation: new estimates of drug development costs. *Journal of Health Economics* **22**, 151-185 (2003).
70. Kola, I. & Landis, J. Can the pharmaceutical industry reduce attrition rates? *Nature Reviews Drug Discovery* **3**, 711-716 (2004).
71. Eder, J., Sedrani, R. & Wiesmann, C. The discovery of first-in-class drugs: origins and evolution. *Nature Reviews Drug Discovery* **13**, 577-587 (2014).
72. DiMasi, J.A., Grabowski, H.G. & Hansen, R.W. Innovation in the pharmaceutical industry: New estimates of R&D costs. *Journal of Health Economics* **47**, 20-33 (2016).
73. Smith, A. Screening for drug discovery: The leading question. *Nature* **418**, 453-455 (2002).
74. Zhang, M., Zhang, Y., Wang, Y., Lv, W. & Zhang, Y. Automated cell-based luminescence assay for profiling antiviral compound activity against enteroviruses. *Scientific Reports* **9**, 6023 (2019).
75. Madoux, F. et al. A 1536-Well 3D Viability Assay to Assess the Cytotoxic Effect of Drugs on Spheroids. *SLAS DISCOVERY: Advancing the Science of Drug Discovery* **22**, 516-524 (2017).

76. Shoemaker, R.H. The NCI60 human tumour cell line anticancer drug screen. *Nature Reviews Cancer* **6**, 813-823 (2006).
77. Mathieu, V. et al. Sphaeropsidin A shows promising activity against drug-resistant cancer cells by targeting regulatory volume increase. *Cellular and Molecular Life Sciences* **72**, 3731-3746 (2015).
78. Frédérick, R. et al. Novel Trisubstituted Harmine Derivatives with Original in Vitro Anticancer Activity. *Journal of Medicinal Chemistry* **55**, 6489-6501 (2012).
79. Mathieu, V. et al. The sodium pump  $\alpha 1$  sub-unit: a disease progression-related target for metastatic melanoma treatment. *Journal of Cellular and Molecular Medicine* **13**, 3960-3972 (2009).
80. Chan, G.K.Y., Kleinheinz, T.L., Peterson, D. & Moffat, J.G. A simple high-content cell cycle assay reveals frequent discrepancies between cell number and ATP and MTS proliferation assays. *PLoS One* **8**, e63583-e63583 (2013).
81. Molla, M.R., Böser, A., Rana, A., Schwarz, K. & Levkin, P.A. One-Pot Parallel Synthesis of Lipid Library via Thiolactone Ring Opening and Screening for Gene Delivery. *Bioconjugate Chemistry* **29**, 992-999 (2018).
82. Ueda, E., Feng, W. & Levkin, P.A. Superhydrophilic-Superhydrophobic Patterned Surfaces as High-Density Cell Microarrays: Optimization of Reverse Transfection. *Advanced Healthcare Materials* **5**, 2646-2654 (2016).
83. Geyer, F.L., Ueda, E., Liebel, U., Grau, N. & Levkin, P.A. Superhydrophobic-Superhydrophilic Micropatterning: Towards Genome-on-a-Chip Cell Microarrays. *Angewandte Chemie International Edition* **50**, 8424-8427 (2011).
84. Feng, W. et al. Surface Patterning via Thiol-Yne Click Chemistry: An Extremely Fast and Versatile Approach to Superhydrophilic-Superhydrophobic Micropatterns. *Advanced Materials Interfaces* **1**, 1400269 (2014).
85. Killops, K.L., Campos, L.M. & Hawker, C.J. Robust, Efficient, and Orthogonal Synthesis of Dendrimers via Thiol-ene "Click" Chemistry. *Journal of the American Chemical Society* **130**, 5062-5064 (2008).
86. Huang, S., Wang, Z., Xu, J., Lu, D. & Yuan, T. Determination of optical constants of functional layer of online Low-E glass based on the Drude theory. *Thin Solid Films* **516**, 3179-3183 (2008).
87. Reidinger, M., Rydzek, M., Scherdel, C., Arduini-Schuster, M. & Manara, J. Low-emitting transparent coatings based on tin doped indiumoxide applied via a sol-gel routine. *Thin Solid Films* **517**, 3096-3099 (2009).
88. Baker, M.J. et al. Using Fourier transform IR spectroscopy to analyze biological materials. *Nature Protocols* **9**, 1771-1791 (2014).
89. Rabe, J.-H. et al. Fourier Transform Infrared Microscopy Enables Guidance of Automated Mass Spectrometry Imaging to Predefined Tissue Morphologies. *Scientific Reports* **8**, 313 (2018).
90. Minnich, C.B. et al. Highly Flexible Fibre-Optic ATR-IR Probe for Inline Reaction Monitoring. *Organic Process Research & Development* **11**, 94-97 (2007).
91. Rosenfeld, A. et al. Solid-phase combinatorial synthesis using microarrays of microcompartments with light-induced on-chip cell screening. *Materials Today Bio* **3**, 100022 (2019).
92. Fox, M.A. & Whitesell, J.K. *Organische Chemie: Grundlagen, Mechanismen, Bioorganische Anwendungen.* (Spektrum Akad. Verlag, 1995).
93. Lide, D.R. *CRC Handbook of Chemistry and Physics: A Ready-Reference Book of Chemical and Physical Data.* (CRC-Press, 1984).

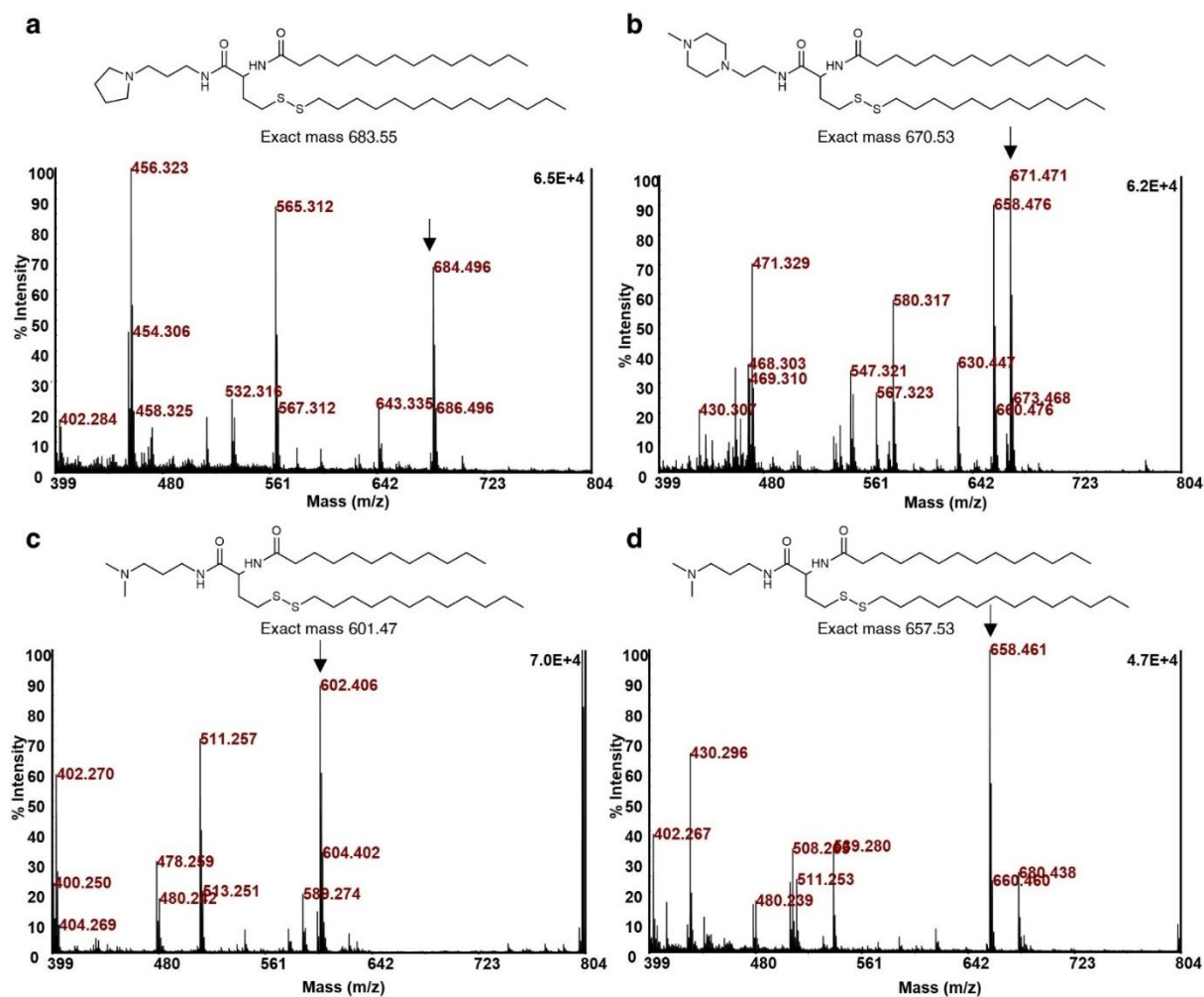
Appendix<sup>7</sup>

**Appendix Figure 1 | Water contact angle measurements.** Advancing and receding contact angle of several solvents ( $H_2O$  and DMSO) were observed on different functionalized surfaces (perfluoro decanethiol (PFDT), cysteamine hydrochloride on rough polymer surfaces (HSTL slides) and bare glass surfaces (LSTL slides)). +/- values are standard deviations,  $n = 3$  (number of replicates). Cited from Ref<sup>1</sup>.

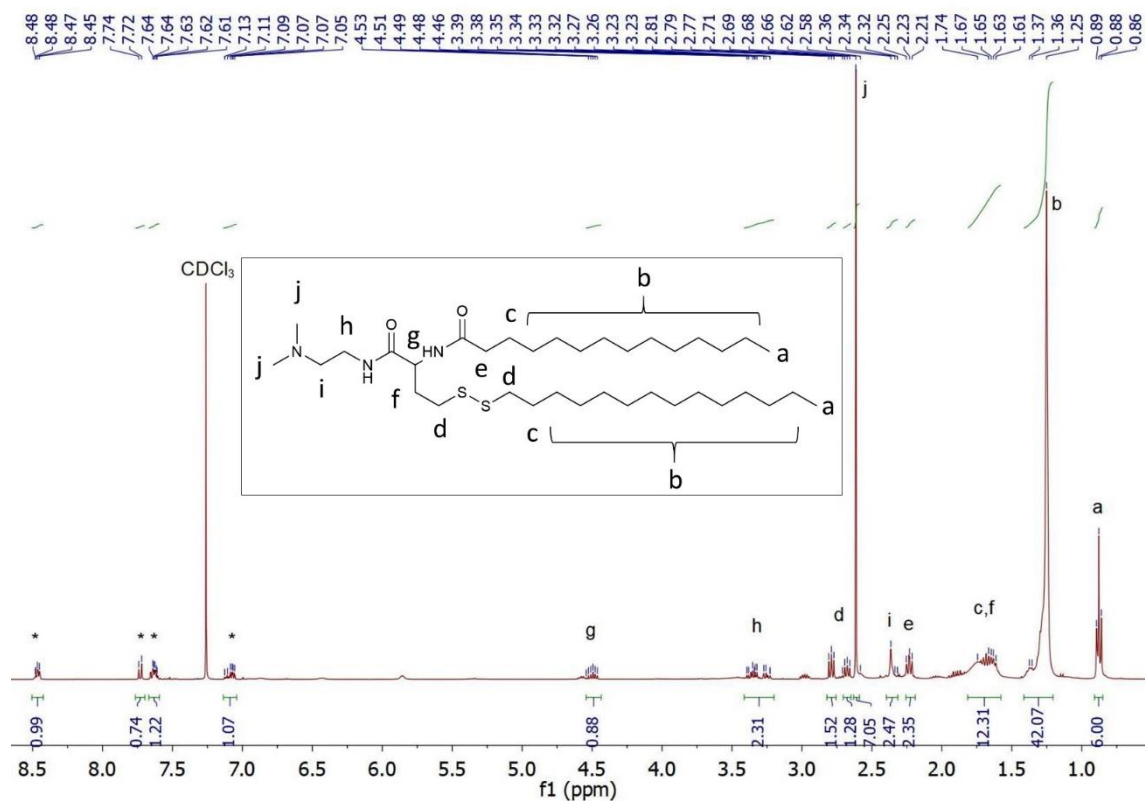
<sup>7</sup> This chapter is adapted from the following publications which are licensed under a Creative Commons Attribution 4.0 International License (CC BY 4.0; <https://creativecommons.org/licenses/by/4.0/>):

Benz, Maximilian, Molla, M.R., Böser, A., Rosenfeld, A. & Levkin, P.A. Marrying chemistry with biology by combining on-chip solution-based combinatorial synthesis and cellular screening. *Nature Communications* **10**, 2879 (2019).

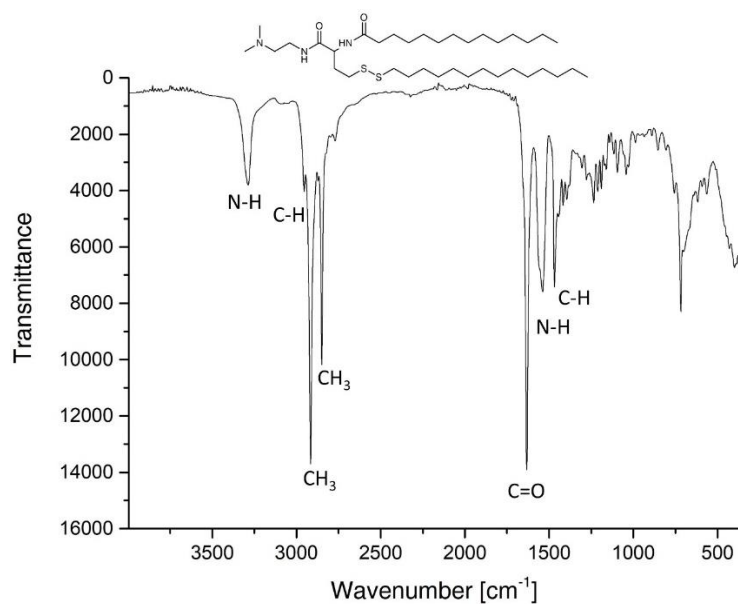
Benz, Maximilian, Asperger, A., Hamester, M., Welle, A., Heissler, S. & Levkin, P.A. A combined high-throughput and high-content platform for unified on-chip synthesis, characterization and biological screening. Manuscript accepted.



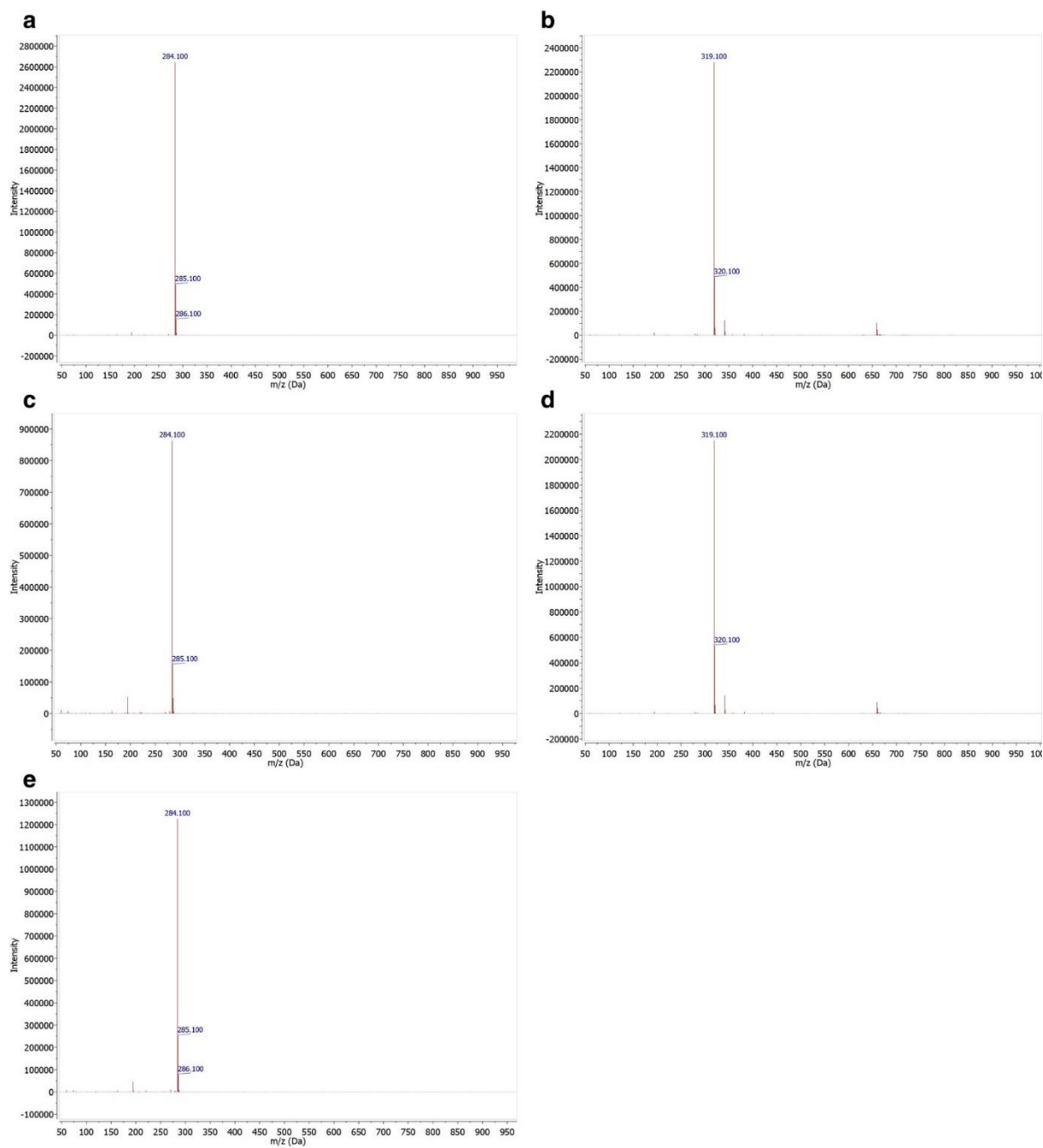
**Appendix Figure 2 | Exemplary mass spectra of several raw products.** (a) A2\_T14\_PY14 – calculated mass (m/z): 683.55; found mass (m/z): 684.496. (b) A3\_T14\_PY12 – calculated mass (m/z): 670.53; found mass (m/z): 671.471. (c) A4\_T12\_PY12 – calculated mass (m/z): 601.47; found mass (m/z): 602.406. (d) A4\_T14\_PY14 – calculated mass (m/z): 657.53; found mass (m/z): 658.461. Cited from Ref<sup>1</sup>.



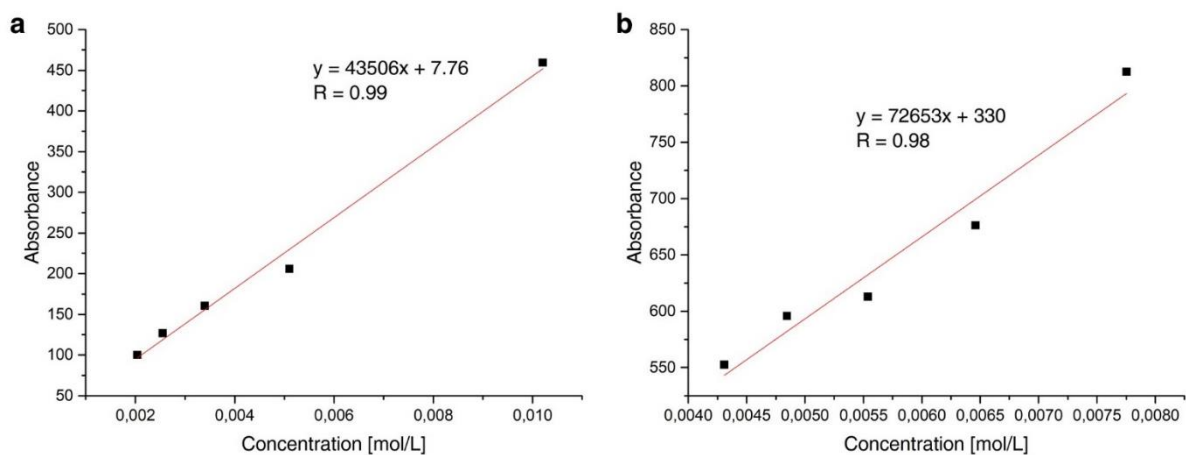
**Appendix Figure 3 | Exemplary  $^1\text{H}$  NMR spectrum of on-chip synthesized raw product A5\_T14\_PY14.**  $^1\text{H}$  NMR (400 MHz, chloroform-*d*):  $\delta$  4.54-4.46 ppm (m, 1H), 3.39-3.23 (m, 2H), 2.81-2.77 (m, 2H), 2.71-2.66 (m, 1H), 2.62-2.58 (m, 7H), 2.81-2.58 (m, 2H), 2.36-2.32 (m, 2H), 2.25-2.21 (m, 2H), 1.74-1.61 (m, 12H), 1.37-1.25 (m, 42H), 0.89-0.86 (m, 6H). Peaks of by-product 2-thiopyridone labelled by \*. Cited from Ref<sup>1</sup>.



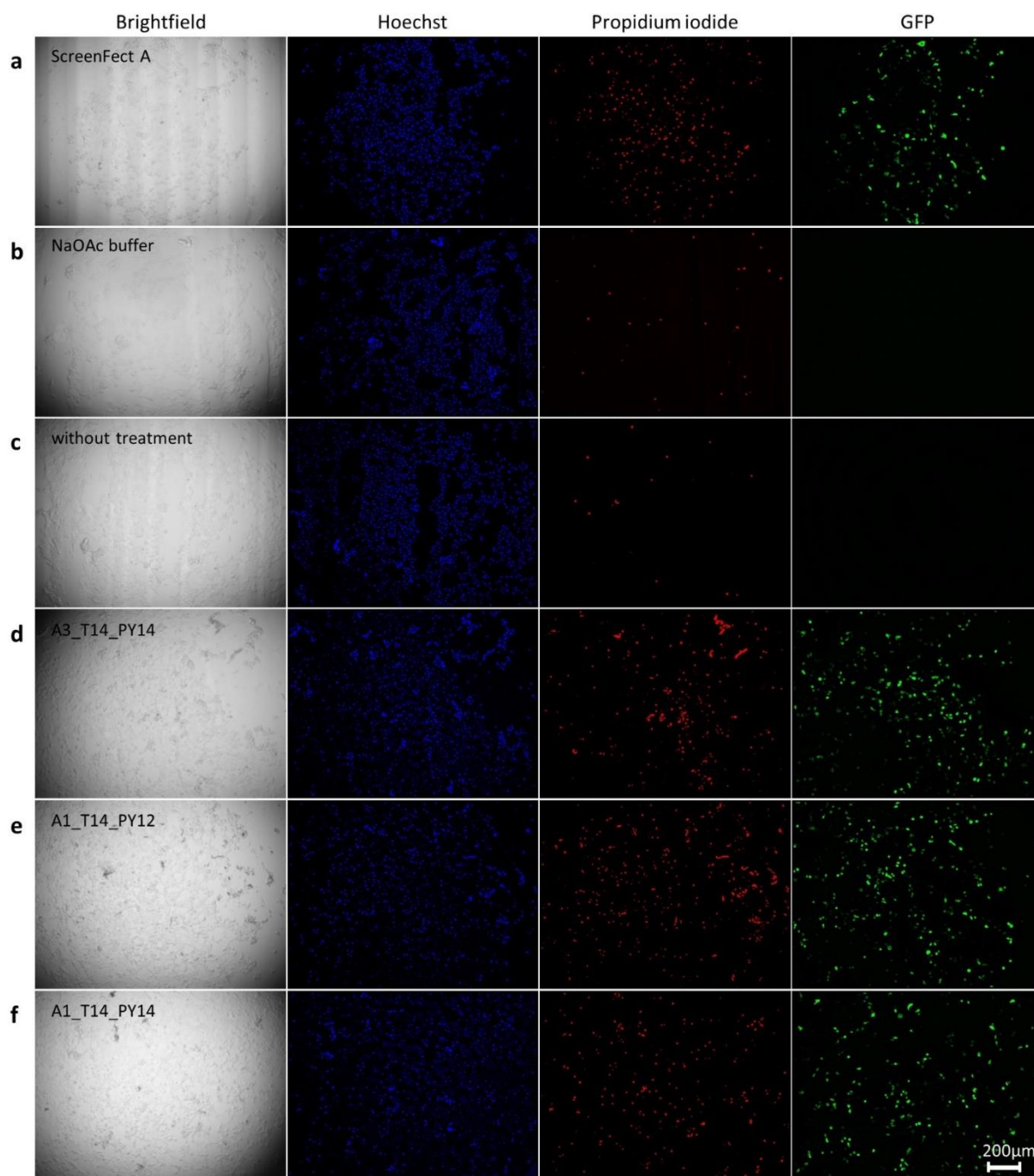
**Appendix Figure 4 | Exemplary IR spectrum of the product A5\_T14\_PY14.** Cited from Ref<sup>1</sup>.



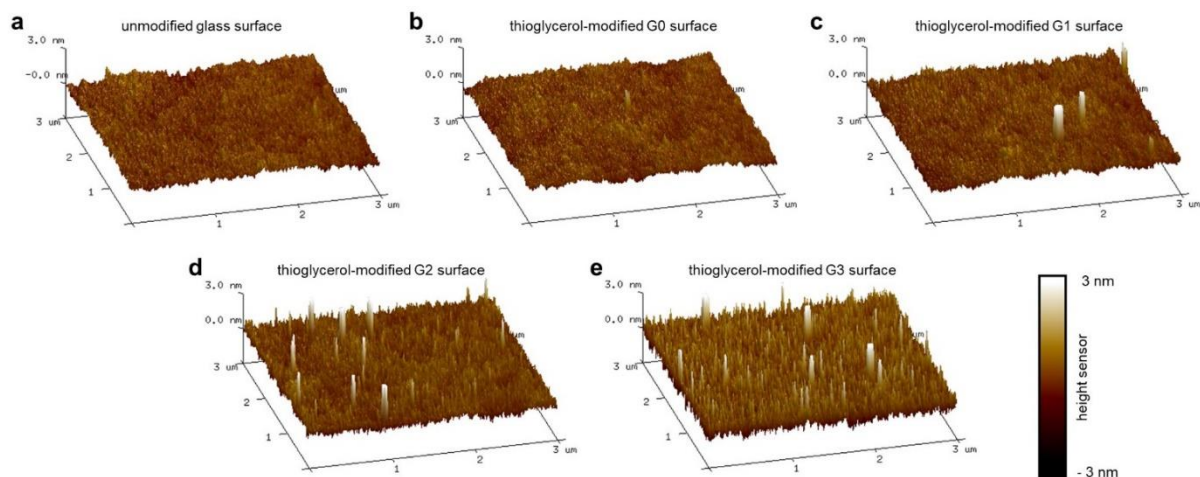
**Appendix Figure 5 | LC-MS spectra.** (a) Mixture; retention time: 5.7 min – calculated mass (m/z): 284.12; found mass (m/z): 284.10. (b) Mixture; retention time: 11.1 min – calculated mass (m/z): 318.14; found mass (m/z): 319.10. (c) Organic phase; retention time: 5.8 min – calculated mass (m/z): 284.12; found mass (m/z): 284.10 (d) Organic phase; retention time: 11.1 min – calculated mass (m/z): 318.14; found mass (m/z): 319.10. (e) Aqueous phase; retention time: 5.7 min – calculated mass (m/z): 284.12; found mass (m/z): 284.10. Cited from Ref<sup>1</sup>.



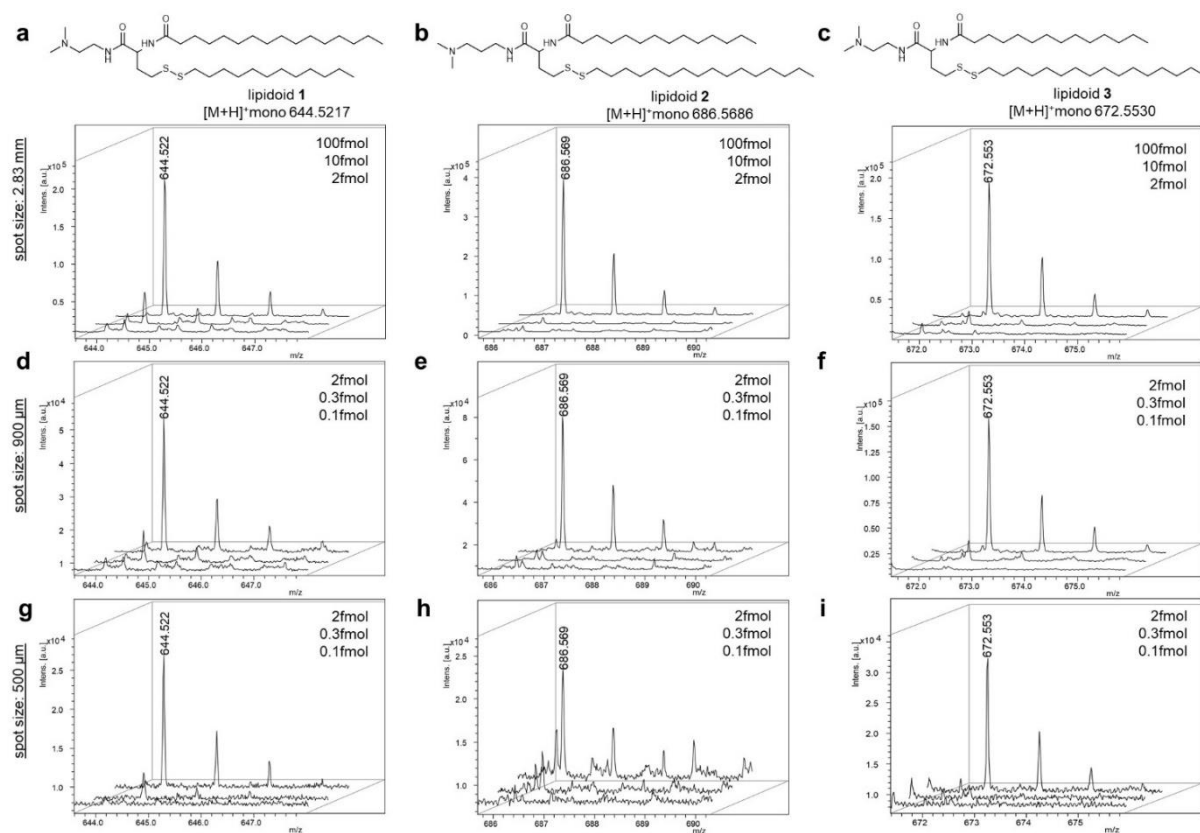
**Appendix Figure 6 | UV-Vis calibration curves.** (a) Calibration curve of Nile red in acetonitrile. The extinction coefficient  $\epsilon$  was estimated to be  $43,506 \text{ M}^{-1}\text{cm}^{-1}$  at 541 nm. (b) Calibration curve of methylene blue in acetonitrile. The extinction coefficient  $\epsilon$  was estimated to be  $72,653 \text{ M}^{-1}\text{cm}^{-1}$  at 654 nm. Cited from Ref<sup>1</sup>.



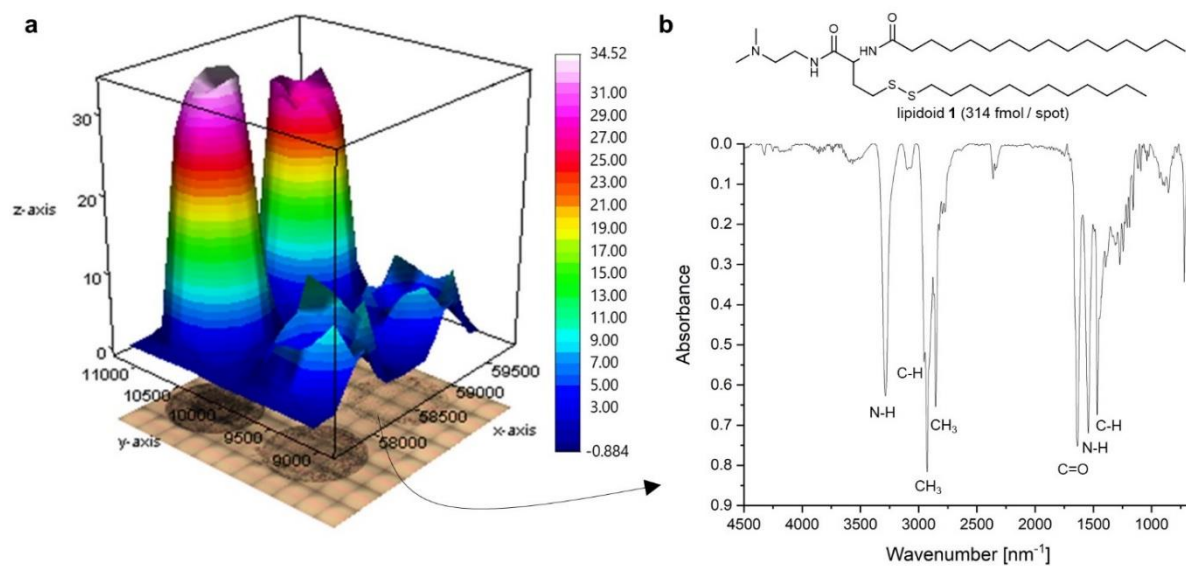
**Appendix Figure 7 | Exemplary microscope images of treated cells after 48h cultivation.** From left to right: brightfield channel, Hoechst 33342 channel ( $\lambda_{\text{ex}} = 400 \text{ nm}$ ), propidium iodide channel ( $\lambda_{\text{ex}} = 595 \text{ nm}$ ), GFP channel ( $\lambda_{\text{ex}} = 505 \text{ nm}$ ); scale bar:  $200 \mu\text{m}$ . **(a)** Cells treated with ScreenFect A as positive control. Transfection efficiency:  $26\% \pm 1\%$ ; cell viability:  $34\% \pm 1\%$ . **(b)** Cells treated with aqueous sodium acetate buffer (50 mM, pH 5) as negative control. Transfection efficiency: 0%; cell viability:  $97\% \pm 1\%$ . **(c)** Cells without treatment as negative control. Transfection efficiency: 0%; cell viability:  $98\% \pm 1\%$ . **(d)** Cells treated with sample A3\_T14\_PY14. Transfection efficiency:  $52\% \pm 4\%$ ; cell viability:  $35\% \pm 11\%$ . **(e)** Cells treated with sample A1\_T14\_PY12. Transfection efficiency:  $50\% \pm 9\%$ ; cell viability:  $36\% \pm 6\%$ . **(f)** Cells treated with sample A1\_T14\_PY14. Transfection efficiency:  $46\% \pm 7\%$ ; cell viability:  $32\% \pm 9\%$ . +/- values are standard deviations,  $n = 3$  (number of replicates);  $N = 3$  (repetitions including lipid synthesis). Cited from Ref<sup>1</sup>.



**Appendix Figure 8 | Atomic force microscopy (AFM) surface characterization.** AFM image of an (a) unmodified, (b) thioglycerol-modified G0, (c) G1, (d) G2, and (e) G3 surface measured in non-contact tapping mode in air. Field-of-view:  $3 \times 3 \mu\text{m}^2$ . Cited from Ref<sup>2</sup>.

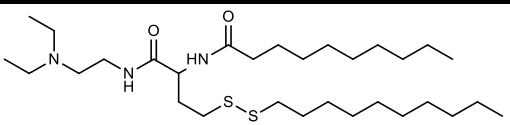
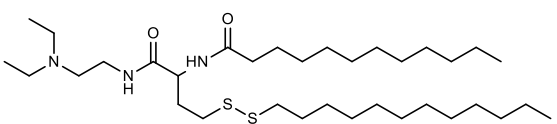
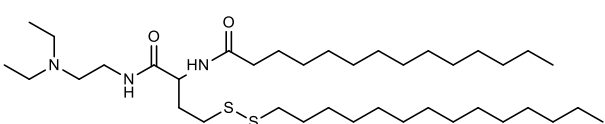
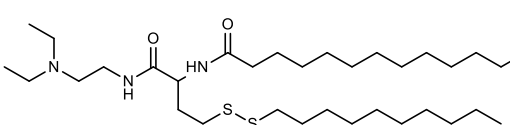
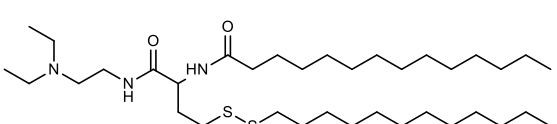
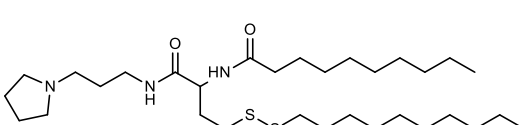
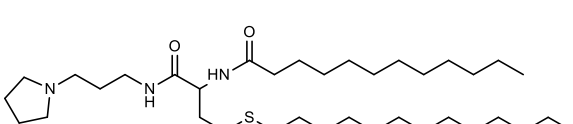
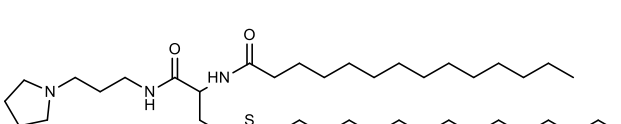
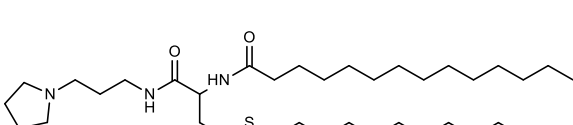


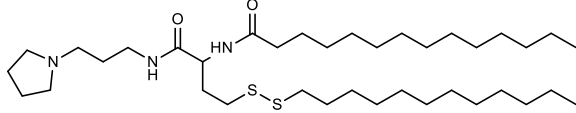
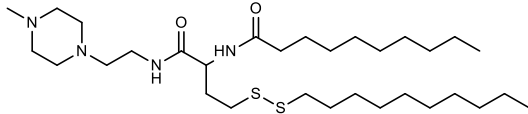
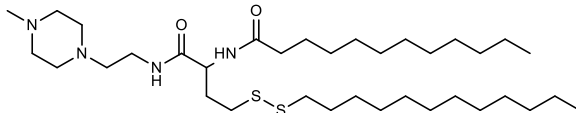
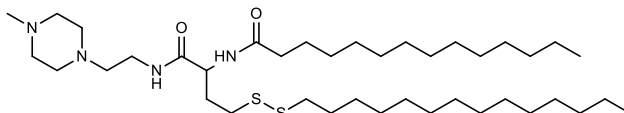
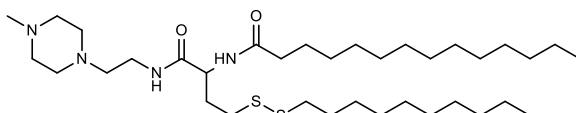
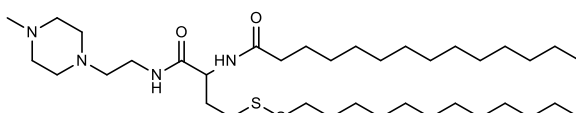
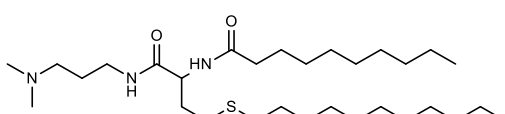
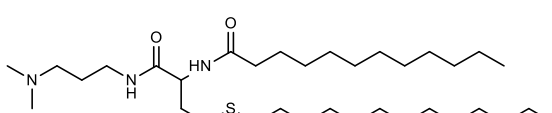
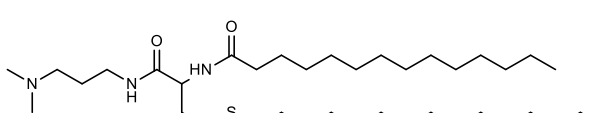
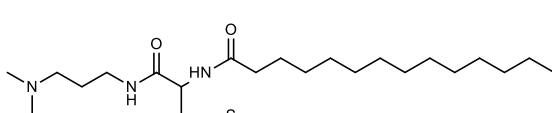
**Appendix Figure 9 | Sensitivity limitation of on-chip MALDI-TOF MS.** MS spectra of lipidoid 1, 2 and 3 of (a-c) 100, 10 and 2 fmol per 2.83 mm spot, (d-f) 2, 0.3 and 0.1 fmol per 900  $\mu\text{m}$  spot, and (g-i) 2, 0.3 and 0.1 fmol per 500  $\mu\text{m}$  spot. Cited from Ref<sup>2</sup>.

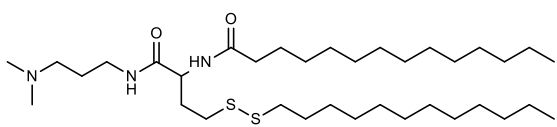
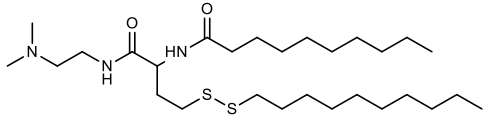
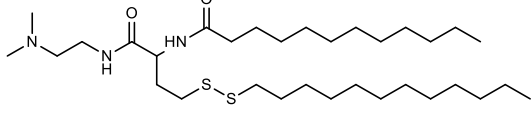
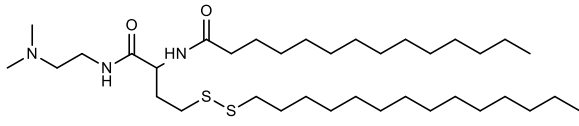
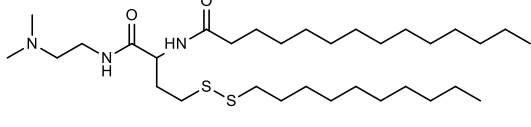
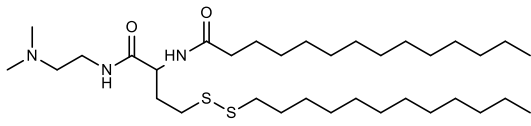


**Appendix Figure 10 | On-chip characterization by IR spectroscopy. (a)** IR imaging of lipidoid **1** applied in different concentrations on an omniphilic-omniphobic patterned ITO surface. **(b)** Corresponding on-chip measured IR spectrum of 314 fmol of lipidoid **1**. Cited from Ref<sup>2</sup>.

**Appendix Table 1 | Synthesized lipidoid library and estimated yield of the reactions appreciated by UV-Vis absorbance measurements of the raw product.** One equivalent of 2-thiopyridone corresponds to one equivalent of lipidoid. Each result based on triplicate control. Cited from Ref<sup>1</sup>.

No.	ID	Product structure	Yield
1	A1_10_10		99±1
2	A1_12_12		98±1
3	A1_14_14		97±3
4	A1_14_10		99±1
5	A1_14_12		97±0
6	A2_10_10		53±1
7	A2_12_12		57±2
8	A2_14_14		53±3
9	A2_14_10		67±4

10	A2_14_12		67±2
11	A3_10_10		91±1
12	A3_12_12		98±0
13	A3_14_14		90±5
14	A3_14_10		93±2
15	A3_14_12		94±2
16	A4_10_10		97±0
17	A4_12_12		99±1
18	A4_14_14		99±1
19	A4_14_10		98±0

20	A4_14_12		98±0
21	A5_10_10		91±1
22	A5_12_12		98±0
23	A5_14_14		90±2
24	A5_14_10		94±2
25	A5_14_12		94±1

---

**Appendix Table 2 | Transfection efficiencies (TE) of test samples observed in three experiments (Exp.).** Each result of a single experiment based on triplicate control. Cited from Ref<sup>1</sup>.

No.	ID	TE(Exp. 1)	TE(Exp. 2)	TE(Exp. 3)	Ø TE [%]	σ TE [%]
		[%]	[%]	[%]		
1	A1_10_10	0	0	0	0	0
2	A1_12_12	15	11	7	11	3
3	A1_14_10	43	17	12	24	14
4	A1_14_12	58	37	55	50	9
5	A1_14_14	51	36	51	46	7
6	A2_10_10	0	0	0	0	0
7	A2_12_12	0	0	0	0	0
8	A2_14_10	0	0	0	0	0
9	A2_14_12	0	0	0	0	0
10	A2_14_14	0	0	0	0	0
11	A3_10_10	0	0	0	0	0
12	A3_12_12	7	14	4	8	5
13	A3_14_10	36	44	50	43	6
14	A3_14_12	36	27	25	29	5
15	A3_14_14	53	56	46	52	4
16	A4_10_10	0	0	0	0	0
17	A4_12_12	9	0	1	3	4

## Appendix

18	A4_14_10	16	14	23	18	4
19	A4_14_12	8	5	12	8	3
20	A4_14_14	12	30	32	25	9
21	A5_10_10	0	0	0	0	0
22	A5_12_12	6	13	7	9	3
23	A5_14_10	36	35	35	36	0
24	A5_14_12	11	11	12	11	1
25	A5_14_14	30	39	29	33	5

---

**Appendix Table 3 | Results of contact angle measurements.** N/A: not tested. Each result based on triplicate control. Cited from Ref<sup>2</sup>.

	solvent	$\theta_{adv}$ [°]	$\sigma_{adv}$ [°]	$\theta_{stat}$ [°]	$\sigma_{stat}$ [°]	$\theta_{rec}$ [°]	$\sigma_{rec}$ [°]
PFDT-modified G3 surface	H <sub>2</sub> O	125	3	116	4	111	3
	DMSO	100	2	97	1	66	2
	DMF	103	1	91	4	67	3
	toluene	89	1	80	2	63	2
	n-hexadecane	86	1	81	2	74	1
	ethanol	80	1	72	2	40	0
Thioglycerol-modified G3 surface	H <sub>2</sub> O	33	2	N/A	N/A	1	1
	DMSO	12	2	N/A	N/A	<1	<1
	DMF	4	1	N/A	N/A	<1	<1
	ethanol	3	1	N/A	N/A	<1	<1

**Appendix Table 4 | Results of surface roughness (Rq) measurements by AFM.** Each result based on triplicate control. Cited from Ref<sup>2</sup>.

$\text{Ø}(\text{Rq}(\text{unmod.}))$	$\text{Ø}(\text{Rq}(\text{G0}))$	$\text{Ø}(\text{Rq}(\text{G1}))$	$\text{Ø}(\text{Rq}(\text{G2}))$	$\text{Ø}(\text{Rq}(\text{G3}))$
[pm]	[pm]	[pm]	[pm]	[pm]
212±8	238±23	335±44	424±61	508±26
	$\Delta\text{Rq}(\text{G0-unmod.})$ [pm]	$\Delta\text{Rq}(\text{G1-G0})$ [pm]	$\Delta\text{Rq}(\text{G2-G1})$ [pm]	$\Delta\text{Rq}(\text{G3-G2})$ [pm]
	26	97	90	83

**Appendix Table 5 | Results of dendrimer layer thickness (d) measurements by AFM.** Each result based on triplicate control. Cited from Ref<sup>2</sup>.

$\text{Ød}(\text{G0})$ [nm]	$\text{Ød}(\text{G1})$ [nm]	$\text{Ød}(\text{G2})$ [nm]	$\text{Ød}(\text{G3})$ [nm]
1.27±0.22	2.03±0.05	2.99±0.19	4.19±0.49
	$\Delta\text{d}(\text{G1-G0})$	$\Delta\text{d}(\text{G2-G1})$	$\Delta\text{d}(\text{G3-G2})$
	0.76	0.95	1.21

**Appendix Table 6 | Dendrimer layer thickness calculation.** Cited from Ref<sup>2</sup>.

<b>bond length [nm]<sup>92, 93</sup></b>	
C(sp3)-S	218
S-C(sp3)	218
C(sp3)-C(sp3)	154
C(sp3)-C(sp3)	154
C(sp3)-O	143
O-C(sp2)	143
C(sp2)-C(sp3)	150
C(sp3)-C(sp3)	154
C(sp3)-C(sp2)	150
C(sp2)-C(sp2)	134
<b>Sum</b>	<b>1,618</b>

**Appendix Table 7 | Mean MALDI-TOF MS Signal-to-Noise (S/N) ratios of lipidoid (L) 1, 2 and 3 measured on 2.83 mm spots before and after on-target washing.** Each result based on triplicate control. Cited from Ref<sup>2</sup>.

Amount on spot [fmol]	L1		L2		L3	
	before	after	before	after	before	after
1,000	312±28	956±169	193±11	652±85	367±256	759±192
100	52±10	116±24	35±23	178±89	27±6	150±33
10	4±1	11±1	2±0	10±2	2±0	10±1
2	2±0	3±1		3±0		4±0

**Appendix Table 8 | Mean MALDI-TOF MS S/N ratios of lipidoid (L) 1, 2 and 3 measured on 900 µm and 500 µm spots after on-target washing.** Each result based on triplicate control. Cited from Ref<sup>2</sup>.

Amount on spot [fmol]	900 µm spots			500 µm spot		
	L1	L2	L3	L1	L2	L3
1,000	2,601±274	2,452±150	2,804±362	2,666±141	2,071±66	2,591±64
100	1,178±108	859±238	767±221	696±120	730±260	818±75
10	137±25	65±15	148±112	155±76	338±264	313±12
2	47±21	34±6	62±22	35±7	13±1	29±20
0.3	9±5	4±1	6±1	10±1	8±3	4±2
0.1	4±1	3±0	3±0	2±0	2±0	3±2
0.05	3±0	3±0		3±1	1±0	1±0

# Curriculum Vitae

## Personal data



Name:	Maximilian Benz
Date of birth:	26.12.1993
Place of birth:	Bruchsal, Germany
LinkedIn	<a href="https://www.linkedin.com/in/maximilian-benz/">linkedin.com/in/maximilian-benz/</a>

## Education

September 2017 – present	Karlsruhe Institute of Technology (KIT), Campus Nord, Institute of Biological and Chemical Systems (IBCS-FMS)  PhD in chemistry
October 2015 – July 2017	Karlsruhe Institute of Technology (KIT)  Master's degree with distinction in chemical biology; focusing in organic chemistry
October 2012 – September 2015	Karlsruhe Institute of Technology (KIT)  Bachelor's degree in chemical biology
September 2004 – July 2012	Schönborn-Gymnasium Bruchsal  Allgemeine Hochschulreife / Abitur – university entrance qualification

**Publications related to the PhD thesis**

- (1) Benz, Maximilian, Asperger, A., Hamester, M., Welle, A., Heissler, S. & Levkin, P.A. A combined high-throughput and high-content platform for unified on-chip synthesis, characterization and biological screening. Submitted (2020).
- (2) Benz, Maximilian, Molla, M.R., Böser, A., Rosenfeld, A. & Levkin, P.A. Marrying chemistry with biology by combining on-chip solution-based combinatorial synthesis and cellular screening. *Nature Communications* **10**, 2879 (2019).

**Other publications during PhD**

- (1) Rosenfeld, A., Brehm, M., Welle, A., Trouillet, V., Heissler, S., Benz, Maximilian & Levkin, P.A. Solid-phase combinatorial synthesis using microarrays of microcompartments with light-induced on-chip cell screening. *Materials Today Bio* **3**, 100022 (2019).

**Patent applications during PhD**

- (1) Benz, Maximilian & Levkin, P.A. Herstellung gemusterter, dendrimerer Oberflächen zur Erzeugung von Tröpfchen-Arrays. DPMA patent application No.: 102019001137.6. Munich: Deutsches Patent- und Markenamt. Patent application submitted (2019).
- (2) Benz, Maximilian, Levkin, P.A., Molla, M.R., Rosenfeld, A. & Brehm, M. Karlsruhe Institute of Technology, Verfahren zur Behandlung von mindestens einer Zelle mit einem chemischen Syntheseprodukt in einem Microarray. DPMA patent application No.: 102018002880.2. Munich: Deutsches Patent- und Markenamt. Patent application submitted (2018).

## Oral presentations

- (1) Benz, Maximilian & Levkin, P.A. DrugMicroarray – Hochdurchsatz Synthese- und Analyse-Plattform auf Basis bioinspirierter Tröpfchen-Arrays, Ideenwettbewerb Biotechnologie – „Von der Natur lernen“ (Ministerium für Wissenschaft, Forschung und Kunst Baden-Württemberg), Stuttgart, Germany, 2019.
- (2) Benz, Maximilian. Unifying On-Chip Solution-Based Combinatorial Synthesis, MALDI-TOF MS Characterization and Biological Screening in Early Drug Discovery, SLAS Europe 2019 Conference & Exhibition, Barcelona, Spain, 2019.
- (3) Benz, Maximilian. ChemBIOS: A Miniaturized Platform Combining Chemical Synthesis, Characterization and Biological Readout Using Droplet Microarray, BIF-IGS seminar, Eggenstein-Leopoldshafen, Germany, 2019.

## Poster presentations

- (1) Benz, Maximilian & Levkin, P.A. chemBIOS – A Multidisciplinary Platform for Unifying Early-Stage Drug Discovery, SLAS 2020, San Diego, USA, 2020.
- (2) Benz, Maximilian & Levkin, P.A. DrugMicroarray - Hochdurchsatz Synthese- und Analyse-Plattform auf Basis bioinspirierter Tröpfchen-Arrays, Ideenwettbewerb Biotechnologie – „Von der Natur lernen“ (Ministerium für Wissenschaft, Forschung und Kunst Baden-Württemberg), Stuttgart, Germany, 2019.
- (3) Benz, Maximilian, Böser, A., Molla, M.R. & Levkin, P.A. chemBIOS: Marrying Chemistry with Biology in Drug Discovery, SLAS Europe 2018 Conference & Exhibition, Brussels, Belgium, 2018.

## Awards during PhD

March 2020	<b>Carl Roth Förderpreis 2020</b> Carl Roth & Gesellschaft Deutscher Chemiker (GDCH)
January 2020	<b>Tony B. Award</b> Society for Laboratory Automation and Screening (SLAS)
September 2019	Subsequent funding for winning the <b>ideas competition</b> <b>“Biotechnologie – Von der Natur lernen”</b> Ministerium für Wissenschaft, Forschung und Kunst Baden-Württemberg
July 2019	3 <sup>rd</sup> price of <b>NEULAND innovation competition</b> Karlsruhe Institute of Technology (KIT)
June 2019	<b>Tony B. Award</b> Society for Laboratory Automation and Screening (SLAS)
July 2018	Feasibility study for winning the <b>ideas competition</b> <b>“Biotechnologie – Von der Natur lernen”</b> Ministerium für Wissenschaft, Forschung und Kunst Baden-Württemberg
June 2018	<b>Tony B. Award</b> Society for Laboratory Automation and Screening (SLAS)

Last update of CV: 04.06.2020